Evaluation of Advanced Wound Healing Products from an Operational and Financial Perspective

A thesis submitted to the University of London

for the degree of

Engineering Doctorate

by

Betty Lin, MEng

Advanced Centre for Biochemical Engineering

Department of Biochemical Engineering

University College London

Torrington Place

London

WC1E 7JE

June 2008

ProQuest LLC
789 East Eisenhower Parkway
P.O. Box 1346
Ann Arbor, MI 48106-1346

Abstract

A shift in the global chronic wound care market from traditional wound dressings to advanced bio-derived products has demonstrated the demand for the 1st generation of skin substitute products. Although these demonstrated the proof-of-concept for tissue engineering, the manufacturing processes were mainly laboratory based, labour intensive and not amenable to scale-up. The aim of this thesis was to carry out a technical and economical evaluation of alternative manufacturing options for the next generation of cell-derived wound healing products delivered in an amorphous gel format.

Experimental work was carried out to demonstrate the feasibility of an alternative manufacturing process culturing human dermal fibroblasts (HuFFs) to generate extracellular matrix. A microcarrier-based process was selected and results showed the HuFFs proliferated well on both Cytodex 2 and biodegradeable Vicryl discs. Limitations with both approaches are discussed.

Economic feasibility of the microcarrier based processes was evaluated, and this was compared to the conventional manual and automated roller bottle processing route. Impact of manufacturing options on the cost of goods and net present value were assessed. Deterministic analysis indicated that the key process economic drivers are the cell density and the ratio of cells to extracellular matrix. Additionally, stochastic analysis was applied to rank each process options in terms of risk-reward characteristics and this showed sensitivity to the production capacity required. Further process economics analysis evaluated the feasibility behind recombinant growth factor production using both *E.coli* and yeast processing routes, and the analysis highlighted critical titre levels required for this option to be feasible.

The work in this thesis demonstrates the use of simulation tools and risk analysis to support the quality of decision making to enable a cost effective manufacture of advanced wound healing products.

Acknowledgements

I would like to thank the many individuals who helped and inspired me to walk this road. I would like to express my gratitude to my supervisor, Dr. Suzanne Farid, for the continual encouragement and constant support from the beginning, and throughout this process. Her advice and enthusiasm has always been an unfailing source of energy which has been priceless. I would also like to thank Dr. Susanna Levy for the advice and support.

I would like to express my gratitude to Nick Medcalf, Dr. Mary-Ann Dowling, Dr. Mark Smith for the guidance and helpful advice. Thanks to Dr. Jonanthan Maughan, Sophie Hidden for help with cell culture, to Sarah Freestone for help with immunostaining, and special thanks to Andrew Prior for all the help with histology staining and sectioning. Most of I would like to say thanks to the many people I have met at Smith & Nephew RC of which this project would not have been possible.

I would like to say thanks to my colleagues at UCL for their constant support. Special thanks to Tarit Mukhopadhay, Wellae Williams-Dalson and Naveraj Gill for their friendship, and the many discussions shared over the teas and coffees. Thanks to Edmund George for help in code writing to run the simulations of the cost models.

Funding by the Engineering and Physical Sciences Research Council (EPSRC) and Smith & Nephew (S&N) is gratefully acknowledged.

I would also like to thank my family for their love and support, and to my partner in life, Kirk, for his unwavering love and support.

Contents

List of Tables

List of Figures

ABBREVIATIONS

aRB	Automated roller bottle
ATS/SN	Advanced Tissue Sciences/Smith & Nephew
bFGF	Basic fibroblast growth factor
CIP	Cleaning-in-place
COG	Cost of Goods
DMEM	Dulbeccos' modified eagles' media
DSP	Downstream processing
EMEA	European medicines evaluation agency
FDA	Food and Drug Administration
HVAC	Heating ventilation and air-conditioning
HuFF	Human dermal neonatal foreskin fibroblasts
IRR	Internal rate of return
KGF-2	Keratinocyte growth factor 2
k_La	mass transfer coefficient for oxygen transfer
MADM	Multi-attribute decision-making
MCDM	Multi-criteria decision-making
MDCK	Madin-Darby cainine kidney cells
mRB	Manual roller bottle
MTT	[3-(4,5-dimethyldiazol-2-yl)-2,5 diphenyl tetrazolium bromide]
NHS	National health service
NPV	Net present value

OCT	Optimal Cutting temperature compound
PBS	Phosphate buffer saline
PDGF	Platelet derived growth factor
QA	Quality assurance
QC	Quality control
RB	Roller bottle
RC	Research centre
SIP	Steam-in-place
STR	Stirred tank reactor
TE	Tissue engineered
TEPC	Total equipment purchase cost
TGF-β1	Transforming growth factor--β1
TGF-β2	Transforming growth factor--β2
TGF-β3	Transforming growth factor--β3
UCL	University College London
USP	Upstream processing
WFI	Water for injection

CHAPTER 1

SCOPE AND BACKGROUND

1.1 Introduction

The pioneering 1st generation tissue engineered products were skin substitute products developed for wound healing. It has been met with many challenges and one of the conclusions drawn by people in the industry is that the manufacture of these advanced wound dressings is subject to costs similar to drug manufacture and yet the profit margins are that of medical devices (Bouchie, 2004). Thus, there is a growing pressure to reduce the development costs. Chronic wounds include pressure ulcers, venous ulcers, and diabetic foot ulcers and these can persist for years, requiring cost-intensive treatments. A leg ulcer is defined as the 'loss of skin below the knee on the leg or foot, which takes more than six weeks to heal' (NHS CRD, 1997). In the U.S. alone, the incidence of chronic wounds is estimated at 3 to 5 million which is costing $2.8 billion dollars annually. Venous leg ulcers are a common, chronic, recurring condition. They are estimated to have a prevalence of 1.5 to 3 per 1000 of the UK population (NHS CRD, 1997). This prevalence increases with age, and is estimated at 20 per 1000 aged 80 years (Royal college of Nursing, 2000a). The economic cost of leg ulcers to the NHS is estimated at £300-600 million a year (Simon et al, 2004). Between 17% and 65% of people with a leg ulcer experience severe or continuous pain with a major impact on the quality of life (Briggs and Nelson, 2003).

Foot complications are also common in people with diabetes. The prevalence of neuropathy in people with diabetes is 23 to 42%, and that of vascular disease is 9-23%

(SIGN, 2001). It is expected that 15% of people with diabetes will develop a foot ulcer associated with peripheral neuropathy or ischaemia or both (NHS CRD, 1999). Again, the diabetic foot ulcer is also very painful and hard to heal. The danger associated with these chronic ulcers is the risk of amputation and morbidity.

For many burns victims, the use of their own skin for grafting is not an option because the patient is too weak for surgery, or simply put, does not have enough healthy skin available. Thus, clinicians will use cadaver skin or animal skin as a temporary solution, even though these will be rejected eventually anyway. In Western Europe, it is estimated that severe burns, with about 150 patients per year to be treated by tissue-engineered skin substitutes, represent a much smaller market (Jones et al., 2002).

The global wound care market is a growing industry that is shifting from traditional wound dressings to advanced wound dressings (Frost and Sullivan, 2004). This is due to the aging population, which leads to an increase in the incidence of chronic wounds and the increase spending in health. Table 1.1 is from the report carried out to examine the future prospects of tissue engineering.

Table 1.1 Maximum market potential for cell derived skin products

Market	Market size 2001 (millions of euros)	Region	Source
Global wound management market potential	6,250	World	Landesbank Baden-Wurttemberg Equity Research, 2001
Maximum market potential for tissue-engineered skin, only applicable to chronic wounds	625	World	Landesbank Baden-Wurttemberg Equity Research, 2001
Global market for skin replacement products for wound repair	800	World	Russell & Cross, 2001
Market for skin substitutes	300	USA	Russell & Cross, 2001

Although these products demonstrated the proof of concept, they have faced many challenges getting to market. The poor business model of high development costs and low profit margins contributed to major players filing for bankruptcy in 2002 as sales were too low to cover operating costs (Bouchie, 2004). In addition, the previous lack of regulatory framework, especially in the EU has contributed to the demise of some of these products, since they lie in the overlap between the biologics and devices (Moore, 2002). This has caused delays in getting approval and consequently led to massive overspending, with the net result of being sold to a larger company (Bouchie, 2004).

1.2 Advanced Wound-healing products

The skin is the largest organ in the body and serves to form a protective barrier against the environment. Significant losses of portions of skin due to injury or illness can lead to debilitating conditions and the possibility of death. Besides acute injuries such as burns, the social and financial tolls of chronic wounds are very high. Thus scientific breakthroughs in wound management have led to the use of cell derived skin substitutes (e.g. Apligraf®, Dermagraft®, Transcyte®) and recombinant growth factors (Regranex® gel). The dynamics of a chronic wound are quite different from that of acute wounds but it is thought that the introduction of cells and the appropriate factors into the engineered skin product will address the imbalance and promote wound healing.

The first products to reach the market were approved for the treatment of severe, full thickness burns e.g. Epicel (Genzyme Biosurgery, US), Integra (Integra Life Sciences, US), and Transcyte (Advanced Biohealing Inc, US). Most of the first generation tissue-engineered products are developed to mimic the human skin as closely as possible. Some of the first products that were developed to treat chronic wounds and severe burns are listed in the table below. (These are situations where the wounds are hard-to heal and it can become a life-threatening situation). Apligraf (Organogenesis, US) was the first product to gain approval from the FDA for the treatment of venous leg ulcers. Having emerged from bankruptcy in 2002, Organogenesis now has the greatest market share with this product. Table 1.2 shows the estimated sales figures of these products.

Table 1.2 Estimation of sales figures for the selected cell derived skin substitutes

Trade Name	Company	Year	Sales (Millions of euros)
Apligraf	Organogenesis Inc (USA), Novartis (USA/CH)	2006	44.6
Dermagraft†	Advanced Tissue Sciences(USA), Smith & Nephew (UK)	2003	10.4
CellActiveSkin*	IsoTis (NL)	2002	0.545
Epidex‡	Modex Therapeutics (CH)	2002	0.157
BioSeedS, BioseedM, MelanoSeed	BioTissueTechnologies (D)	2002	0.450
Epicel**	Genzyme Biosurgery (USA)	2001	n.a. 75 patients treated annually worldwide

†Production stopped in 2005 and business sold to Advanced Biohealing Inc, US.
*Production stopped in late 2002 because the product was not profitable.
‡Production was stopped by Modex Therapeutics (CH), product licensed to Autoderm (Germany) in spring 2003.
**No FDA approval needed as it was considered as a medical procedure.

According to Pruitt and Levine, (1984), Smith, (1995), Ehrenreich and Ruszczak, (2006), the ideal synthetic wound dressing, or biologic skin substitute should have the following characteristics:

- absence of antigenicity
- tissue compatibility
- absence of local/systemic toxicity
- impermeable to exogenous microorganisms
- water vapour transmission e.g. like skin
- rapid and sustained adherence to wound surface
- conformable to the surface irregularities
- elasticity to permit motion of underlying tissue
- resistant to linear and shear stresses
- tensile strength
- inhibition of wound surface flora and bacteria
- long shelf life, and minimal storage requirements

- biodegradable
- low cost
- minimize the nursing care of the wound, and patient discomfort
- translucent to allow observation of the wound healing
- reduction in healing time
- not increase the rate of infection
- patient acceptance and compliance

These cell derived advanced wound healing products brought to market were expensive (Jones et al., 2002) and this delayed the adoption of these products by the market. One of the reasons for the high price of these products was due to the high production costs involved. Additionally, the set size was also one of the limitations. The short shelf-life made the logistics of transportation of these products to the patient a critical issue. Thus the need to address some of these limitations exists for the next generation of cell derived biological dressings.

1.3 Aims and organisation of thesis

The preceding section has provided a general background to the field of cell derived products for wound healing e.g. skin-substitutes, and Chapter 2 presents a more in-depth literature review. As highlighted in this introductory chapter, the first generation cell derived products for wound healing have struggled to achieve their potential market success. This has been largely attributed to inflexible, labour-intensive and costly manufacturing processes that are not amenable to scale-up. Thus, the aim of this project was to explore an alternative approach for generating second generation products that would provide increased flexibility and lower costs. This was based on the provision of products in a radically different formulation as a gel which would open up the way for more robust and scalable manufacturing process. Additionally, this project will seek to identify the crucial parameters involved in making the next generation of cell derived products for wound healing by examining the process economics as well.

Chapter 2 starts with the introduction of the biology of wound-healing, and then presents a more in-depth analysis of the current products and the processes of manufacture. It then examines the manufacturing challenges and reviews the various bioreactor designs, followed by the culture conditions required for the culture of human dermal neonatal foreskin fibroblasts (HuFFs).

Chapter 3 gives the methodology required for the technical experiments and this section describes the methods and assays used. Chapter 4 presents the results of the experimental work, beginning with the initial characterisation of the dermal fibroblasts, the static culture and then the results from bioreactor cultures in stirred tank fermenters. It then expands to discuss other equipment issues in scaling up and discuss the technical limitations.

Chapter 5 explains the framework presented for the economic modelling. It presents a methodology for modelling the process economics and shows economic indicators such as net present value (NPV), and cost of goods (COG) can be incorporated as the outputs. Chapters 6 shows the case study for comparing the different reactor options, namely roller bottles (RBs) to stirred tank reactors (STRs) and the disposable Wave bioreactor. The results of deterministic analysis and stochastic analysis using Monte Carlo simulation were presented. Chapter 7 present the economic analysis of growth factor manufacture using the microbial routes and the main limiting factor was identified to be the titre level. Sensitivity analysis showed achieving a critical titre level of greater than 100mg/L meant profitability for the process routes.

Chapter 8 covers the regulatory issues faced by these TE-products. Finally, Chapter 9 provides a summary of the key conclusions and then presents suggestions for future work. Finally, titles of the drafted papers by the author to be submitted for publication are mentioned as Appendix A. Protocols used for the experimental work are included as Appendix B. Additional details involved in the economic cost modelling are included in Appendix C.

CHAPTER 2

LITERATURE REVIEW

2.1 Introduction

This chapter provides the literature on skin replacement products, and the manufacturing processes for them. It starts with a brief background on the biology of wound-healing which is a very complex process and then delves into the existing treatments and processes. A discussion of manufacturing choices for adherent cells is then discussed. Finally, culturing conditions published in the literature are reviewed so as to provide a basis for the experimental work.

It was the breakthrough work published in 1975 by Rheinwald and Green, which prompted the revolution in tissue engineering of skin substitutes. Building on previous attempts at skin replacement in the 1960s, they successfully serially sub-cultured keratinocytes. Increasingly, many methods have been published which describe the deployment of autologous and allogeneic cells onto wounds. Currie et al. (2003) and Veazey et al. (2004) demonstrated the use of aerosol sprays to deliver cells to burns. Constructs of fibroblasts/collagen gels (Kuroyangi et al., 2001), fibroblasts and chitosan (Ma et al., 2001), cells and fibrin (Gorodetsky et al., 1999, Cox et al., 2004), cells and plasma products (Ito et al., 2003), tissue equivalents (Eaglestein and Falanga, 1998), cells and other polymeric surfaces (Yamato et al., 2001) have been also developed. The use of biodegradable microspheres for regeneration of wounded skin has been proposed by LaFrance and Amstrong (1999). Wound healing is a complex condition involving a myriad of factors and some information about wound biology is given.

Wound repair is a dynamic process, but follows a time sequence and can be considered in stages of inflammation, tissue formation and tissue remodelling. Immediate wound coverage is generally one of the key cornerstones of therapy, thus in the past grafts from other sources such as cadavers or animals have been used. However, this has its associated risks (e.g. transmitting infection), thus there is the need for bioactive cell derived biological dressings. Additionally, these grafts are eventually rejected thus making them a temporary solution rather than a permanent one.

The skin comprises of the epidermis and the dermis, where fibroblasts and keratinocytes are the main cell types, which produce and maintain the extracellular matrix (ECM). Fibroblasts are one of the key cells, which migrate to the wound site and secrete a variety of factors and matrix proteins to stimulate wound healing. The ECM laid down by the cells is a complex mixture of cross-linked proteins and glycosaminoglycans (GAGs). This ECM interacts with the cells in a crosstalk manner. The growth factors, which are involved in wound healing are listed in Table 2.1.

Table 2.1 List of growth factors and cytokines used in wound healing

PDGF	Platelet derived growth factor
TGF-β	Transforming growth factor-β
TGF-α	Transforming growth factor-α
FGF	Fibroblast growth factor (acidic, basic)
KGFs	Keratinocyte growth factors
EGF	Epidermal growth factor
IGF-1	Insulin-like growth factor 1
VEGF	Vascular Endothelial Growth Factor
TNF-α	Tumour necrosis factor α
IL-1-α	Interleukin-1-α
IL-1-β	Interleukin-1-β
IFN γ	Interferon γ
IFN α-2β	Interferon α-2β

These cytokines and growth factors act in a concerted manner and control wound healing; thus identifying the key ones would be desirable as well as controlling the level expressed. Collagen is the primary structural protein and many forms exist. Adhesion

proteins bind to these collagen proteins. Typically, the predominant form of collagen of interest will be type I, secreted by the human foreskin fibroblasts (HuFFs) since this will be present in significant quantities.

Fibronectin is a globular protein and again interacts with the cells. Proteoglycans are part of the multifunctional ECM and act as important cell surface molecules. One of the small proteoglycans, decorin binds to collagen fibrils and plays a role in the fibril assembly. Additionally, it has an effect on the cell morphology and can modulate the binding of cells to the matrix constituents such as collagen and fibronectin. These small proteoglycans also helps to sequester the growth factors within the ECM (Hildebrand, 1994).

With normal wound healing, the first response is clot formation and at the same time, inflammatory cytokines are released to do a variety of functions: recruit macrophages and lymphocytes to fight off infection, regulation of blood flow to the affected area; stimulate angiogenesis and deposition of ECM. The latter processes form granulation tissue. This is very important because it fills the wound with tissue that brings inflammatory cells to provide protection and at the same time a substrate for re-epithelialization. After the wound closes with an epithelium, factors such as TGF-β stimulate the remodelling into a scar.

With the case of impaired healing, it is postulated that there may no longer be a granulation response because the fibroblasts and keratinocytes at the wound perimeters may have stopped proliferation and start to senesce (i.e. the cells have grown old and are no longer able to grow). It could also no longer be responding to the cytokine stimulation. It has been reported that the expression and proteolysis of VEGF is increased in chronic wounds (Lauer et al. 2000). Therefore, it is believed that providing either living healthy cells or altering the level of cytokines such as the case of Dermagraft® (Advanced Biohealing Inc) and Apligraf® (Organogenesis) will shift the imbalance at the wound site to the normal healing response (Gentzkow et al., 1996). Thus, it would be useful to observe how environmental factors can affect the levels of growth factors or cytokines

and thus vary the final composition of the bioactive cell derived product. For example, in peritoneal fibroblasts, it has been shown that increasing the concentration of glucose stimulated the production of type I collagen and TGF-β1 mRNA levels (Saed, 2003). Thus by altering the levels of glucose, the levels of TGF-β will be affected and thus affect the collagen secretion by the cells.

Additionally, if the mode of action for accelerated wound healing is to use biologically active matrix, then the development of a biomass product rich in a variety of growth factors is a viable approach. Indeed, cell derived biological dressing such as Dermagraft and Apligraf probably act as a vehicle for delivering growth factors to wounds (Eaglestein and Falanga, 1997). It has been demonstrated that Apligraf does not survive transplantation for more than six weeks in acute human wounds and serves a temporary role as a biological dressing (Griffiths et al., 2004).

2.2 Current Products and Process review

The current products brought to market can be divided into three categories: autologous skin grafts, allogeneic skin substitute products, and growth factor therapy. At present, an example of commercial autologous therapy is Myskin, produced by CellTran (UK). Launched in 2004, Myskin is used to treat burns and chronic wounds. This product is only available in the UK, partly due to logistic and transportation issues. The pricing of Myskin is quite attractive, as it is expected to have an average price of £500 for several applications.

Myskin is made up of a flexible medical-grade silicon substrate backing polymer coated with a chemically controlled plasma polymer film that supports the growth of keratinocytes, derived from a small biopsy obtained from the patient. This silicone layer is formulated with a surface coating that has been deposited by plasma polymerisation of acrylic acid. This polymer film is engineered to promote cell growth, and subsequent release when applied on to the wound. During the manufacturing process, the keratinocytes are co-cultured with irradiated murine cells. It is supplied as a 5cm

diameter circular disc of surface area 19.6 cm^2, and individually packaged on a sterile, buffered, serum-free mixture of DMEM(76%) and HAMS F12 (23%) in an agar gel form.

Both Apligraf and Dermagraft originate from neo-natal foreskin and hence are allogenic therapies. Apligraf® (developed and manufactured by Organogenesis, marketed by Novartis until June 2003, formerly known as Graftskin, Living Skin Equivalent) was first approved in the treatment of venous ulcers and subsequently, the treatment of diabetic foot ulcers. Apligraf (Organogenesis) is a bilayered skin substitute consisting of living cell and structural proteins. The lower dermal layer is a bovine type I collagen fibroblast-containing matrix and the upper epidermal layer is formed by viable keratinocytes. The process of manufacturing Apligraf is a modification of the procedure used by Bell et al. (1981) and subsequently described in detail by Parenteau et al. (1992). The total manufacturing time takes 17 to 20 days (Eaglestein and Falanga, 1997).

Essentially, the basic steps to the process are cell stock preparation, formation of the matrix, epidermalisation, stratification and maturation. Fibroblasts and keratinocytes are obtained from screened neonatal foreskins and used to establish the cell banks (Wilkins et al., 1994). Solution of purified acid-extracted bovine type I collagen is mixed with fibroblasts and is cast onto the porous membrane of the culture insert and the neutralised mixture solidifies into a gel. This then is cultured, and after 4-6 days, the fibroblasts cause this mixture to contract and form a dermal equivalent. Finally, keratinocytes are seeded onto this dermal equivalent in the epidermalisation stage and cultured for another 2 days to allow coverage. This is then exposed to air to allow stratification of the epidermis and the bilayer is cultured at the air-liquid interface to ensure epidermal organization and maturation.

This product is supplied as a circular dish, which is approximately 75mm in diameter and 0.75 mm thick. The packaging is a sealed polyethylene bag with a 10% CO_2/air atmosphere and an agarose nutrient medium. It is shipped overnight based on the date of

patient application and stored at room temperature. The shelf life of the product was about a week, but has been extended to 10 days and retails at $1199 (Medicare, 2004).

Transcyte is a temporary covering derived from fibroblasts. It is made by seeding cells onto a nylon mesh in fiberglass casings, and when closed the casing acts as a bioreactor. The bioreactors are stacked together in an incubator. This is used to treat burns. Problems from manufacture are that tiny perturbations caused shear stresses which affect the formulation of scaffold. It is not space efficient or very robust, and dependent on the skill of the operator. This was also delivered in a fixed format only. Dermagraft® was first approved to treat diabetic foot ulcers, and it was developed by Advance Tissue Sciences (ATS), in collaboration with Smith & Nephew. After ATS filed for bankruptcy in 2002, the product was subsequently bought out by Smith and Nephew. In Nov 2005, Smith and Nephew announced the sale of the Dermagraft and Transcyte business, and this was purchased by Advanced Biohealing Inc in May 2006. Dermagraft (Advanced Biohealing Inc) is a living, metabolically active, immunologically inert dermal tissue. It is cryopreserved and human fibroblast-derived. It consists of cultured neonatal fibroblasts, which are seeded on to bioresorbable polyglactin mesh. The product is supplied frozen in a clear bag that contains one piece measuring 2inch x 3inch and sold for $450 (Naughton, 2002).

The basic manufacturing steps are cell stock preparation, matrix formation, and cellular in-growth. Screened fibroblasts obtained from the neonatal foreskins by enzymatic isolation are cultured and banked at passage 5. Cells are expanded in roller bottles. These dermal fibroblasts are seeded onto polygalactin acid mesh (Vicryl®, Ethicon Inc) which was laser welded to the pouch. This is then cultured for 15 days. This semi-automated system consisted of several bags stacked next to each other and attached to a manifold which circulated media at a slow recirculation rate. Dermagraft is supplied frozen with a shelf life of one year.

Byproducts from the manufacturing processes of Apligraf and Dermagraft are the spent media, which is rich in soluble growth factors and have been sold off to make anti-aging

facial creams. For example, Nouricel (ATS/S&N) comprises the spent media from the Dermagraft process and was sold to Biozhem Cosmeuticals Inc (Mckenna, 2002). Organogenesis are also utilising the spent media from the culture of their Apligraf for similar purposes as well, in targeting the cosmeuticals industry, with their own product, Revitix, which will be on sale in 2007. Neocutis is another company that is selling creams for anti-aging purposes with growth factor mixture derived from cultured fetal fibroblasts. Gold et al. (2007) reported on the use of growth factors and cytokines as such in a topical cream to reduce the appearance of wrinkles.

Another company in this field is Ortec International where its primary product is Orcel, and this is a bilayerd cellular matrix aimed at the chronic and acute wounds market. Orcel consists of bovine type I pepsinised collagen sponge seeded with keratinocytes and fibroblasts derived from the neo-natal foreskin tissue. However, they still need to complete clinical trials for the ulcers market. The culture duration is 10 to 15 days and expected be on the market at $1100.

Intercytex, another UK company, is seeking to commercialise its lead products, ICX-PRO for chronic wounds, ICX-TRC for hair regeneration and ICX-SKN for skin grafts. Again, the cells are derived from US neo-natal foreskins. ICX-PRO is human dermal fibroblasts presented in a fibrin-based gel matrix and Intercytex hopes to bring this product to market in 2008. It has a shelf life of 21 days.

These 1st generation cell derived advanced wound healing products are produced as 'tissue bandages' in the form of discs or sheets. However, this fixed size limitation requires hospitals to have stocks of material and surgeons to alter the shape to cope with the variation of wounds seen with each individual patient. Original manufacturing methods were largely based on laboratory practice and were slow, labour-intensive and did not implement much automation. The repetitive nature of the work represented a problem for retaining skilled labour, and resulted in high staff turnover ratio.

Since emerging from Chapter 11 bankruptcy, Organogenesis has moved successfully from a manual process requiring skilled technicians to one that is semi-automated to control media additions to the Petri dish like vessels (Mason and Hoare, 2007). Although Dermagraft was produced by a more automated process, it has been reported that many batches of product had to be discarded due to uneven growth in the pouches, thus increasing overall production costs (Moore, 2002).

Transportation of these cell derived advance wound healing products has been a major stumbling block and added to the financial drain on the company's resources. Some of these cell derived advanced wound products are shipped fresh for use in therapy, but the short shelf life meant that any delays in transportation resulted in useless expired product. Although cryopreservation overcomes this limitation and allows off the shelf use, couriering a product in dry ice to attempt to keep it frozen is expensive. Additionally, this requires the hospital to invest in infrastructure such as -70°C freezers and maintenance of them to store the frozen product. Most clinics do not possess this necessary infrastructure. The doctor, who applies this frozen product, needs to be well trained in the defrosting technique, plus it is important to thoroughly rinse the product free from the toxic cryoprotectant, DMSO, dimethylsulfoxide.

A different approach for treatment of wounds has been the use of growth factors e.g. Regranex gel (Johnson and Johnson), Fiblast spray (Kaken Pharmaceuticals). The active ingredient in Regranex gel is a recombinant platelet-derived growth factor (PDGF). Fiblast spray is currently available only in Japan and contains basic fibroblast growth factor (bFGF). Currently, other cytokine products for cosmetic improvement of scars and planned for use in wound healing is under development by a UK company, Renovo. Table 2.2 summarise the details about the products brought to market.

The only growth factor product that has enjoyed commercial success has been Regranex gel and this is probably due to the fact that wound healing being such a complicated process, has meant that there is not a one simple solution. Different growth factors have

been tested, and the results demonstrating efficacy have been shown for some growth factors e.g. bFGF, (Robson et al., 1992), and PDGF (Wieman, 1998).

Table 2.2 Description of growth factor therapy products

Product	Company	Product and Process Description	Cost	Year approved	Sources
Regranex gel	Johnson and Johnson	Topical application containing a secreted growth factor rPDGF Kept refrigerated	£275 for a 15g tube	1998	www.rxlist.com www.regranex.com
Fiblast spray	Kaken Pharmaceuticals	Topical application containing a bound growth factor rbFGF Freeze-dried powder, reconstituted upon usage.	£60 pounds for a 500ml spray	2001	Annual Report from Kaken Pharmaceuticals
Prevascar	Renovo	Topical application of rIL-10 growth factor	N/A	Expected 2008	www.renovo.com
Juvista		Topical application of rTGF-β	N/A	Expected 2008	www.renovo.com

Thus, provision of 2nd generation cell derived advanced wound healing products in radically different formulations such as an easy-to-use preformed gel delivered via a disposable tube using robust scalable manufacturing processes appears to be an attractive alternative. This approach is explored further in this thesis.

2.3 Manufacturing Choices

2.3.1 Autologous vs. allogenic cells

Before the production can start one of the important determining factors affecting the choice of manufacturing route is the source of cells. Cell based therapies that opt for the autologous route usually delivers the product 'fresh' to the patient and cryopreservation is not adopted. Choosing the allogeneic route allows for cryopreservation which increases the shelf life of the product, and the product can be shipped a great distance to the patient

(IPTS report, 2003). It is felt that the autologous route will be based on a service-driven industry model, rather than the product-driven model. The source of cells for the allogeneic route has been derived from neonatal foreskins for the products brought to market. There is a belief that because these cells are very young that they contribute towards a scarless healing, and this can be considered a marketing advantage over the autologous route. The autologous route will represent a lower regulatory burden when compare to allogeneic methods.

2.3.2 Scaffold choices

The cells require a scaffold to grow on and this can be incorporated into the product to form part of the cell delivery vehicle. A wide variety of biodegradable scaffold materials are being developed, which can be separated into many categories, but essentially, there are natural and synthetic biodegradable polymers. Examples of natural biodegradable polymers are fibrin, collagen, gelatin, albumin, starch, dextran, chitosan, and chitin. Synthetic biodegradable polymers are polylactic acid, polyglycolic acid, poly(lactide-co-glycolide), polyorthoesters, polyhydroxybutyrate, polyhydroxyvalerate, polyanhydride. There are some other classes of scaffolds which change their physical properties in response to external stimuli e.g. pH sensitive and thermoresponsive polmers (Kidchob et al., 1998, Recum et al., 1998, Yamato et al., 2001). However, for the scope of this project, the biodegradable material used will be the synthetic material, PLGA (polylactide glycolic acid), with the commercial name, Vicryl.

2.3.3 Reactor vessel choices

The last dominant variable to be considered is the type of reactor vessel which is suitable and whether to run the culture as batch, fed-batch or continuous and this is reviewed in the following section based on the industrial processes with animal cells. Many systems were developed to match the need for the production of mammalian cells and this has been demonstrated by the successful manufacture of vaccines, tPA, human interferon, blood proteins such as Factor VIII. However, the development of bioreactors for adherent

cells for tissue engineering is still very much of a challenge since the cells are primary and are more delicate.

Since these cells are primary cell lines, the cell expansion step prior to production culture cannot be too long, thus this implies an upper size limitation to the reactor. Hu at al. (1985) showed that for FS-4 fibroblasts serially passaged over 3 consecutive microcarrier cultures decreased from 2.2 doublings in the 1st passage to 1.5 doublings in the third passage. Van Wezel et al. (1967) reported the decrease in the final density achievable for kidney cells from monkeys with each successive subculture, until the cells ceased to grow at the sixth or seventh passage altogether.

The use of adherent cells limits the possibilities in reactor choice, and in general, the next step up from lab-scale experiments in T-flasks has been to conduct the cell culture in roller bottles. These are cylindrical screw-capped bottles, which are usually made of plastic or reusable glass. The size of the bottle is about 1 litre or so and is filled to about 30% of culture medium. These bottles are then placed on a roller rack and rotated slowly, and incubated either, in an incubator or an incubation room. The cells attach to the inner wall of the bottle. This cell layer is bathed into the medium, and there is alternate exposure of the gas phase and medium as the bottle slowly rotates.

Eventually the entire surface is covered by the cell, and normal diploid cells will suffer from contact inhibition and stop growing. They are then detached by enzymatic treatment e.g. trypsin, and then inoculated into other roller bottles. Roller bottles have been used commercially for the production of erthropoetin EPO by Amgen (Tsao et al., 1992, Eridani, 1990). This worked well for Amgen, as it allowed them to get product into clinical trials quickly, and meet the total estimated demand in the US in 1998 which was 1 kg per year (Kretzmer, 2002). The use of spiral designs, ceramic packing, glass tubes in the roller bottles are methods to increase the surface area and still retain the monolayer culture. Table 2.3 compares some different systems and it can be observed that roller bottles may not be the most efficient system to culture cells.

For small-scale production, roller bottles (RBs) have many advantages. RBs are inexpensive to set up and allows for a rapid change of throughput in response to need. The relative simplicity to replace the cell growth medium to one that is designed for product formation is an advantage, for example, replacing the serum-containing medium with serum-free medium for production of viruses. The transparency of the roller bottles allows quick visual inspection and microbial contaminated bottles can be quickly identified and discarded.

The disadvantages become obvious for large-scale production. Numerous bottles are required, and there is no on-line environmental monitoring and control, as it is impractical and virtually impossible. The aseptic handling of the bottles means that labour has to be extensively well trained to ensure success. The risk of microbial contamination is high, since each batch requires many bottles and there are several manual steps. The advent of automation has allowed some of these problems to be addressed but the cost of the robotic arm is, certainly not cheap.

Table 2.3: Culture systems available for growth of anchorage-dependent animal cells

Source: Taken from Atkinson and Mavituna, Biochemical Engineering and Biotechnology Handbook, pg 476

The reasoning behind the use of multitray units such as the Cell Factory is the ease in scale up, as it is like lego bricks. Nunc's cell factories are disposable, polystyrene, ventable chambers that come in stacks. Inoculation, feeding, and harvest are straightforward. No specific training is required and the cells can be visualised directly in the chambers via an inverted microscope (Meisenholder, 1999). The CellCube from Corning Science Products is an easily expandable system for growing adherent cells. With these disposable polystyrene modules, each holds about 3.5L of media and contains 25 parallel plates for a total growing area of 21,000cm^2 per cube. The interlinked cubes stand on one another with media entering the bottom and exiting the top (Griffiths, 2001).

These units are supplied, assembled and sterile ready for use. Also been made of disposable plastic meant the issue of risk of contamination is lower. However, the potential disadvantage is that it requires a lot of medium. Additionally, the inability to completely remove all the cells from the trays is quite a disadvantage. This problem can be turned around by adding fresh medium to the remaining cells, which can act as inoculum for the next culture. However, this maybe suitable for initial cell expansion but it is not an option as a final reactor for cell derived skin substitute, due to the inability to retrieve the final product without compromising sterility.

Rotary reactors, such as the NASA device, have been developed. However, this system is not applicable to large scale due to its complexity. There has been some mention in literature of various configurations, which uses rotary motion. It has been reported that a rotary column reactor was used for anchorage dependent cells (Nakao et al., 1996). It could be that the rotary motion is conducive to enhance the secretion of extracellular matrix by fibroblasts. Fig 2.1 shows the rotary column reactor that was used.

The idea of culturing adherent cells on microcarriers was proposed in 1967 by Van Wezel, and a few decades on, a variety of microcarriers have been developed and used in cell culture for the production of biologicals such vaccines, and proteins (DePalma, 2002). Microcarriers are spherical beads of 150-200μm diameter, which can be

suspended in a culture medium. Cells can attach and grow on the bead surface, as a monolayer of up to 100-200 cells per microcarrier.

Figure. 2.1 Experimental set-up of rotary column bioreactor. The arrows with *indicate the flow of the culture medium. 1 = Level sensor, 2 = pH sensor and 3 = DO sensor. (Nakao et al., 1996)

Microcarrier cultures are generally considered to have the greatest advantages for scale up of anchorage-dependent cells, and this quasi-suspension culture is space saving and cost-effective with regard to use of culture media and expensive supplements such as serum (Malda and Frondoza, 2006). Use of microcarriers opens up the options normally only available to suspension cell cultures. Simple stirred tank batch fermenters can be easily adapted to suit the mixing conditions required to maintain a homogeneous culture of microcarriers, and such cultures have been operated at a scale of 1000L. The cell yield from such batch cultures typically reaches a maximum of ~ 10^6 cells/ml (Wurm, 2004).

Medium re-feeding or perfusion can raise cell yields to $>10^7$ cells/ml. Thus it is important to appreciate that it is not only the volume of the bioreactor that determines the scale of operation – a 100L microcarrier culture operated by medium perfusion may produce a higher yield than a 1000L culture operated in a batch mode (Boedecker et al., 1994).

This established technology has been used extensively for viral vaccines (Van Wezel et al., 1980, Montagnon et al., 1984, Barteling and Vreemijk, 1991, Moran, 1999), and a wide variety of cell lines has been tested. Culture of chrondrocytes on microcarriers was first suggested by Freed et al. (1993), additionally, other cells lines such as human adult mesenchymal stem cells (Doctor et al., 2002), and hepatic cells (Werner et al., 1999), pancreatic islets (Del Guerra et al., 2001), and a variety of fibroblast cells has been demonstrated to attach and proliferate on microcarriers (Nilsson et al., 1986, Forestell et al., 1992). Most of the conventional microcarrier systems employ the use of solid microcarriers.

With the conventional microcarrier system, the available surface area for growth is limited, since increasing the microcarrier concentration beyond a certain limit will not lead to an increase in cell concentration because the increased agitation which is needed to suspend the microcarrier slurry becomes damaging to the cells. Thus, macroporous microcarriers were developed to overcome this limitation. The development of macroporous microcarriers allowed an increase in cell density per litre of culture, due to the increase in surface area (Nilsson et al., 1986). Macroporous microcarriers are commonly made from gelatin (Gustafson et al., 2007), collagen, cellulose, glass, polyethylene and polystyrene. (Nikolai and Wu, 1992) After inoculation of the cultures, the cells attach to the external surface of the microcarriers and subsequently migrate inwards to populate the interior of the beads.

Issues of concern documented by the use of microcarrier culture have been the hydrodynamic shear from stirring and sparging (Cherry and Papoutsakis, 1986, 1988, Lakhotia and Papoutsakis, 1991, Croughan et al., 1987, Croughan and Wang, 1988), lack of sound, scale up approaches (Aunins, 1993) and oxygen limitation, especially with

macroporous microcarriers (Kong et al., 1999). Additionally, some investigators found that the cells grew well but when infected to produce the virus particles, the cells detached from the microcarriers and died, resulting in low productivity. Thus, they resorted to using the Cell cube as the processing route (Buckland, 2006).

Microcarrier cultures have typically used stirred tank reactors but recent efforts using the disposable Wave bioreactor have been reported; the Wave bioreactor is a disposable sterile bag bioreactor upon a rocking-cradle platform (Singh, 1999). MDCK cells for influenza virus vaccine production have been shown to be cultured successfully in the Wave bioreactor and demonstrated better attachment compared to the stirred tank reactors (Genzel et al., 2006). This requires the use of a rocking cradle to give a wave agitation, which is gentle but sufficient to provide nutrient distribution. Moreover, cell damage due to gas bubbles is reduced, as there is no sparging of air. As it utilises the principle of disposables, it requires no cleaning or additional sterilization. It is easy to operate, and maintains sterility through a high containment. The bioreactor is completely closed and additions and samples are done via needless syringe connectors or tube-fuser. Vent gases are sterilised through filters. However, the downside to Wave bioreactor is that the rocking cradle is expensive and it only gives a scale-up of up to a working volume of 500L.

The next section discusses the culturing conditions reported in literature and formed the basis for the culturing conditions applied in the technical work carried out.

2.4 Cell culturing conditions

Carbohydrates provide a variety of functions in mammalian cells. The early work by Eagle et al. (1958) and others have led to development of many different media to be used. The operating medium of choice is Dulbecco's modified Eagles's medium (DMEM) supplemented with bovine calf serum, glutamine, ascorbate and nonessential amino acids. It has been shown that at a glucose concentration of 80μM the glucose utilised by human diploid cells is only 7% of that utilised by cultures initially at 5mM

(Zielke et al., 1984). Much work has been carried out by the same team into the glucose and glutamine metabolism. Additionally, the same group has shown glucose metabolism and glutamine metabolism are interlinked and the concentration of one can act to inhibit the other (Zielke et al., 1978). The presence of 2mM of glutamine inhibited glucose-6-^{14}C oxidation by 88% and stimulated the glucose-1-^{14}C by 77% in log phase cells (Zielke et al., 1978) and normal growth is maintained if the glucose concentration is above 25μM. They showed that as glucose concentration increased from 0 to 10mM the oxidation rate of L-(1-^{14}C)-glutamine decreased from 80 to 15 mmol $^{14}CO_2$ released /mg protein hr (Zielke et al., 1984). The level of glucose is very important since high glucose concentrations affect the expression of collagens and fibronectin and it has been shown by Benazzoug et al. (1998) to affect the ratio of collagens production.

Glutamine can also be used as a major source of energy for cells. Barnabe and Butler (2000) estimated that in the presence of high glucose concentrations, glutamine provided the energy of maintenance of up to 28% of the intracellular ATP pool and remainder is then provided by glucose metabolism for murine hybridomas. It is estimated that glutamine oxidation provides around 30% energy requirement of human diploid fibroblasts (Zielke et al., 1976, 1978, 1984). Glutamine is a necessary supplement to be added for the proliferation of fibroblasts. It serves to act as a key link between the carbon metabolism and proteins. It is not very stable and decomposes readily to form ammonia and glutamate. Glutamine can also act to stimulate collagen production in collagen producing cells, Karna et al. (2001). They found that that the intermediates of glutamine interconversion: glutamate and pyrroline-5-carboxylate (P5C) also act to stimulate the production of collagen however, they evoke different levels of response. Thus, it is considered that the glutamine-induction of collagen biosynthesis is through its intermediate (Karna et al., 2001). Therefore it would be important to monitor the levels of glutamine throughout the culture.

Ascorbate is added to the culture to stimulate the production of collagen. Ascorbate in low concentrations is necessary for the crosslinking of collagens, and the formation of hydroxyproline. The half-life of ascorbate is very short, and 88 to 98% of the compound

will have degraded after 24hr, (Peterkofsky, 1972) thus it is expected to be added constantly. It has been reported that the levels of ascorbate will affect the expression of collagens (Booth et al., 1980, Davidson et al., 1997, Fisher et al., 1991, Leveque et al., 2003, Phillips et al., 1994, Tajima et al., 1996).

When components of human or animal origin are added to the culture medium, there is a potential risk of transfer of viruses, and or prions. Thus if these components are added to the culture medium the sources have to be identified and contaminants inactivated or removed. Yet, despite the use of serum from 'disease-free' countries, the reliability of testing and inactivation are called into question and the regulatory authorities have advised the use of serum-free media. Thus without serum, there is the need to search for the right serum-free media, or somehow wean the cells off the dependence on serum. Additionally, the protective effects of serum against shear will have to be replaced and this perhaps can be done by the use of chemical agents such as Pluronics. Cell protectants have been added to suspension cells to help improve the viability of the cells. These media additives have helped to cope with shear and hydrodynamic effects (Croughan et al., 1987, Murhammer and Goochee, 1990, Christi, 2000, Van der Pol and Tramper, 1998). They lower the interfacial tension and help to prevent cell-to-bubble attachment. Pluronic F-68 is a block copolymer and is supplemented into the medium at 0.2% (w/v). Pluronic L-35 at 0.2%(w/v) has also been used and demonstrated to offer protection. This is a smaller molecule than Pluronic F-68 and a superior foam suppressor. Pluronics and Methocel A15LV have been deemed most effective.

Part of the serum component also consists of lipids and fatty acids, thus the use of lipids and fatty acids such as linolenic acid has been tested. It has been reported that linolenic acid has beneficial effects in the prevention of shear damage to cells (Butler et al., 1999). It has been reported that the use of dexamethasone and EGF has enabled passages to be carried out of primary human diploid fibroblasts (Baker et al., 1978, Bettger et al., 1981) in serum-free media. Due to time constraints and resources, all experiments will be carried out using serum, and it is believed, that the development of serum-free media is a field to itself, thus will not be covered in this thesis.

The measurement of oxygen uptake rate (OUR) provides a good estimate of intracellular oxygen demand when the supply rate of oxygen is constant. Active cell cultures will deplete the oxygen from the medium at a rate that is proportional to the cell mass, if there is no other limiting metabolite. Thus oxygen uptake rate (OUR) can be used as a tool to estimate cell mass and to control the cell culture process (Zabriskie, 1985). OUR values ranging from 0.05 to 0.5mmol O_2 /10^9cells/hr have been reported for various mammalian cells (Butler, 1987). The OUR of mammalian cells is affected by the glucose concentration and higher OUR at low glucose concentrations have been reported (Frame & Hu, 1985).

The supply of oxygen to the cells in culture is a particular problem when culture volumes are increased from the laboratory scale. The solubility of oxygen in aqueous solution is relatively low – 0.2 mmol per litre of culture. At a typical consumption of 0.05 - 0.5 μmol/10^6cells/hr, this means that for a litre of culture (at 10^6 cells/ml) would be depleted of oxygen in 0.4 - 4 hrs unless there is a constant supply of oxygen. Oxygen plays an important role in cellular metabolism, the most important is the electron transfer oxidase system, and additionally acts as the final carrier. In order to promote fibroblast proliferation and the production of collagen, oxygen is required. This is because oxygen is incorporated by two amino acids, proline, and lysine in the collagen chain synthesis. Collagen will not be synthesised unless adequate amounts of both proline and lysine are hydroxylated with oxygen. Synthesis requires one atom of oxygen for every three amino acids in sequence. Thus, maintenance of a sufficient level of dissolved oxygen is required.

Much literature has accumulated reporting that hypoxia induces collagen synthesis in tissues. It has been reported that hypoxic conditions accelerates the posttranslational process of collagen synthesis in cultured fibroblasts. The right level of oxygen required for HuFFs need only be about 4.3% O_2, since greater than this the concentration becomes increasingly toxic to fetal tissues. It has been shown that skin fibroblasts grow best at 31mm Hg (Balin et. al., 2002). The level of oxygenation may not need to be so high since it has been shown that hypoxia (i.e. absence of oxygen) can act to stimulate the cells and

up-regulate the production of collagen (Yoko Horino et al., 2002, Yuji Takahashi et al., 2000).

Waymouth (1981) indicated that the optimal pH for mammalian cell growth for two human skin fibroblasts cell lines were pH7.5 – pH7.6, and pH7.6 – pH7.8. In the bioreactor, the pH is stabilized with the use of buffers. It is normally recommended to use an additional organic buffer like HEPES (N-2-hydroxyethylpiperazine-N'-2-ethanesulfonic acid) and 1-2mM bicarbonate to maintain adequate concentrations of dissolved CO_2. HEPES is relatively expensive but it is frequently used because its pKa falls in the physiological range (7.31 at 37°C). The direct effect of temperature on cells is obvious, but the temperature will also affect the pH of the medium due to increased solubility of CO_2 at lower temperatures. The pKa of buffer and the degree of ionization of serum components is also affected by temperature. The pH of a typical medium at room temperature is around 0.2 units lower than at 37°C. Therefore, a room operating temperature solution at pH7.55 would be 7.31 when warmed to operating temperature. (HEPES is usually used in the range of 10 to 50mM.) At concentrations of more than 15mM the buffer is sometimes growth-inhibitory. Phenol red is used in small-scale culture as an indicator of pH but it can become toxic, especially in serum-free conditions. Therefore, for large-scale manufacturing, it must be avoided. The optimum operating temperature will be controlled around 37°C since this will simulate body temperature. Temperature is an environmental variable that can affect a variety of animal cell parameters such as growth, shear sensitivity, cell morphology.

2.5 Conclusion

Reviewing the literature has shown the possibility of using established equipment of stirred tanks and microcarrier technology to be a way forward for the use of culturing cells for tissue regeneration. The literature published about culturing conditions has provided a set of conditions which will be used in the technical experiments. The next two chapters describe the assays and experimental protocols used followed by results and conclusions of the technical investigations.

CHAPTER 3

MATERIALS AND METHODS

3.1 Introduction

This chapter serves to explain the assays and the general cell culture techniques used in the technical experiments carried out to test the feasibility of the culture of fibroblasts to develop a TE-product and to develop a scalable process for a primary human fibroblast cell-derived wound healing product. The cells used in all the experiments were kindly donated by Smith and Nephew RC, and are neonatal human dermal foreskin fibroblasts, which were from the Master Cell Bank used for Dermagraft production, frozen at passage 5. These cells have been through rigorous testing to demonstrate their safety and are free from adventitious agents. Where necessary, protocols written up for use are included in Appendix B.

3.2 Culture conditions

All cell culture, including media preparation was carried out in class II laminar flow biological safety cabinet. The operating media used was Dulbecco's modified Eagles medium (DMEM) with 10%(v/v) foetal calf serum (FCS). Additionally, there was a need to supplement the media and the following table shows the various amounts added. The various reagents and basal media were obtained from Sigma, UK.

Table 3.1 The required amount of supplements to add to the basal media

Supplements	Working Concentration	Stock concentration	Volume percentage
Foetal Calf Serum	10% (v/v)	Neat	10%
HEPES Buffer	20mM	1M	2%
L-Glutamine	2mM	200mM	1%
Penicillin/Streptomycin	50 IU/ml P	5000IU/ml P	1%
	50μg	5000μg/ml S	
Non Essential Amino acids	1%	100 x	1%

Glutamine keeps well as a dry powder however once made up into solution it must be kept frozen to prevent degradation. It is the most unstable of the essential amino acids and decomposes rapidly to form the pyrrolidine carboxylic acid and ammonia in solution. Additionally, many components of the medium cannot be heated together. Cystine and ascorbic acid cannot be autoclaved in the same solution, the ascorbic acid becomes oxidised and destroyed. Thus where necessary, medium or supplements were sterile filtered. Glucose and ascorbic acid are destroyed in alkali solutions. Therefore ascorbic acid was ordered in crystalline form for stability, and when needed, dissolved in the DMEM solution, and then sterile filtered through a 0.22 μm filter.

The incubator was set at 37°C and 5% CO_2. When resurrecting the cells from its cryo-preserved state, DMEM with all the supplements added in was used. It is important to avoid excessive alkalinity of the medium during the recovery of the cells. Thus prior to the addition of the vial contents, the culture vessel containing the growth medium was placed into the incubator for at least 15 minutes to allow the medium to reach its normal pH.

Some cell lines may undergo osmotic shock if a large volume of fresh medium is added too quickly to the cell suspension upon thawing. Several smaller volume stepwise additions (1 to 2ml each time) of fresh medium to the cell suspension at 20 to 37°C over a period of 10 to 20 minutes may improve their recovery and survival.

Passaging of cells occurred at a frequency of every 3 to 4 days depending on microscopic observation of flasks to avoid reaching overconfluency. Additionally media exchange would take place to ensure sufficient nutrients are supplied and waste is removed. See protocols in Appendix B.

3.2.1 Static cultures

Triplicate 25cm^2 flasks were seeded at 1.5 x 10^4 cells/cm^2, and maintained for 28 days. The cells were bathed in 5ml of media and for each time point flasks were either trypinsinsed to give a time point, or scraped using a cell scraper to give small lump of biomass to be analysed for collagen content. The media were collected for measuring metabolites levels and presence of growth factors.

3.2.2 Stirred tank microcarrier cultures

Cells were mainly grown in t-flasks and roller bottles to generate the required cell numbers required to inoculate the bioreactor. For stirred tank cultures, a 5L bioreactor (Sartorius, UK) was utilised at UCL, and a 3L (Applikon, UK) at York RC. The microcarriers tested were Nunc 2D microhex, Cytodex 2 and finally Vicryl discs. The nunc 2D microhex was cultured at a microcarrier concentration of 5g/L in 5L bioreactor for 28 days, after initial promising experiments in shake flasks. Cytodex 2 was carried out at a microcarrier concentration of 10g/L for 1L working volume culture in the 3L reactor and the Vicryl discs was at 1g/L at working volume of 1L in the 3L reactor as well. However, the spin filter on the Applikon reactor blocked, thus overall media working volume for Cytodex 2 and Vicyl discs were maintained at 1.5L.

The commercial microcarriers were prepared according to manufacturer's instructions. Briefly, Nunc Microhex was transferred via aseptic pouring or pumped into the reactor through a peristaltic pump. Cytodex 2 beads were hydrated in PBS and then autoclaved in the bioreactor, and then media rinses were used to remove the PBS and condition the

Cytodex microcarriers before use. Vicryl discs after hole punched and collected by picking it up using surgical forceps were collected into a glass jar and gamma irradiated to sterilize prior to use. These discs were then pumped into the bioreactor through a sterile inlet. The next following parameter to consider was to establish what suspension speeds are required for cell culture.

The flow regime within the vessel is crucial to ensure sufficient mass transport to the cells and although increased agitation promotes the transport this is offset by detrimental shearing forces (Cherry and Papoutsakis, 1988, Croughan et al., 1987, Lakhotia et al., 1992). Zweitering's correlation (Zweitering, 1958) was used to calculate the minimum suspension speeds to operate at based on the just suspension speed, N_{JS}.

$$N_{JS} = \frac{S\,\upsilon^{0.1}\,d_p^{0.2}\,(g\,\Delta\rho/\rho_L)^{0.45}\,X^{0.13}}{D^{0.85}} \qquad (1)$$

S = dimensionless constant accounting for impeller and reactor geometry
υ = kinematic viscosity (m^2/s)
d_p = diameter of a particle (m)
g = gravitational constant ($9.81 m/s^2$)
$\Delta\rho$ = density difference between the particle and the fluid (kg/m^3)
ρ_L = density of the fluid (kg/m^3)
X = weight of the solids/weight of the liquid x 100, dimensionless
D = diameter of the impeller (m)

Just complete suspension exists when all particles are in motion and no particle remains on the tank base for more than 1 to 2 seconds. Under this condition, all the surface of the particles is presented to the fluid, thereby ensuring maximum surface area is available for the cells in the fluid to attach and proliferate.

To calculate the maximum speed for the system, Kolmogorov microscale of isotrophic turbulence, λ, was used. According to Cherry and Papoutsakis, (1988) and Croughan et al. (1988) detrimental effects occur when the Kolmogorov scale for eddy size drops below $^2/_3$ to $^1/_2$ the diameter of the microcarrier. The interaction of microcarrier beads

only with eddies smaller than the microcarrier could result in shear stresses on the surface of the microcarriers that are harmful to the cells. Eddies larger than the microcarrier surround the microcarriers completely and may rotate or translate them without creating an excessive amount of stress.

The eddy concentration is proportional to $(\upsilon^3/\varepsilon)^{1/4}$ so relating the three equations allow the calculation of maximum speed.

$$\varepsilon = \frac{\upsilon^3}{\lambda^4} \tag{2}$$

$$\varepsilon = \frac{P}{\rho V} \tag{3}$$

$$N_i = \frac{P}{N_p \rho_L D_i^5} \tag{4}$$

where N_i = Impeller speed

N_p = Power number

ε = local rate of energy dissipation per unit mass of fluid

υ = kinematic viscosity

Additionally, from Zweitering's equation, the minimum suspension speed is seen to be affected greatly by the density difference, and Vicryl having a density of $1.3 g/cm^3$, means that it sinks quite readily, thus carboxymethylcellulose, (CMC), an inert polymer was added to the DMEM media to alter the viscosity of the media for the culture of cells on the biodegradable discs. This allowed the discs to suspend at a speed, which does not kill the cells. CMC did not affect the culture and was not metabolised by the cells. CMC has also been used as a viscosifier and bulking agent in the formulation of bioproducts, toothpaste and in the food industry. See Appendix B for the range of speeds chosen for the STR cultures.

3.3 Metabolite Analysis of the media

Key nutrients and waste products were monitored in the media, to ensure that the cells were being maintained and conditions were adequate. Starvation due to the depletion of glucose can lead to altered glycosylation patterns. The accumulation of waste products such as lactate and ammonia will affect the pH and can inhibit growth, for example, it has been reported the 3mM ammonia can inhibit hybridomas (Mercille and Massie, 1994). Additionally, the presence of growth factors released into the media was traced as it gave an indication of the potential bioactive component for wound healing. Vascular endothelial growth factor (VEGF) is the most soluble and abundant growth factor that is produced by fibroblasts thus this was the chosen growth factor to test. Amino acid analysis was carried out to see if at any time during the culture for the production of the tissue mass, were there any shortages of certain amino acids, which could act as a limiting step in the production of extracellular matrix proteins, e.g. collagen.

Ascorbic acid was also monitored to ensure that the concentration was at the right level and not toxic. Ascorbic acid was measured by means of reduction of the tetrazolium salt MTT [3-(4,5-dimethylthiazolyl-2,5-diphenazinium methyl sulphate) at pH 3.5 to a formazan. Thus to determine the level of ascorbic acid, in a sample blank determination only the L-ascorbate fraction as part of all reducing substances present in the sample is oxidatively removed by ascorbate oxidase (AAO) in the presence of oxygen. The dehydroascrobate formed does not react with the MTT/PMS. Then by taking the difference between the absorbance of the sample and the sample blank, gives the quantity of the ascorbate present in the sample. The ascorbic assay was a test kit purchased from R-Biopharm, UK, Cat. No. 0409677.

3.3.1 Glucose, lactate, glutamine, glutamate and ammonia

Glucose, lactate, glutamate, and glutamine were analysed offline, and measured in triplicates through a biochemical analyzer: YSI Analyzer 2700 SELECT. The glucose

and lactate concentrations from a sample can be obtained simultaneously, likewise, glutamine and glutamate. Table 3.2 shows the chemistry specifications:

Table 3.2 Chemistry specifications

Name	Detection range to	Calibration point	Precision CV, n = 10	Membrane working life (days)
Glucose	9g/L at 25 µl sample size	2.50 g/L	2%	21
Lactate	2.67 g/L at 25µl sample size	0.50g/L	2%	14
Glutamate	10 mmol at 20 µl sample size	5mmol	2%	7
Glutamine	8 mmol/L at 20µl sample size	5 mmol/L	4%	5

The enzyme glucose oxidase is immobilized onto the YSI dextrose membrane and the following reaction takes place:

$$\text{Glucose} + O_2 \xrightarrow{\text{glucose oxidase}} H_2O_2 + \text{D-Glucono-d-Lactone}$$

The enzyme L-lactate oxidase is immobilised in the YSI lactate membrane and the following reaction takes place:

$$\text{L-lactate} + O_2 \xrightarrow{\text{L-lactate oxidase}} H_2O_2 + \text{Pyruvate}$$

Ammonia accumulates throughout the culture, due to degradation of glutamine and is a waste product from metabolism as well. The ammonia assay is a spectrophotometric assay and takes advantage of the Berthelot reaction, where ammonia, hypochlorite and phenol react to produce a dye molecule indophenol blue in an aqueous solution. The concentration of the NH_3 can be determined by monitoring the absorbance of the dye molecule at λ = 640nm. The indophenol blue molecule is also subject to photodegradation, thus the reading is only stable for about an hour.

3.3.2 Vascular endothelial growth factor (VEGF)

The VEGF concentrations in the media were measured in triplicates through an enzyme-linked immunosorbant assay (ELISA). These assays use enzymes for detection and the most common ELISA is a noncompetitive 'sandwich' assay using 96-well plates precoated with the capture antibody. The plates were incubated with the sample to permit formation of the antibody-antigen complex. Then a second, enzyme labelled antibody was then used to tag the complex and the enzymatic activity was determined via a colorimetric reaction. The amount of antigen bound to the wells was determined from a standard curve of absorbance vs. log of antigen concentration. The kit to measure VEGF was purchased from RnD Systems (DuoSet ELISA development kit DY293B).

3.4 Cell Analysis

The analysis of the cells was carried out both qualitatively and quantitatively. This gave indications of the viability and cell yield.

3.4.1 Qualitative measures

Light microscopy was mainly used with the inverted microscope. However, in certain cases, confocal microscopy was used to obtain better images and this was used in conjunction with LIVE/DEAD stain of the cells cultured on the microcarriers. The LIVE/DEAD viability/cytotoxicty kit was obtained from Molecular Probes, Cat. L3224. Scanning electron microscropy was performed to certain tissue samples from the bioreactor culture to determine the level of coverage of cells on the microcarriers.

3.4.2 Quantitative analysis

Cell counts were measured using a haemocytometer for the static culture, but the reactor cultures, MTT assay was applied when cell counting was difficult via the haemocytometer.

The cell count measures the status of a cell culture at a given time and is essential when subculturing or assessing the effects of experimental treatments on cells. Most commonly used is the haemocytometer because it is inexpensive, accurate and versatile. Cell count is often expressed as the no. of cells per ml of medium or per cm^2 of area of attached surface. The Haemocytometer is a modified glass slide, which has been engraved with two counting grids of known areas. Each of the grids contains 9 squares, and each being $1mm^2$ in area. The haemocytometer is supplied with a glass coverslip of a precise thickness, thus when the coverslip is correctly positioned the volume of the liquid placed into the counting chamber is a known constant.

Viability counts for the haemocytometer method generally involve the dye exclusion test, which relies on the ability of living cells to exclude the dye and so the dead cells are permeable and the dye crosses the cell membrane. Note, however, this is really more of an indication of the integrity of the cell membrane but not necessary how the cell is functioning. The dye used is trypan-blue (Sigma, UK)

1. Use the average of the total cells counts to calculate N and derive the cell concentration as follows:

$$C = N_a \times D \times 10^4$$

N_a = average number of cells counted per $1mm^2$ square (cells per chamber divided by the number of squares counted)

C = unknown concentration of cells = cells/ml

10^4 = conversion factor to convert the volume over $1mm^2$ square to 1 ml.

D = dilution factor

2. For viable cell number or percent viability

$$\text{No. of viable cells/ml} = N_v \times D \times 10^4$$

N_v = number of cells unstained

D = dilution factor

$$\text{Percent (\%) viability} = \frac{\text{no. of cells unstained x 100}}{\text{Total number of cells}}$$

There are some precautions to bear in mind with cell counting, and these are that the more cells counted, the more accurate the cell count. Additionally, living cells that have been recently trypsinised for either subculture or thawed from a freezing medium containing dimethyl sulfoxide (DMSO) may have leaky membranes, thus causing them to take up the dye.

Another method of quantifying the cells is to use the MTT [3-(4,5-dimethylthiazol-2-yl)-2,5-diphenyltetrazolium bromide] assay (Mosmann, 1983). The MTT assay is based on the ability of a mitochondrial dehydrogenase enzyme from viable cells to cleave the tetrazolium rings of the MTT to form a formazan product, resulting in a colour change. The number of cells is directly proportional to the level of the formazan product. A modification of the MTT assay can also be used and is known as the WST-1 assay (available from Roche Diagnostics Cat. No.1664807). It does not need the final solubilising step and after incubation with the WST-reagent, the plate can be read straight away.

3.5 ECM analysis

This section looks at the assays involved that were used to try to estimate the level of extracellular matrix proteins produced both qualitatively and quantitatively. Collagen is the most abundant molecule so this was selected as the key marker to track. Neonatal dermal fibroblasts produce mainly of the type I form and some type III initially which is then converted to type I. Glycosaminoglycans (GAGs) are assayed as well.

3.5.1 Qualitative analysis

Immunostaining of the tissue sample for collagen was used to give a qualitative indication of the presence of collagen, and the areas of deposition. Fresh tissue mass samples were first rinsed with PBS to remove any media components and then cryopreserved using OCT compound and then snap frozen using liquid nitrogen. The cryopreserved samples were cryosectioned and prepared onto slides. The slides were defrosted just before the start of the immunostaining protocol. The protocol is described in Appendix B.

Additionally, samples were prepared for histology staining to determine the presence of collagen and GAGs. The samples for histology staining and SEM were dehydrated through an alcohol series from 10 to 100%, with gradual increments of 10%. For the histology staining procedures, the samples were then fixed in chloroform and then wax embedded. Then using the Leica RM2165 rotary microtome, sections were cut at 5μm thickness. Two sections were placed on each slide after being floated out on a water bath at 45°C. Then load the slides into the autostainer.

3.5.2 Quantitative analysis

Each α chain consists of about 1000 amino acid residues and is coiled into an extended, left-handed polyproline II helix and within a collagen triple-helical domain; there are three of these α chains which are in turn twisted into a right-handed superhelix. Collagen is a very stable protein and the stability is due to the hydrogen bonds in this triple helix, which is formed at every third residue of the α chain. Therefore, this amino acid residue has to be glycine since it cannot have side chains and so, the amino acid sequence of each α chain consists of about 300 Gly-X-Y tripeptide repeats, where X can be any amino acid residue and Y is usually proline or hydroxyproline. Additionally, since hydroxyproline is only found when there is collagen present, this mean that the content of collagen could be estimated based on an assumption that a percentage of collagen is hydroxyproline (Woessner, 1961). The oxidation of hydroxyproline to a pyrrole derivative will react with

p-dimethylaminobenzaldehyde (p-DAB) in an acid medium to give a coloured product. This colour can be enhanced with organic solvents. The assay was carried out in a 96-well microplate, and using a plate reader to determine the absorbance at 570nm. The tissue samples underwent a papain digestion prior to the hydroxyproline assay.

The dimethylmethylene blue (DMB) assay to measure the amount of sulphated glycosaminoglycans (s-GAG) also relied on the digestion of the tissue with papain solution followed by staining with dimethylene blue, the absorbance, which was then read in a spectrophotometer and translated into an amount by comparison with a calibration standard curve chrondroitin-4-sulfate.

This completes Chapter 3 which describes the various methods used and the next chapter presents the results from these experimental studies.

CHAPTER 4

OPERATIONAL EVALUATION OF THE PRODUCTION PROCESS OF AN ADVANCED WOUND HEALING PRODUCT

4.1 Introduction

Many tissue-engineered solutions for the treatment of chronic non-healing wounds depend on the delivery of cells to the injured site, e.g. Dermagraft (Smith & Nephew), Apligraf (Organogenesis) (Balasubramani et al., 2001). Although there have been very promising results in a laboratory set-up, large scale production of cell laden matrices is expensive and quality control is difficult to manage. An alternative approach is to design a frozen cellular-based bioactive matrix that is conductive and inductive of the key responses in the tissue cells surrounding the wound that affect the essential healing processes. This chapter explores possible methods for generating this bioactive matrix by culturing human dermal fibroblasts on microcarriers. This can then be reformulated into a gel or a bioactive patch for application.

The use of microcarriers as initial supports for cell growth has long been recognised. (Van Wezel, 1967). The benefits of using microcarriers for the culture of adherent cells include cost savings in labour, process consumables, and laboratory space. Using particulate culture gives a greater surface area to volume ratio, and allows for a high-density culture of cells with more effective use of media. In this chapter, the suitability of smooth, solid microcarrier discs and microporous microcarrier beads is assessed. Solid mcirocarriers typically allow for easier handling when washing and harvesting the cells from the carriers (Lundgren and Blüml, 1998). On the other hand, porous microcarriers

provide a larger surface area to volume ratio for cells to attach and deposit extracellular matrix (Ng et al., 1996). For regenerative medicine approaches, the use of a biodegradable microcarrier is particularly attractive, since product harvest is greatly facilitated; the cells and extracellular matrix (ECM) do not need to be stripped from the microcarriers (e.g. by trypsinisation) since the microcarriers will degrade leaving the bioactive matrix (Curran et al., 2005). Gorodetsky et al. (1999) demonstrated the use of fibrin microbeads as biodegradable carriers for the culture of cells for wound healing. Hence, this chapter also evaluated the potential of a biodegradable carrier.

Aggregation is often seen in extended microcarrier cultures with fibroblasts (Varani et al., 1996). This chapter explores when aggregation occurs and whether it results in a detrimental effect on the cell viability, for example, by creating creating diffusional limitations or localized build up of waste metabolites. On the other hand the interstitial spaces formed within the aggregates may facilitate deposition of extracellular matric and potentially trap growth factors. This will be explored in the chapter.

Section 4.2 presents the results of the static culture of these human dermal fibroblasts, and then identifies the extent of deposition of extracellular matrix by the cells. The results from the microcarrier studies are presented in Section 4.3 and this is compared to the static culture. The microcarriers studied were smooth polystyrene disks (Nunc 2D Microhex), crosslinked dextran microporous spheres (Cytodex 2) and finally, biodegradable Vicryl discs. Finally, Section 4.4 looks at equipment considerations for the large scale processing, and discusses the implications of the processing route suggested.

4.2 Static culture studies

This section outlines the key results from the static culture studies that were carried out using 25cm^2 t-flasks for 7 days, and 28 days using complete media. Preliminary growth curve studies were carried out first to determine the growth rate of the neonatal dermal fibroblasts and their morphology. Fig. 4.1 highlights the cell morphology as streaky, long

and narrow as expected. Fibroblasts have an elongated form which can exhibit a width of less than 5μm, in contrast to other cell types that often exhibit a diameter of about 8-15μm. As can be seen from Fig. 4.1 the fibroblasts initially attach and spread on the surface (Day 2) and by Day 5 they were found to be confluent and packing more densely. Thus when cells have reached overconfluency, the cells will be packed together very tightly. The specific growth rate was calculated to be $0.0127hr^{-1}$, i.e. a doubling time of 55hours, (similar to the 45 hours doubling time found by researchers at Smith and Nephew using the same cell line). Croughan et al. (1987) reported a specific growth rate of $0.016hr^{-1}$ for FS-4 fibroblasts on Cytodex 1 microcarriers. Confluency in the static t-flask generally yielded a minimum of $1x\ 10^5$ cell/cm^2 cell density.

a) b)

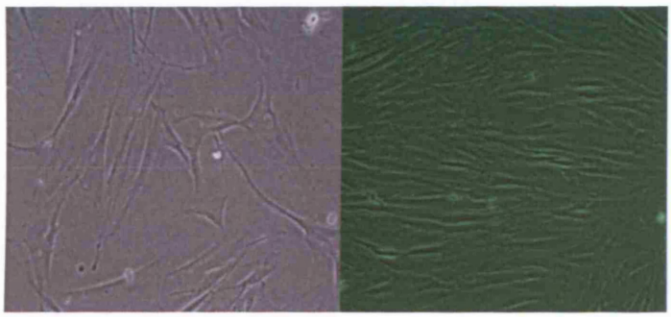

Day 2 Day 5

Figure 4.1 Light microscopy pictures of human dermal fibroblasts cultured in T-flasks at a) Day 2 and b) Day 5. A green filter was used in order to give better detail and contrast at Day 5.

The ratio of cells:ECM is an important indicator of productivity of the reactor. Here the ECM content was considered proportional to the collagen yield since collagen was considered to be the most abundant extracellular matrix protein. Collagen was found to require long culture times of 28 days for it to be detected quantitatively. Hence the static culture study was set up for 28 days to determine the cells to collagen ratio and compare it with the microcarrier cultures. In order to maintain the culture for 28 days, full media exchanges were carried out every 4 days using the low and high glucose media

respectively. Media samples were taken before and after each media exchanges to verify the glucose and lactate concentrations. Each flask was sacrificed each day to obtain a cell count, or scraped using a disposable cell scraper to harvest the biomass to check for collagen. Scraping was used rather than trypsinisation since the use of trypsin may destroy the extracellular matrix laid down (personal communication with N. Medcalf, Smith & Nephew RC, York). Fig. 4.2a shows the growth curves obtained and the cell densities achieved. This is comparable to values reported by Varani et al. (1985) where a maximum monolayer cell density of HuFFs at 2.4±0.8 x 10^5 cell/cm^2 cell density was achieved after a 20 day period.

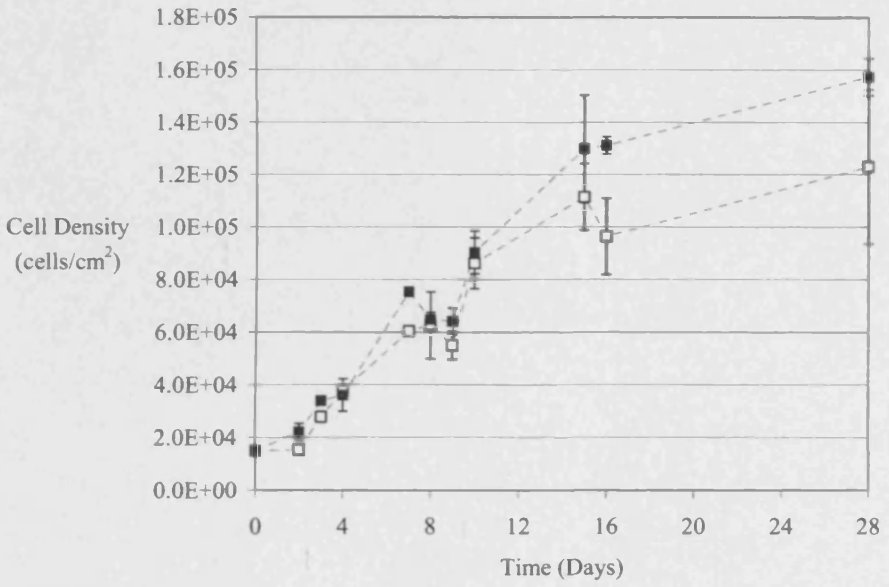

Figure 4.2 Growth curves of the static culture. Cells were seeded at 1.5 x 10^4 cells/cm^2, and cultured for 28 days. The conditions of high (4.5g/L) glucose (--□--) and low (1.0g/L) glucose (--■--) media were tested using replicate flasks.

The impact of using a high glucose media (4.5g/L) and low glucose media (1.0g/L) was investigated and the results summarized in Fig 4.2 to 4.4. From Fig 4.2 it can be seen that the glucose concentration does not significantly affect the cell growth rate. However, different consumption and production rates were observed as shown in Fig. 4.3.

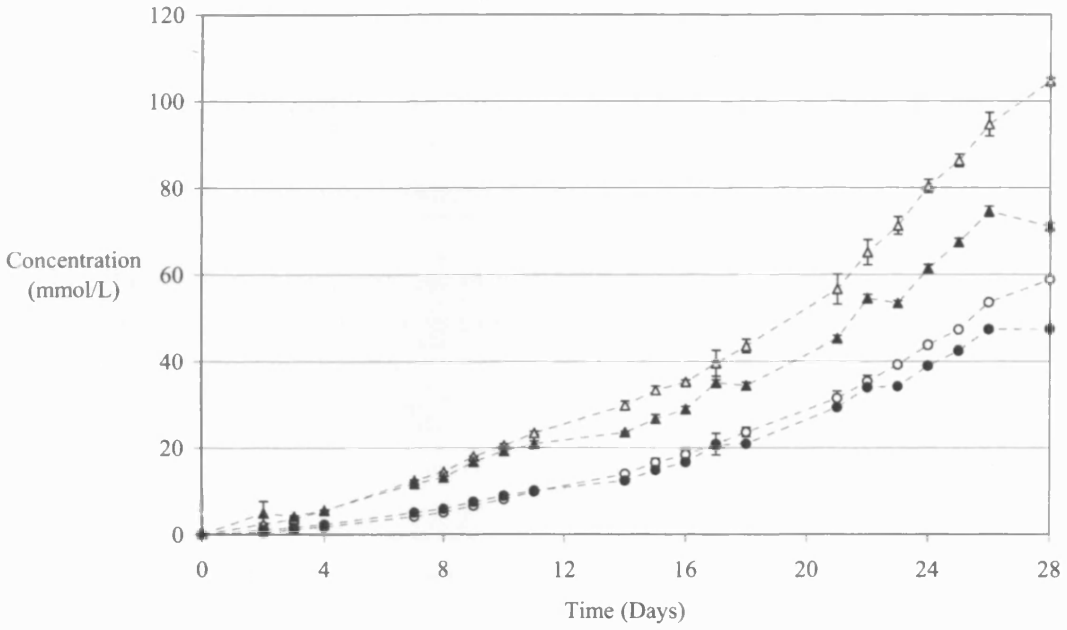

Figure 4.3 Cumulative glucose consumption and lactate production plots.
--○-- denotes glucose consumption, --Δ-- denotes lactate production in high (4.5g/L) glucose formulation. --●-- denotes glucose consumption, and --▲-- lactate production in low (1.0g/L) glucose formulation.

Translating the data into lactate production to glucose consumption ratios as shown in Table 4.1 indicated that low glucose media gave better control of lactate waste production. Therefore, high levels of accumulation of lactate in the media did not occur in the low glucose media compared to the high glucose media used.

The specific rate of production of ammonia and consumption of glutamine was not affected by the difference in glucose concentration, and subsequently gave the same ratio. The specific rate of production for VEGF corresponded to those reported by Pinney et al. (2000) of 0.5-4ng/24hrs/10^6cells for human neonatal fibroblasts cultured on a lactate-glycolate copolymer scaffold for 12 to 16 days.

Table 4.1 Summary of the metabolite analysis data for static culture of fibroblasts

High glucose DMEM media	
Specific glucose consumption rate (mmol/10^6cells/hr)	0.20
Specific lactate production rate (mmol/10^6cells/hr)	0.35
Lactate:Glucose molar ratio	1.7
Specific glutamine consumption rate (mmol/10^6cells/hr)	0.04
Specific ammonia production rate (mmol/10^6cells/hr)	0.02
Ammonia:glutamine molar ratio	0.5
Specific VEGF production rate (pg/10^6cells/hr)	10.02
Low glucose DMEM media	
Specific glucose consumption rate (mmol/10^6cells/hr)	0.13
Specific lactate production rate (mmol/10^6cells/hr)	0.19
Lactate:Glucose molar ratio	1.5
Specific glutamine consumption rate (mmol/10^6cells/hr)	0.05
Specific ammonia production rate (mmol/10^6cells/hr)	0.02
Ammonia:glutamine molar ratio	0.5
Specific VEGF production rate (pg/10^6cells/hr)	13.42

This indicated that a more optimal feeding strategy could be implemented in the manufacturing, by the use of low glucose media and a concentrated glucose solution addition; this will give rise to a reduced need of media exchanges to remove the waste products and replenish the nutrients. This, in turn will allow the growth factors to accumulate to a higher concentration in the culture. Additionally, a more efficient usage of media is possible and can contribute towards lowering the cost of culture in manufacturing. The most efficient culture for manufacturing would be to operate in fed-batch mode during the growth phase, and then switch to perfusion mode to maintain the culture from stationary phase onwards; this approach was adopted in microcarrier culture studies.

The spent media from the static flasks were also checked for levels of vascular endothelial growth factor (VEGF), and this is presented in Fig. 4.4

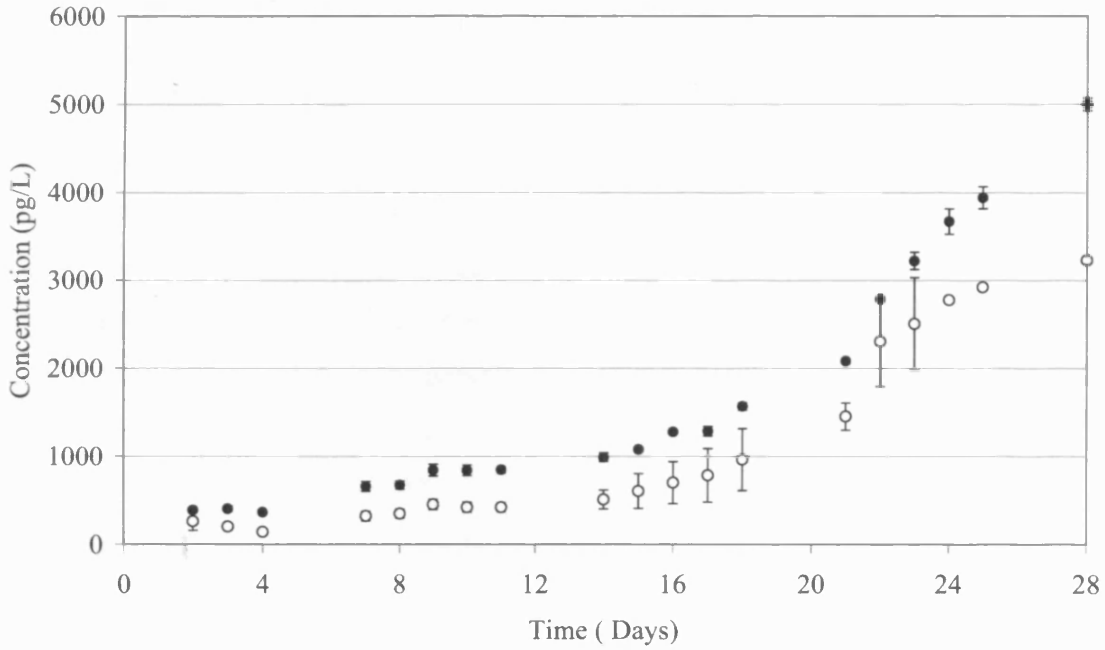

Figure 4.4 Cumulative VEGF production in the static t-flask culture. --○-- denotes VEGF levels in the high (4.5g/L) glucose fed flasks, and --●-- denotes VEGF levels in low (1.0g/L) glucose fed flasks.

The level of VEGF accumulated to an overall level of 1000pg/ml in the media samples during the first week of culture, and from the Day 1, it was produced. As VEGF is the most abundant growth factor in the media, this would be easier to detect. Fig 4.4 indicated that VEGF is produced throughout the culture period. The results suggest that the lower glucose concentration of 1g/L encourages a slightly higher production of VEGF throughout the culture period than the 4.5g/L glucose concentration. Literature reports differ in their findings on the relationship between glucose concentration and VEGF production. Reports with similar trends to those presented here include Sone et al., (1996), who found for bovine retinal pigmented epithelial cells that VEGF production significantly increased when glucose concentration decreased from 5.5 to 0.5mM; however, no change was found when glucose concentration decreased from 33 or 16.5 to 5.5mM. Additionally, Noriko et al., (2002) found that prolonged culturing under high

glucose conditions led to impaired growth rate and lower VEGF levels. In contrast some authors (Omori et al. 2004, Williams et al. 1997, Kim et al. 2000) have cited that high glucose concentrations induce higher VEGF production for many other cell types.

The deposition of collagen over time with the low and high glucose media is illustrated in Fig. 4.5. When a cell density of 10^5 cells/cm^2 was achieved, the cells were deemed to becoming over confluent and from Fig. 4.5, collagen production in static culture did not really start until the cells were confluent. The hydroxyproline assay was used to determine the amount of collagen present. Fig.4.5 indicates that this is a time-dependent process and that to get a detectable amount of cross-linked mature collagen requires a culture period greater than a month.

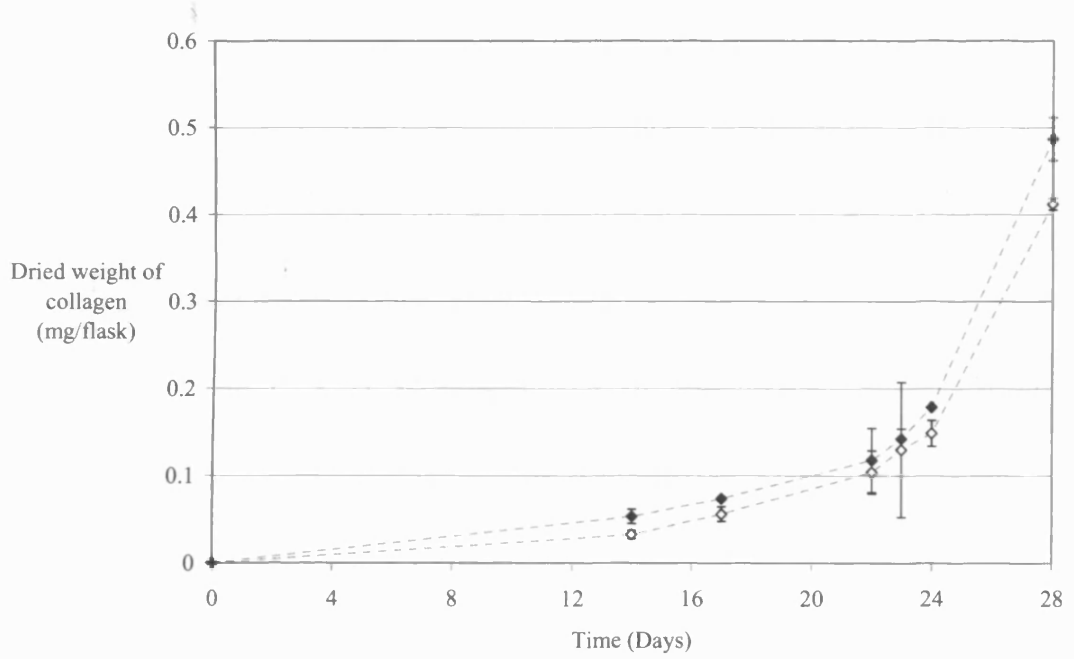

Figure 4.5 Production of collagen in the static t-flask culture. --◊-- denotes production of collagen in the high (4.5g/L) glucose fed flasks, --♦-- denotes the low (1.0g/L) glucose fed flasks.

This behaviour has been reported for mouse fibroblasts by Goldberg and Green, (1964) and they showed that collagen could not be detected during the log phase, and upon start

of stationary phase the collagen begins to accumulate. Indeed, they reported that significant quantities of collagen production were detected around Day 22. Examining the yield of collagen in static culture to the number of cells present gave an indication of cells to matrix ratio of 3:5. This piece of information was then used for the economic study and forms the basis to some of the assumptions made in the case study presented in the subsequent chapters. Fig 4.5 also seems to suggest that the fibroblasts fed with low glucose media produced higher levels of collagen than those fed by high glucose media. Although the presence of ascorbic acid helps to stimulate the collagen and proteoglycans production but according to Fisher et al. (1991), this effect is inhibited by glucose at a concentration of 25mM. Thus as both the low and high glucose fed flasks had ascorbic acid addition, the higher levels seen in the low glucose condition was attributed to this. Thus for manufacture, the optimal level of glucose concentration to maintain log phase would be 1g/L.

4.3 Microcarrier culture studies

The growth characteristics of fibroblasts and the production of ECM were explored on different types of microcarriers: smooth, microporous and biodegradable (Table 4.2). Commercial carriers were then examined and two types of microcarriers were selected for comparison: a non-porous carrier, Nunc 2-D Microhex, and a microporous carrier, Cytodex 2. The Nunc Microhex was tested first, since the material is similar to tissue culture plastic, thus the attachment kinetics and cell proliferation were assumed to act in a similar manner. Nunc Microhex is supplied sterile, thus the microcarriers were transferred into the culture aseptically.

Cytodex 2 was tested since the micro-porous nature of the microcarrier is expected to contribute towards the attachment and proliferation of the cells (personal communication with production engineer, Mark Baumgartner, Smith & Nephew, La Jolla). Additionally, the microporous nature also molecules of up to molecular weight of 100kDa to penetrate this microporous layer, thus this encourages the cell to secrete the adherent materials to ensure attachment (Lundgren and Blüml, 1998). This was supplied as a dried powder,

which required hydration and sterilization prior to use. As it was autoclavable, this makes it quite an attractive choice for commercial manufacturing. Cytodex 2 is made from cross-linked dextran, the microcarrier can be degraded away by dextranase quite effectively. Thus after the culture, the microcarrier can be removed through enzymatic digestion and centrifugation to retain the biomass (Lindskog et al., 1987).

It would be ideal to have a biodegradable microcarrier, but currently there is not a commercial one available. Therefore, as it is known that cells proliferate well on Vicryl mesh, which is biodegradable and biocompatible, 2mm disks were made by hole-punching the mesh, and then using forceps, placed into a preweighed glass vial. Vicryl mesh will start the degrading process if wetted, thus the work surface for hole punching was first wiped with 70% ethanol, and allowed to dry before hole punching began. This was then gamma sterilized before culture. Clearly, from a manufacturing perspective, to spray dry the polymer to form microspheres would be the more suitable method to produce the required biodegradable microcarriers.

Table 4.2 Properties of the microcarriers used in the culture

Microcarrier	Material	Density	Surface Area $cm^2 g^{-1}$	Shape and Size range
2D-Microhex	Polystyrene	1.05	760	Regular hexagon, side length =125 μm, 25 μm in thickness
Cytodex 2	Cross-linked dextran, with positively charged trimethyl-2-hydroxyaminopropyl groups at the surface	1.04	4400	Spherical, micro-porous Diameter = 114 - 198 μm
Vicryl Mesh	PGLA	1.3	N/A	Diameter =2mm circular disc, porous, thickness = 0.016cm

4.3.1 Nunc 2D Microhex culture

Nunc 2D Microhex carriers were first utilised to determine if the dermal fibroblasts could grow on microcarriers. Experiments were carried out in 125ml shake flasks initially (in the incubator at 37°C, 5% CO_2), and the cells that were attached were trypsinised to

enable viable cell count to be determined. Initial stirring speed of 45 rpm to set on the shaker plate to just suspend the carrier, and after attachment this was raised to 55rpm during the shake flask culture. Fig.4.6 shows the dermal fibroblasts were able to attach and proliferate to form clumps. The cells still retain their morphology and it was observed that when the carriers reach confluency, the carriers become much more opaque. The presence of empty carriers was still seen at Day 9. Some dead cells were observed to be present in the supernatant, and it was considered that these could be cells that failed to meet the microcarrier and attach onto it. Since cells meeting microcarriers in suspension is considered to be a random event, it is quite likely, that if the cells have not attached within the first 24hrs of inoculation they will die. These shake flask cultures showed that the cells were able to attach and grow as presented by Fig.4.6, thus bioreactor runs were then attempted.

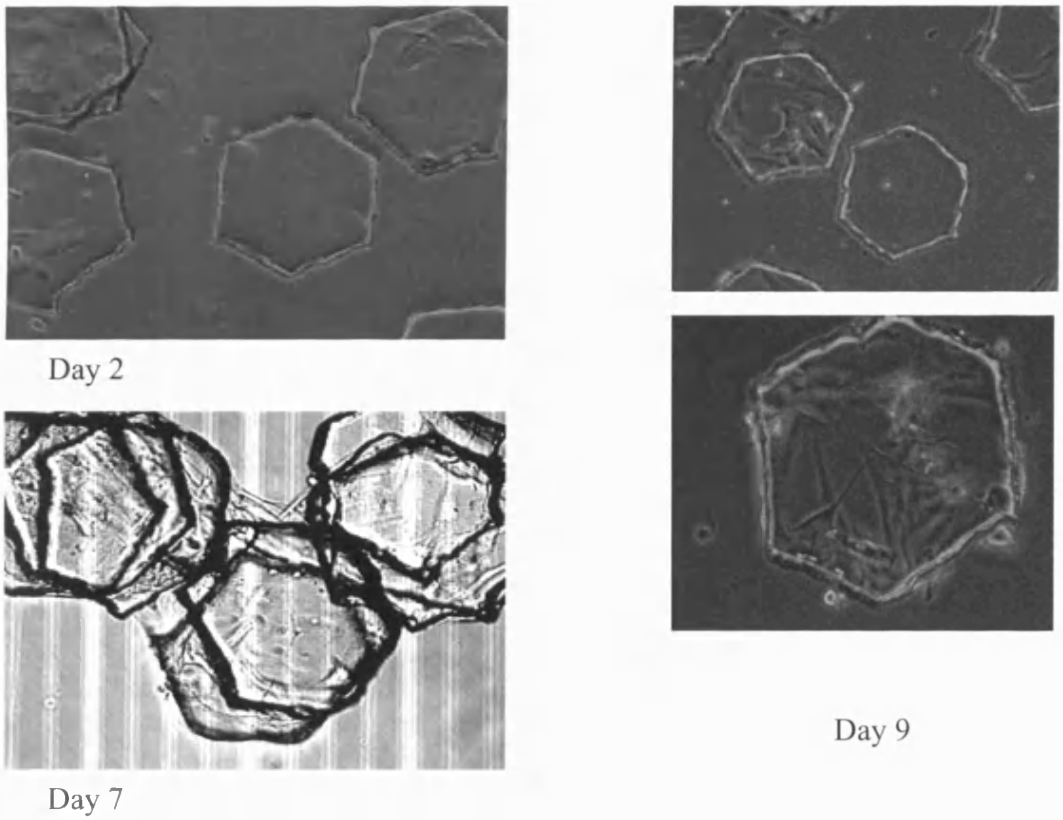

Figure 4.6 Light microscopy picture showing the dermal fibroblasts attached and proliferating on the Nunc 2D Microhex, Day 2 (initial attachment), Day 7 proliferate to stick together to form clumps and Day 9 of the shake flask culture.

Bioreactor runs using Nunc 2D Microhex carriers indicated that the cells were not able to proliferate well and accumulate extracellular matrix, and plenty of empty carriers were observed (See Table 4.3 for summary of results comparing the static and various STR cultures).

Further microscopy showed that straight scratches were sometimes seen on the flat 2D microcarriers and this led to the speculation that cells attached to the carriers could be sheared off as the microcarriers slid over each other. Furthermore, since the cells growing on the surface are exposed, they are more susceptible to turbulence created by the rotating impeller. Analysis showed that significant quantities of collagen could not be detected. Thus although these experiments served to show that particulate culture with dermal fibroblasts was possible, it was concluded that this was not a suitable microcarrier for cell expansion or extracellular matrix production. Varani et al. (1985) reported that the substrate surface affected the morphology and growth characteristics of microcarrier cell culture.

The next section investigates the potential benefits of employing a microporous carrier to overcome the limitations seen with the Nunc carriers.

4.3.2 Cytodex 2 culture

Cells were resurrected and expanded from RBs initially, and then subsequently inoculated into the STR at 4.5 x 10^3 cells/cm^2. This initial low starting cell density helps to control the aggregation that takes place when culturing dermal fibroblasts on microcarriers. The culture time was 34 days. The reactor used was 3L and operated at 1L initially, and then eventually fedbatched to 1.5L. Stirrer speed increased from 60rpm to 80rpm over time, as the aggregrates got bigger. Temperature of 37°C was maintained using a heating jacket, and a mixture of complete high glucose and low glucose DMEM was used. When lactate levels reached above the 1g/L mark, perfusion was started. However, after 2 days of perfusion culture, the spin filter blocked, thus, it was decided to

operate using 0.75L media exchanges, by allowing the aggregates to settle and pump out the spent media. This was carried out based on the monitoring of glucose concentration, thus when glucose was below 0.5g/L, 0.75L of media exchange took place. The culture with Cytodex 2 carriers showed that the cells were able to proliferate as can be seen from the light microscropy pictures and the LIVE/DEAD staining in Fig 4.7 and 4.8. Additionally, for prolonged culture, extracellular matrix was laid down and collagen was detected, as can be seen qualitatively, from Fig.4.9 and 4.10. There was some distortion of the spherical nature of the microcarrier following the immunostaining protocol as can be seen Fig. 4.9. This was partly due to the snap freezing by liquid nitrogen. Again, the distortion of the spherical nature of the microcarriers was observed, in the histological stains in Fig 4.10 due to the dehydration required for the histology staining during the sample preparation. The microporous nature of the microcarrier can be seen to have absorbed more of the histological staining.

The better growth characteristics on the Cytodex 2 microcarriers was partly attributed to the spherical nature of the microcarriers which probably caused less sliding and shear effects upon the cells compared to the Nunc Microhex culture. The microporous nature of the carriers also facilitated the deposition of matrix proteins thus increasing the strength of adherence.

Cellular morphology was examined by scanning electron micrograph (SEM) and revealed the presence of three dimensional multicellular aggregates consisting of cell covered Cytodex 2 beads all bridged together. The substantial aggregation involving the cells and the beads can be seen very clearly by the SEM pictures that were taken as shown by Fig 4.11. This shows that the fibroblasts have been deposited in the voids and that the outer surfaces of the beads still have some empty areas.

Fig 4.12 a and b show that the dense growth of the cells; the extracellular matrix laid down on Cytodex 2 beads indicated presence of channels throughout this lump of tissue. This helps to support the thinking that there were no transfer limitations or nutrient

starvation. Furthermore apoptosis was not observed and the ratio of lactate to glucose of 1.1 further supports this since values close to 1 indicate aerobic cell metabolism.

a)

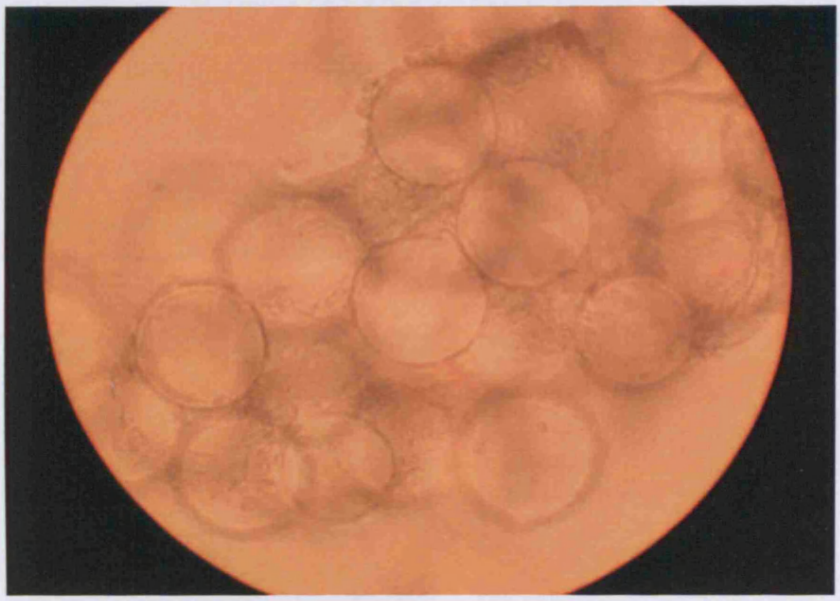

b)

Figure 4.7 Light microscopy pictures of fibroblasts on Cytodex 2 spherical beads, at x10 magnification at a) Day 18 and b) Day 25.

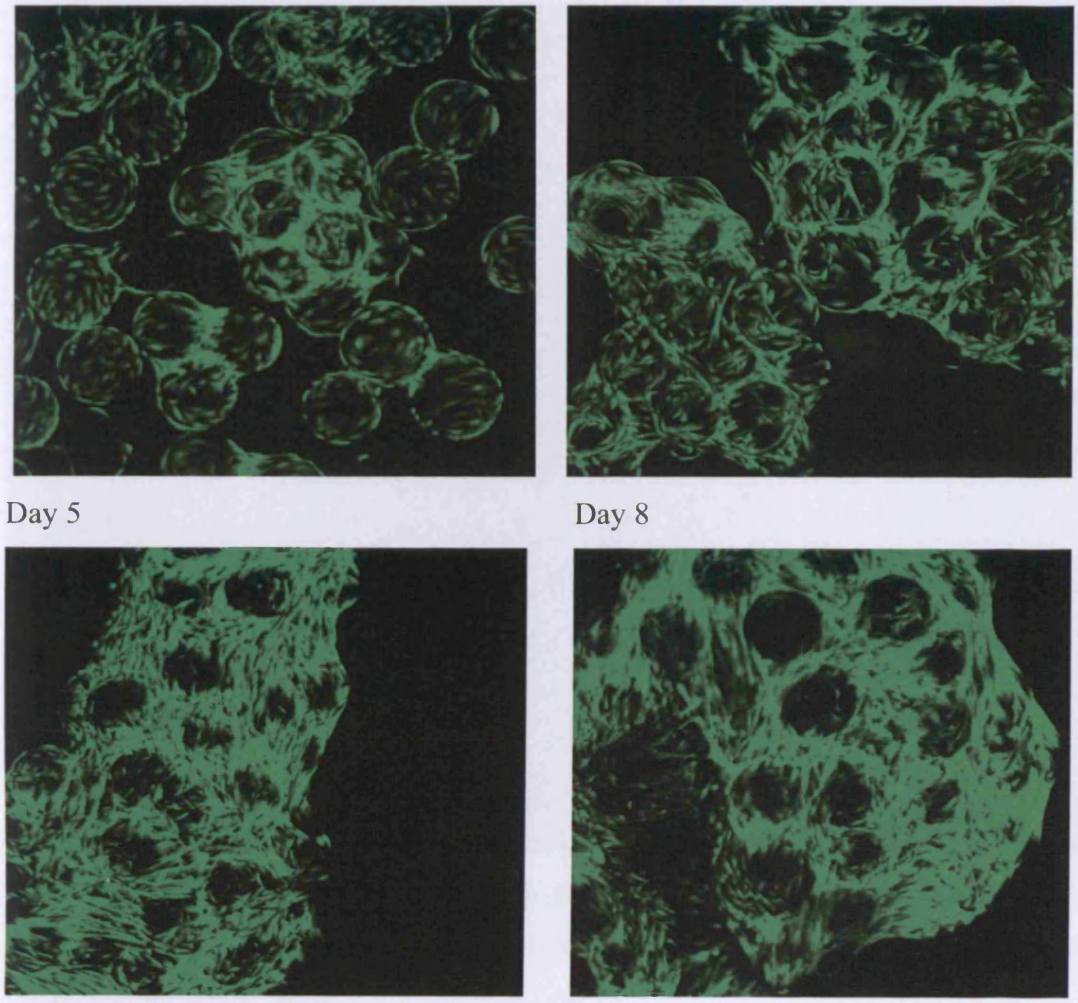

Figure 4.8 LIVE/DEAD staining of fibroblasts on Cytodex 2 beads at Day 5, 8, 28 and 34. Green indicates the cells are alive, and red indicates dead cells.

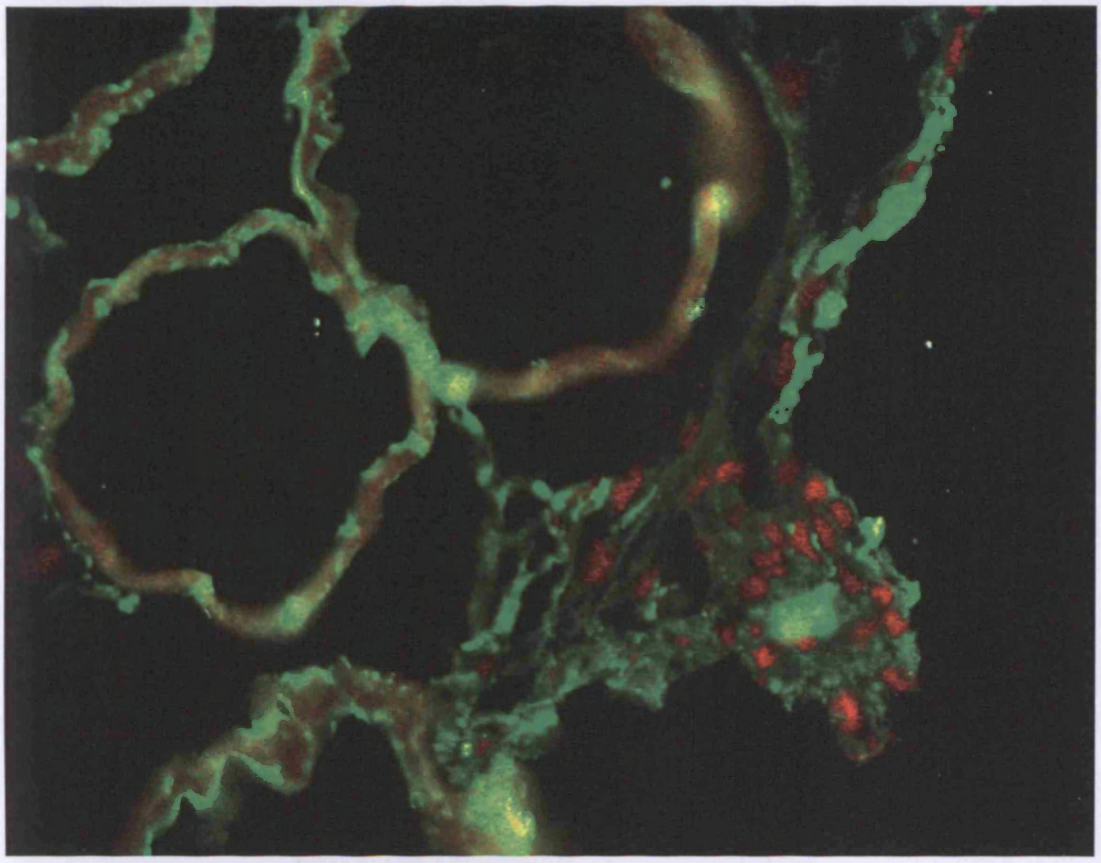

Figure 4.9 Immunostaining of Cytodex 2 microcarriers and cells to show where the collagen is laid down. Green fluorescence shows the presence of collagen and the red is the propidium iodide stain for the cells at Day 28.

a)

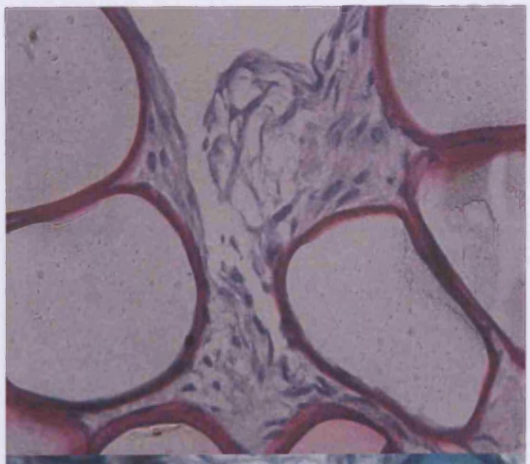

b)

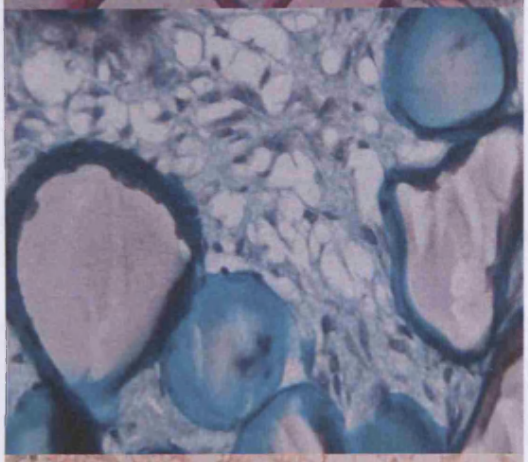

c)

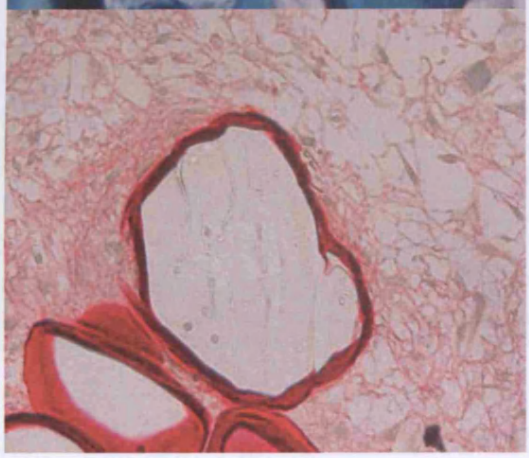

Figure 4.10 Histological stains to show the presence of cells, and ECM being laid down surrounding the microcarriers. All taken at x 20 magnification, at Day 34 using light microscropy. a) H&E stain to show the cells and the architecture of the tissue. b) The stain for GAGs, and c) Sirius red stain for Collagen.

a)

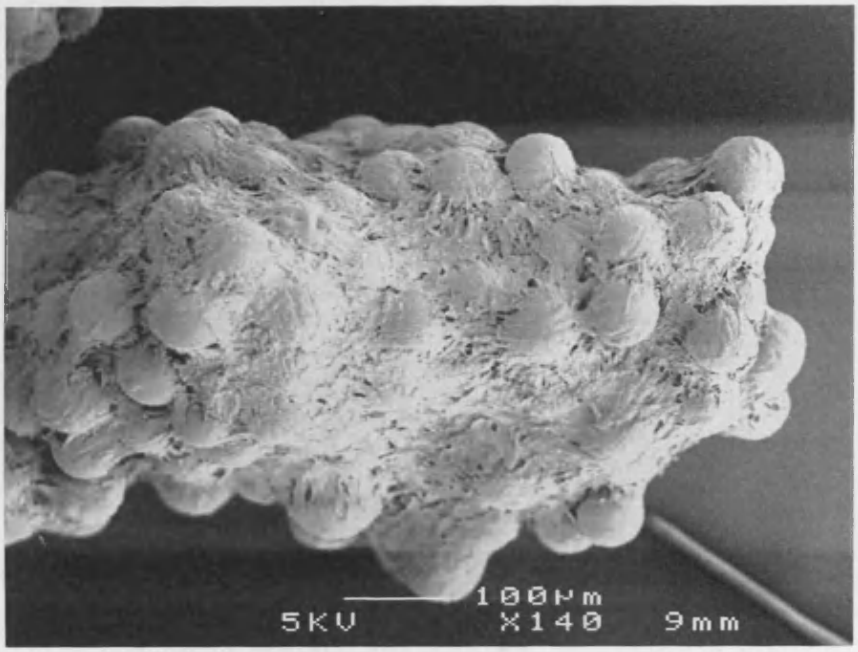

b)

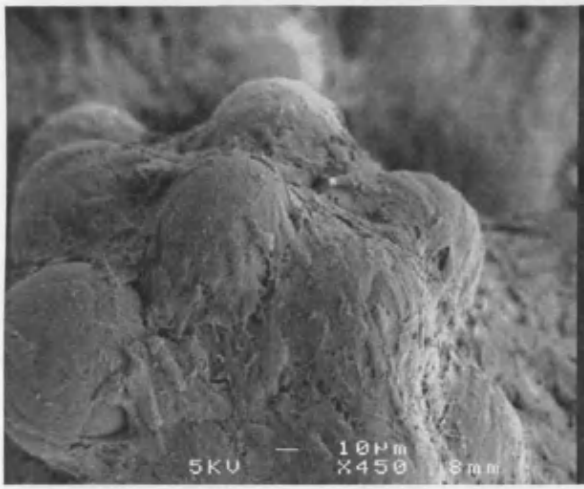

c)

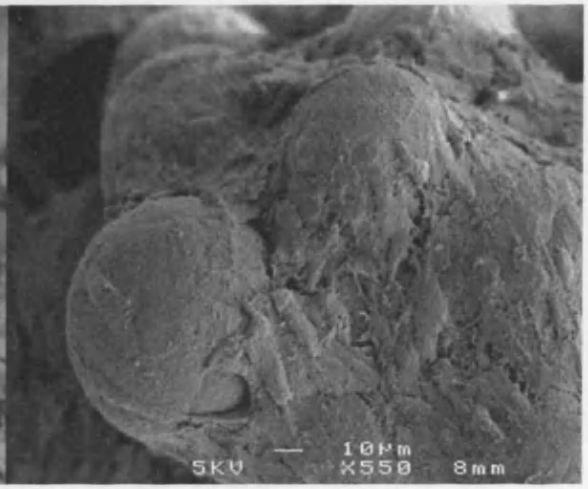

Figure 4.11 SEM pictures showing the aggregate of Cytodex 2 beads and cells grown in the STR with increasing magnification.

a)

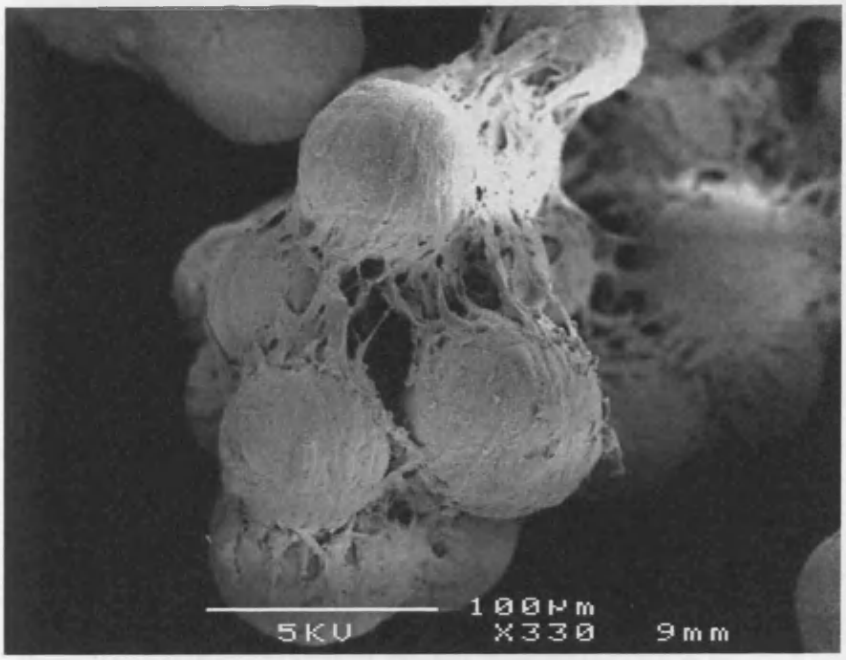

b)

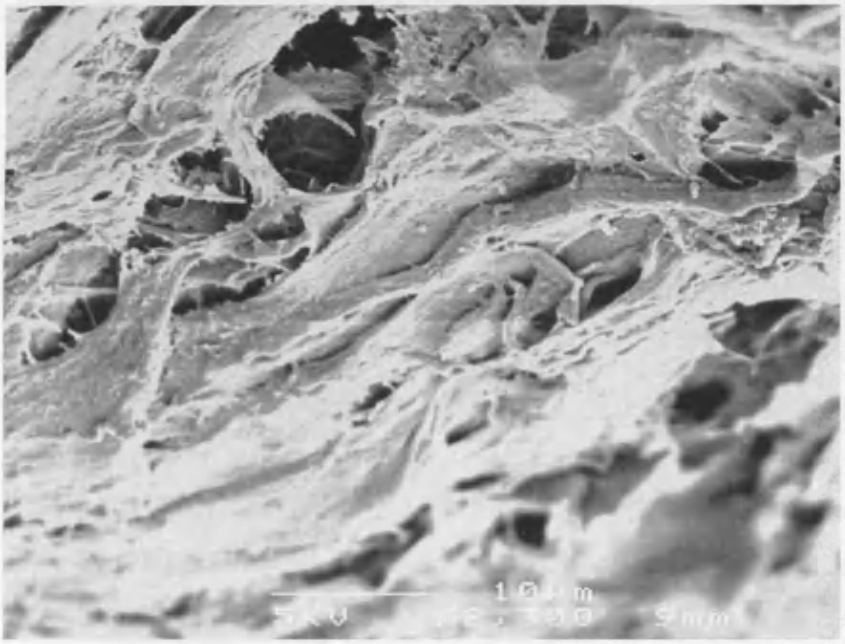

Figure 4.12 SEM pictures to show a) loose aggregate of cells and Cytodex 2 beads, b) the cells and extracellular matrix laid down. Clear fibrils can be observed.

It was concluded that Cytodex 2 would be a suitable candidate for the process as the cells proliferated and over the course of culture were able to secrete extracellular matrix as the cell clumps and beads got larger and heavier. Dextranase can be used to dissolve the carriers leaving only cell clumps which could be harvested using centrifugation or tangential flow filtration. The spent media could be concentrated using ultrafiltration to give a rich cocktail of growth factors to use in the formulation to enhance the bioactivity of the gel. Thus for manufacturing, the growth factors could be concentrated, and then diafiltered into a stable buffer to produce a spray to be used in conjunction with the gel, or simply sold off for cosmetic use.

A simpler and neater manufacturing approach would be to adopt a biodegradable microporous microcarrier; this would avoid the need and potential damage and loss in yield caused by the use of enzymes in between the transfers during the cell expansion and also for the final harvest. Ideally, the biomaterial of the microcarrier would be engineered to last the period of culture, thus harvesting the cells could be carried out easily by a simple centrifugation step of the contents of the bioreactor. As Dermagraft was grown on Vicryl mesh, it was decided to purchase the mesh and hole punch to create discs for the cells to proliferate upon due to the constraints of time and resources of the project, rather than spray drying to make biodegradable porous PGLA microspheres.

The next section describes the culture of a biodegradable microcarrier.

4.2.4 Biodegradable culture

Vicryl discs were seeded into a 3L bioreactor at 1L working volume, and eventually to 1.5L maximum working volume. This culture was seeded at a higher cell density of $3.8x10^5$ cells/cm^2, in order to shorten the time for the cells to reach confluency over the carrier and thus shorten the culture time to 21 days. Settling of the vicryl discs laden with cells occurred constantly, and the stirring speed was raised to 80 rpm intermittently to ensure movement of all the discs with cells to avoid merging into one very large aggregate.

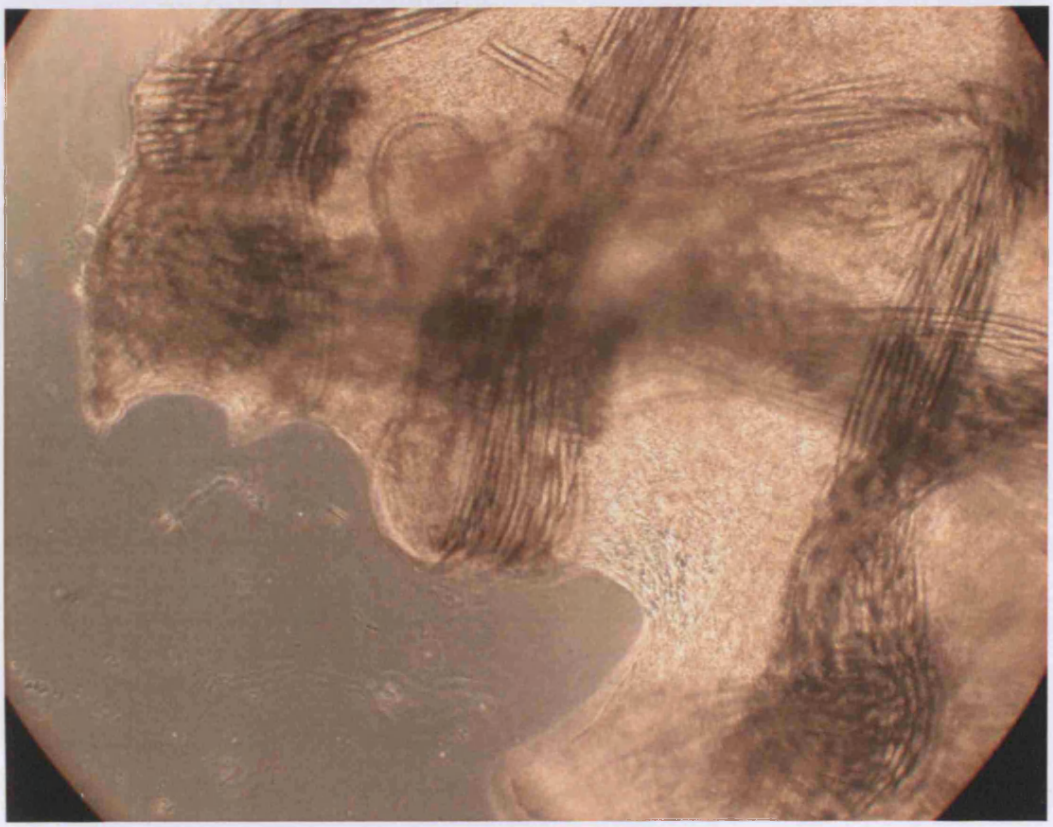

Figure 4.13 Fibroblasts cultured on Vicryl mesh discs in a 3L bioreactor. Light microscopy at x40 magnification.

Light microscopy showed that the cells grown in the reactor were able to attach and proliferate on the Vicryl mesh discs, and also acted in the similar manner observed for Dermagraft which was that the cells were able to fill in the gaps of the mesh. This can be observed clearly in Fig. 4.13 where the fibers of the mesh can be seen very clearly, and the cells have covered the disc. Fig. 4.14 shows the immunostaining of the collagen deposited after 15 days. This culture was maintained for 21 days and then harvested since previous degradation studies carried out by Smith and Nephew RC indicated that the Vicryl degrades completely after this period making it difficult to obtain tissue samples for immunostaining. Without the rigidity of the mesh fibers, the cell mass formed at this stage is too premature and can dissolve and disintegrate into the media supernatant.

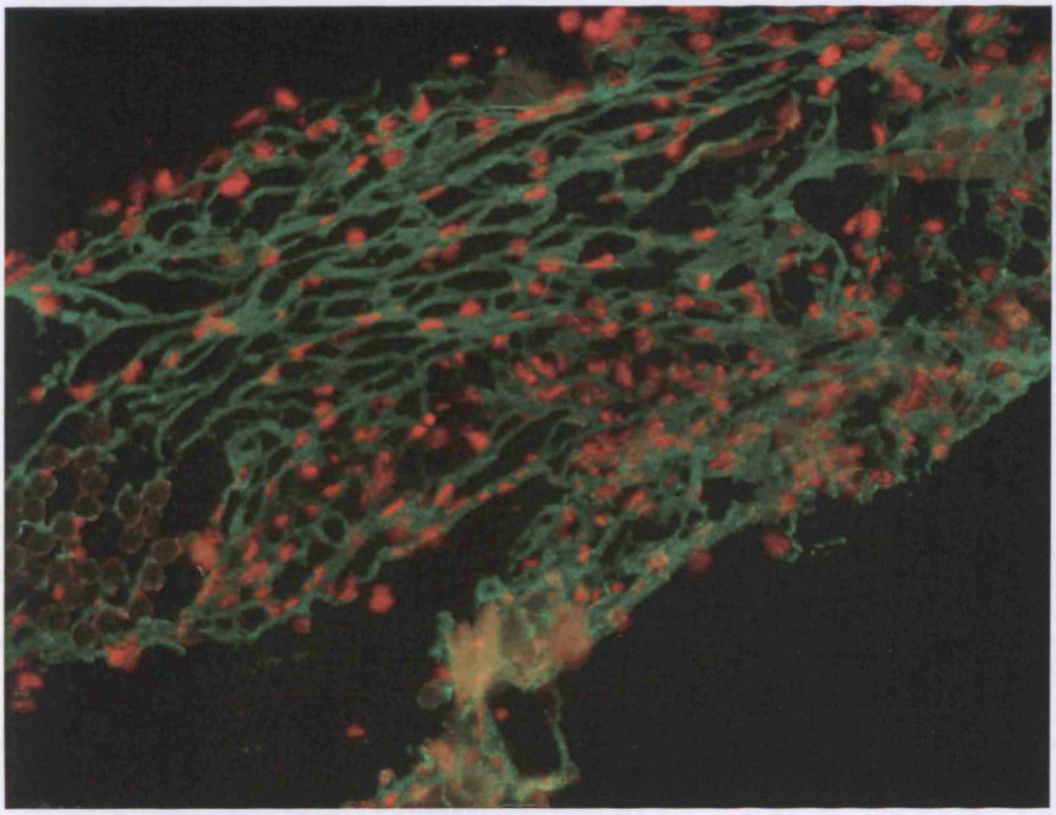

Figure 4.14 Immunostaining of the Vicryl disc culture. The green is where the collagen has been deposited and the red is the propidium iodide stain for the cells. Immunostaining and the confocal microscope were utilized to take the picture.

Table 4.3 summarises the key results and highlights the differences between the static and the stirred tank (STR) cultures. Neves et al. (2005) showed that for fibrochrondrocytes the stirring-induced mixing was able to increase the deposition of GAGs and collagen for cartilage constructs. Thus it can be observed there was more deposition of collagen with the STR culture when compared to the static culture. (An additional 3 x 5ml t-flask static culture was cultured and maintained alongside the stirred tank culture with the Cytodex 2 beads and harvested at the same time, and the collagen content of this was similar to the 28 days static culture. These cells in the t-flasks were kept and maintained initially to serve as a check that the cells for inoculation were fine in the event the STR culture failed due to a contamination. The biodegradable discs had lower collagen content because they were not cultured for 28 days. Most of the collagen deposition only really takes

place after 4 weeks into culture, as it becomes sufficiently crosslinked to enable detection using the hydroxyproline assay.

Table 4.3 Summary key metrics for the static and STR cultures

	Static culture	Bioreactor culture (Nunc)	Bioreactor culture (Cytodex 2) 10g/L	Bioreactor culture (Vicryl discs) 1g/L
Seeding density (cells/cm^2)	1.5 x 10^4	1.0 x 10^4	4.5 x 10^3	3.8 x 10^5 *
Final cell density (cells/cm^2)	~1.5 x 10^5	~1.9 x 10^4	~7.54 x 10^4	~5.9 x 10^5 *
Collagen yield % of biomass	7%	N/A	17%	3%
VEGF levels (pg/ml)	400-1000	~1800	~2500	~2000
Overall Lactate/Glucose ratio	1.5 (low gluc) 1.7 (high gluc)	2.8	1.1	2.3
Overall Ammonia/Glutamine ratio	0.5	1.4	0.1	0.9
Duration Time (days)	28	28	34	21

[* the surface area for growth is based on nominal surface area (π x d^2/4). 1g in total of 2mm diameter disks was used. Approximately 1875 discs were used in total.]

The results showed that the STR cultures have higher levels of VEGF than static culture, and this phenomenon is similar to what has been reported by Pinney et al. (2000), where the investigators found the presence of VEGF mRNA was 22-fold greater in three-dimensional cultures compared to monolayer cultures. This can be attributed to more efficient media usage, as the STR cultures have more cells per media volume than the static cultures. Table 4.3 also shows that a similar 10-fold expansion of cells was achieved for both the static culture and the bioreactor Cytodex 2 culture.

Table 4.3 indicates the ratio of waste products to substrates as lactate to glucose and ammonia to glutamine. Having the lactate/glucose ratio closer to one meant the culture was operating in the more aerobic region, and probably that the nutrients were consumed and eventually incorporated into the production of extracellular matrix rather than just waste products, lactate and ammonia. This was observed in the Cytodex bioreactor culture and to a lesser extent in the static culture. Values above 2 typically indicate anaerobic metabolism.

The high lactate/glucose ratio for the Vicryl seemed to indicate the possibility of oxygen limitation however there was sufficient oxygenation as the culture had intermittent sparging to maintain DO. Thus with the intermittent sparging and the higher ammonia/glutamine ratio, this indicated that the cells were probably exposed to more stressful conditions than the Cytodex culture. As CMC was utilized to increase the viscosity of the DMEM media to allow suspension of the Vicryl discs this probably increased the diffusional limitations thereby contributing to the higher ratios for the Vicryl culture. Thus this implies the importance of having density that is only slightly heavier than water, so the microcarriers both suspend easily and settle readily. This also implies that altering the viscosity of the media utilized alters the diffusivity profiles of the nutrients, thus for scaling up this would not be ideal, as diffusional limitations are more likely to be compounded upon scale up.

4.4 Proposed process for generation of biomass

4.4.1 Introduction

This section is a summary of what the proposed process could be for the generation of biomass consisting of cells and extracellular matrix. It will then discuss some of issues and limitations in scale-up that should be considered and explored further. Thus from the experimentation, two process culture routes are possible, whereby the first is to utilise the commercially available Cytodex 2 microcarriers and subsequently include an incubation

step with the dextranase enzyme to remove the microcarriers, followed by a centrifugation or filtration step to harvest the biomass generated. The second would be to culture the cells on the biodegradable Vicryl mesh formed as beads and harvest the entire lot to formulate into the gel, thus minimising the level of purification required. Vicryl has been used as medical sutures, thus biocompatibility is not as much of an issue, and indeed could form part of the formulation. There would be necessity to control the pH of this formulated gel, as the degradation of the polymer could cause a pH drop, and this could inhibit the bioactivity of the biomass gel. Tatard et al, (2005) proposed the use of PLGA microcarriers coated with adhesion molecules for cell therapy, and demonstrated the use of these microparticles for PC12 cells. Fig. 4.15 shows the process flowsheets that are proposed. Advantages and disadvantages of each route are discussed in the following sections.

4.4.2 Processing Issues and Equipment Considerations

Process route (I) is more complicated and (II) has less steps. However, the fermenter culture for route (I) is easier to operate as Cytodex 2 microcarriers suspend better. Additionally, as the Cytodex 2 microcarriers are autoclavable sterilizing in situ is an attractive advantage in comparison to route (II). It would be necessary to characterize the biodegradable characteristics of the microcarrier first so as to allow sufficient control of process (II) to ensure the correct harvest time. This is balanced by the fact that Process (I) needs studies to characterize the amount of dextranase required and time of incubation to degrade away the dextran, and then a rinse and centrifugation to remove the enzyme.

The maximum size of reactor would be the 1000L as any bigger size would probably require too long a cell expansion chain and hence the passage number of the cells. Experimental results shown earlier in the chapter, indicate it would be desirable to use the low glucose DMEM at 1g/L and have an intermittent feed of glucose solution to replenish.

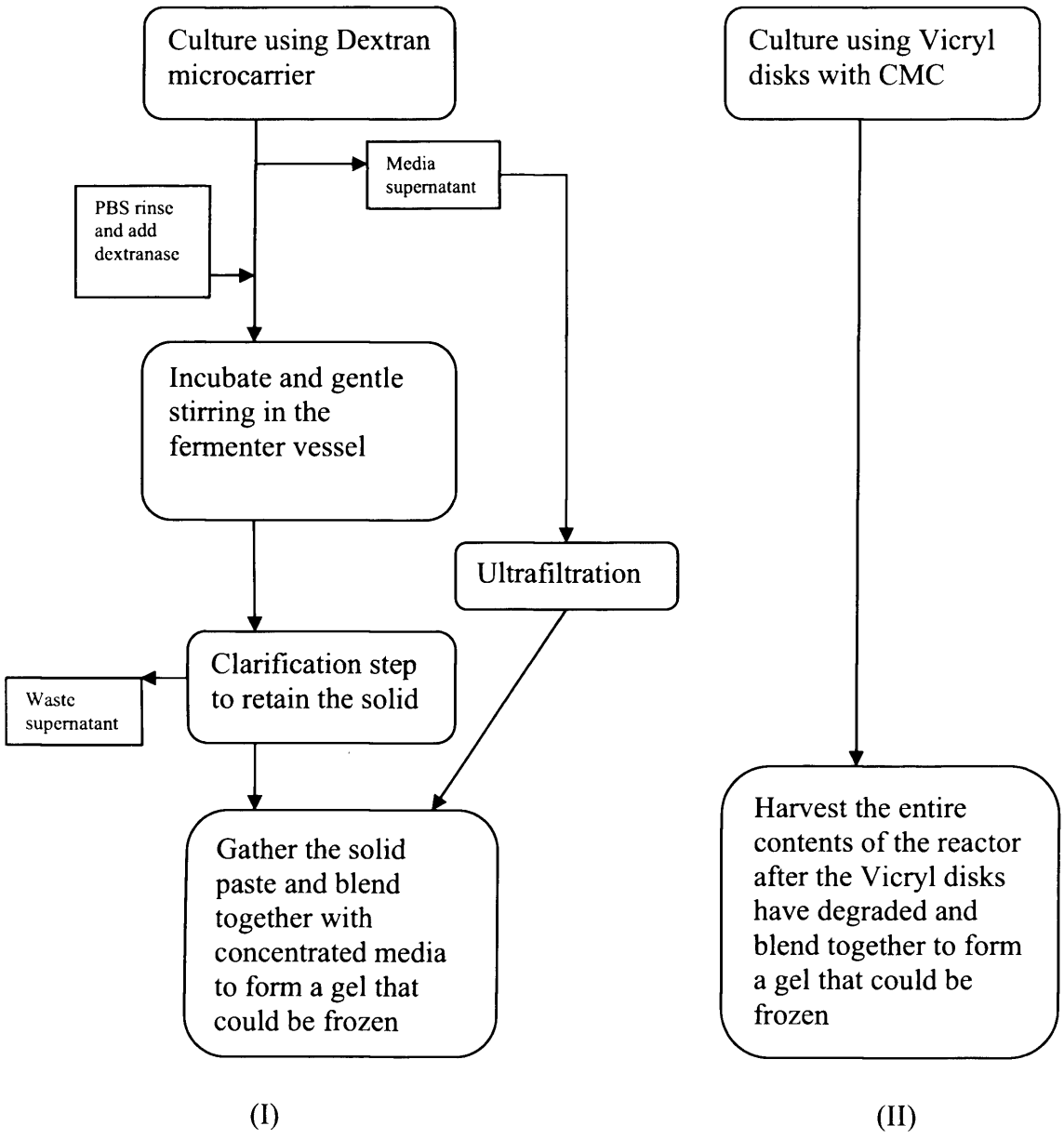

Figure 4.15 Process Flowsheet to indicate the unit operations required for the routes adopting (I) the dextran microcarrier, and (II) the Vicryl microcarrier.

Additionally, rather than stopping the impeller and letting the microcarriers settle, in order to carry out the media exchanges it would be better to siphon the spent media at a slow flow rate constantly through a settling tube. This process stream could be filtered to ensure no particulates which could block the UFDF membranes and this then can be concentrated and diafiltrated remove the lactate and ammonia and buffer exchange the growth factor-rich solution into the fresh DMEM to recirculate back into the reactor. This should be able to supply the culture with nutrients needed and reduce the amount of expensive serum and media required, thus reduce costs even further.

The media used is certainly not cheap and this economic driver will dictate the use of powdered or liquid concentrate medium as shipment and storage of large volumes of complete medium is impractical. From a 10L reactor culture, over a period of 2 weeks, 84L of complete media was utilized (personal communication with Mary-Ann Dowling, Smith &Nephew RC). This indicates that a 1000L culture would be utilizing at least 8,400L of expensive complete media. Additionally, the ideal culture mode to operate would be in perfusion mode and this will need constant preparation of medium. Thus, application of liquid concentrates would allow media preparation to take place in-line, by automatic dilution of the concentrates with water of the appropriate quality.

Scale-up considerations would be the mass transfer and oxygen transfer limitations which would take place. This will be finely balanced with providing sufficient agitation to ensure adequate nutrient mixing and suspension of microcarriers, whilst avoiding shearing the cells from the microcarriers, especially, as the aggregates gets bigger over the course of time. Multiple impellers would be required at the larger scale. Intermittent sparging with air would be needed, thus investigation into the designs for the sparger would be required.

Ability to use a disposable reactor rather than the standard stainless steel STR would take out the CIP and SIP and speed up production.

4.5 Conclusions

The experimental work here has shown that the culture of human dermal neonatal fibroblasts could be cultured on particulates successfully to generate the ECM and that cell expansion via the bulk reactor would be more efficient for large scale processes to satisfy potential demands. However, the extensive aggregation although favourable for biomass generation, made sampling difficult, and thereby making it difficult to monitor the cell density with any accuracy throughout the culture. Thus for the STR cultures, only the initial and final cell densities could be reported with confidence.

CHAPTER 5

ECONOMIC METHODOLOGY AND IMPLEMENTATION

5.1 Introduction

This chapter explains the methodology used in setting up the economic models to assess the potential of process alternatives for producing advanced wound healing products. Process planning early on can help to enhance manufacturing operations, and in the field of regenerative medicine, which is quite a new industry, ability to be able to address the questions regarding process economics can be quite beneficial. Experience from the bioprocessing industry showed that choices made early in the development process are hard to change later on due to regulatory constraints on process modification. When examining the technical feasibility for the process, the performance of the unit operations can be modelled based on experimental data, and this can be combined with business modelling to enhance decision-making in the manufacturing process.

Based on decision-support tools developed for the biopharmaceutical industry, the framework used is implemented via the spreadsheet software, *MS Excel XP* (Microsoft, USA). By using easy accessible software, the models developed can be examined and adapted quite simply for other processes. This chapter will start with explaining how the software platform is used to implement the model and the cost appraisal. The last section will explain how risk is analyzed and implemented.

5.2 Modelling Framework

The framework for capturing and organising process and cost data was adapted from Farid et al. (2000, 2005). Setting up the model initially required the creation of unit cost databases with the specifications of the resources within the facility being evaluated and their costs. The resources were identified and categorised as equipment, materials, utilities, and labour. Fig. 5.1 below is a schematic to explain the set up of the model.

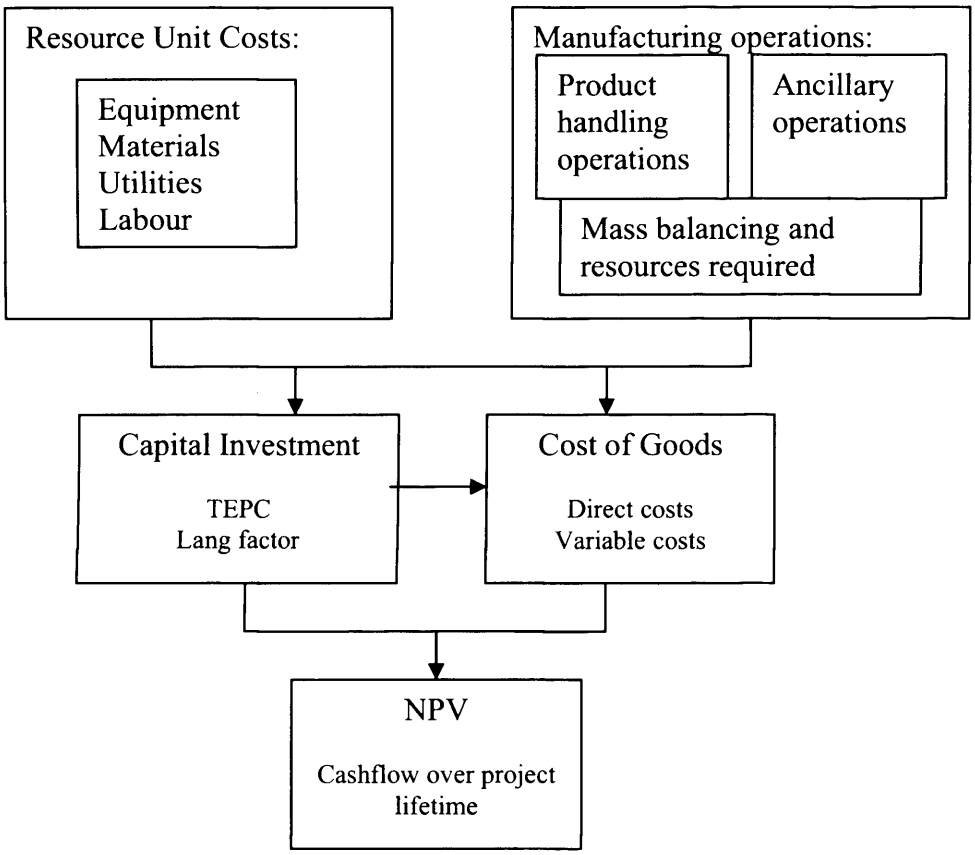

Figure 5.1 The hierarchical framework adopted.

Separate spreadsheets were created to define the task sequences and their resource requirements. The manufacturing operations were categorised as product-handling operations (e.g. cell culture) and ancillary operations to prepare the equipment (e.g. CIP)

or intermediates (e.g. media preparation). This helped to ensure all relevant activities and hidden costs were captured in a transparent fashion. For each unit operation relevant design equations and short-cut mass balance models were encoded to compute the output of each step and the equipment sizes and numbers required to meet the demand. This is further discussed in section 5.3.1.

5.3 Data collection

Parameters in the process models have certain default values, which come from the following sources: industrial experts, historical data, literature, and vendors. For example, equipment costs relating to the disposable Wave bioreactor were obtained by consultation with the vendor, Wave Biotech. Certain equipment costs, which may not have exact quotes, were estimated using the sixth-tenths rule and the use of cost indices.

$$\text{Scale-up factors: } \text{Cost}_2 = \text{Cost}_1\left(\frac{Size_2}{Size_1}\right)^R \quad \text{, where } R < 1.$$

$$\text{Inflation factors: } \text{Cost}_2 = \text{Cost}_1\left(\frac{Inflation\_index_2}{Inflation\_index_1}\right)$$

There are certain caveats to the use of these indices, for example, the inflation index calculations become increasingly inaccurate as the time interval between the data points increases, thus a 5 year difference will result in a more accurate calculation than a 20 year one (Remer and Mattos, 2003). Additionally, scale-up factors can only be used in the capacity range for which the factors were developed.

Frequent discussions with experts were carried out (N.Medcalf, M.Smith, M.Dowling at Smith and Nephew RC, York, UK) to ensure data values were sensible for the manufacturing operations. They were also consulted to validate the structural modelling assumptions. Databases of the information on costs gathered are shown in Appendix C.

5.3.1 Process models

The process alternatives presented in Chapter 6 each involved a series of operations that proceed from inoculum grow-up to fermentation and product recovery. The alternatives in Chapter 7 also required purification steps primarily by chromatography. This section presents the key principles behind the process models are used to calculate the composition of the process streams, and certain process variables. A summary is presented in Table 5.1. In general the rule of mass conservation is applied, in that the sum of the total process streams going in must equal the total of process streams out.

Inoculum grow-up of mammalian cells generally involves a vial of cells being seeded into roller bottles, which are passaged until the desired cell concentration is achieved. Roller bottle expansion is generally considered in terms of split ratio and knowledge of the final cell density achieved. From experimental work, a 1500cm^2 confluent roller bottle will generate ~5x 10^7 human dermal fibroblasts.

Fermentation is a process step whereby substrates undergo a reaction to give cell growth and product. Thus this step can be modelled using mass-stoichiometry to describe the link between the substrates and the products over a cycle. Information such as the titre of product or cell density achievable can be found from pilot plant studies, historical records or literature sources, and these can be used facilitate a quick calculation of the output streams from a mass balance. The maximum size of the reactor for production fermenter was fixed at 1000L, thus depending on the demand, the spreadsheet was set to first increase the number of batches until the maximum is reached and then to increase the number of reactor trains. The 1000L reactor limit was set, because working with primary cell lines, means that it is not feasible to have too long a cell expansion train and therefore dictates the final size of reactor. Furthermore, the maximum size of a disposable reactor is 1000L with a 500L working volume.

Centrifugation is used to separate solids from liquids in component mixtures and typically used to remove cells from the liquid broth. Ultrafiltration is very often used to

concentrate the process stream and diafiltration to allow for buffer exchange. Chromatography is used to purify the target product and typically considered to operate with the various stages of loading, wash, elute and regeneration of matrix. Knowledge of the number of column volumes, linear velocities and height of the columns are required and this can be taken from literature sources, manufacturer's recommendations, or experimental work.

Table 5.1 Summary of key inputs for each process model

Unit Operations	***Process Models***
Inoculum Grow up	Seeding densities, split ratio, final cell densities achieved.
Fermentation	Stoichiometry, extent of reaction
Centrifugation	Solids carry-over, Solids volume fraction in sediment
UFDF	Flux, Rejection coefficients, Number of Diavolumes
Chromatography	Flowrates, Column volumes, yields, binding capacities

Equations utilised are shown in Appendix C.

5.4 Key output parameters

The main outputs from the model are the fixed capital investment (FCI), cost of goods (COG) and net present value (NPV). The following sections explain how they were calculated.

5.4.1 Fixed capital investment

The method to derive the fixed capital investment was from the approach proposed by Lang, (1948), who predicted the total plant construction cost based upon the delivered cost of plant equipment. The method was based on the analysis costs of previous projects, and subsequently derived 'Lang Factors' whereby multiplying this with the total equipment purchase cost quickly provides an estimate of the fixed capital cost.

This is summarized by the equation:

$$FCI = TEPC \times Lf$$

where TEPC = total equipment purchase cost

Lf = Lang factor

The proposed Lang factor accounts for cost factors for items such as the electrical work, piping, instrumentation, contractor's fees etc. Depending on the type of plant that is to be installed, the value of the factor will vary, for example, chemical engineering plants typically will have lower values, ranging from 3 to 5. Biopharmaceutical plants are considered to required higher values of 4 to 8 because the need for specialised facilities, e.g. aseptic processing plant. Additionally, the variation will also occur depending on whether it is a disposable, hybrid or stainless steel plant. Derivation of the Lang factors is based on the method reported by Novais et al. (2001) and Petrides et al. (1995). Novais et al. (2001) reported that although the specific value for such a factor application to bioprocessing plants is not easily available from the literature it can be obtained from the sum of the individual factors that constitute capital investment. (Table.5.2)

Table 5.2 Individual factors, f_i, for a stainless steel bioprocessing plant and the corresponding derived Lang factor (Novais et al., 2001).

5.4.2 Cost of Goods

The cost of goods was defined as the cost of manufacturing, therefore it does not include the sales and distribution costs. The COG model used was based on Farid, 2000 and shown in Table 5.3.

The direct costs i.e. variable costs were based upon utilization by each of the unit operations. The indirect, i.e. fixed costs were estimated from the fixed capital investment. The term general utilities was to account for the HVAC systems and the aseptic requirements since the direct utilities did not account for the ongoing utility charges in running the facility.

Table 5.3 Breakdown of the COG/g model used (Farid et al., 2000)

The indirect raw materials accounted for miscellaneous material costs such as safety clothing, aseptic gowning requirements. Labour was treated as a function of utilization, i.e. the cost for the number of man-hours required for that task, and not as an annual fixed-salary based staff.

5.4.3 Cashflow model and Net present value (NPV)

A spreadsheet taking in account of the costs and revenue was set up. (See Appendix C). The total annual cost of goods was then fed into this spreadsheet to produce a cashflow to enable the calculation of NPV. Income was based on the amount produced multiplied by the sale price. Sales prices were determined based on information on commercial products currently on the market and adjusted based on expected market capture. Working capital was assumed at 15% of the FCI and was expected to be recouped at the end of the 10 year lifetime. Sales and distribution costs were assumed at 3% of the sales revenue. Corporation tax of 30% was applied.

The net present value (NPV) was chosen as the main output for the economic parameter to determine whether the project was considered economically feasible or not. This is a standard method to determine the profitability between competing projects and required a cash-flow to be generated. The simplified cashflow analysis was generated assuming that target sales would be reached in all years for the 10 years of operation.

A discount rate was also required to discount the future cash flows to their present values. Most companies take the weighted average cost of capital after tax, or the use of higher discount rates used for riskier projects (personal communication, Dr. K. Sutherland). The following equation defines the calculation for NPV.

$$NPV = \sum_{t=0}^{n} \frac{C_t}{(1+i)^t}$$

where t = time of the cash flow

n = total time of the project

i = discount rate

C_t = cashflow at that point in time

If the NPV is positive, i.e. greater than zero, then the project is deemed economically feasible and it is then recommended to the company to invest in the project.

5.5 Dealing with uncertainty: Risk Analysis and Monte Carlo simulation

Economic studies should also be able to point out the impact of potential changes and uncertainties on the expected output. This gives an idea on the robustness of the process, and how risky the process is as well. Thus, sensitivity analysis was carried out to determine the impact that the key variables and assumptions within the model had on the results. The extreme ends of the range of the variables were chosen to see the departure away from the base case value. The results from this were then shown graphically in tornado plots.

A Monte Carlo Simulation involves several iterations of the model and each one, a random number generator selects a value for each uncertain variable. Values are chosen within specified ranges for each variable and with a frequency proportional to the shape of the probability distribution associated with each variable. The process models created utilised triangular distributions for the key uncertainties. Usually 1,000 to 10,000 cases were needed to reach convergence in the output distributions. The Monte Carlo simulations were set up using code written in Microsoft *VBA* which manipulated the models in MS *Excel XP*. The speed to run the iterations ensured that the calculations required were carried out in a day. The Monte Carlo simulations were used to obtain frequency distributions of the key economic metrics, COG and NPV. This enabled potential risk against the reward to be analysed more clearly.

5.6 Conclusions

This modelling approach allows the user to compare process alternatives to be compared in terms of yield, resource demands, cost and profitability. The next two chapters present the results of the economic analyses using the model to compare different flowsheets for producing advanced wound healing products.

CHAPTER 6

ECONOMIC ASSESSMENT OF MANUFACTURING STRATEGIES FOR ADVANCED WOUND HEALING PRODUCTS

6.1 Introduction

In parallel with the experimental work presented in Chapter 5, an economic evaluation of manufacturing strategies was also carried out. As highlighted earlier, the 1st generation of tissue-engineered (TE) skin substitutes are regarded as interactive drug delivery systems (Harding et al., 2002) providing cytokines and growth factors to the wound bed. Hence it is possible to envisage the 2nd generation products as bioactive ECM reformulated as a gel or patch. Consequently, the assumption that the 2nd generation TE skin products do not need to be administered as flat skin equivalents to be effective opens the door to several possible bioreactors designs as successors to the conventional planar devices. In this chapter, a simple multi-criteria decision making technique was used to score the alternative designs in order to select the most promising designs for further investigation. These selected designs were then subjected to a more rigorous economic evaluation which was extended to incorporate the impact of uncertainties on the cost and profitability. Stochastic modelling with Monte Carlo simulations was used to minimise the risk of incorrect conclusions due to variability in the assumptions that form the basis of the models such as process parameters such as cell yields and product yields. This strengthens the key conclusions that can be drawn from the economic evaluation.

The structure of this chapter is as follows: Section 6.2 presents the assessment of the various bioreactor designs using a MCDM technique; Section 6.3 covers the background

to the more detailed case study and in Section 6.4 the deterministic analysis of the problem is presented. The uncertainties in the problem are then identified, and addressed, using a sensitivity scouting analysis in Section 6.5. Monte Carlo simulation is then used to imitate the randomness inherent in the problem and this is presented in Section 6.6. Finally, Section 6.7 examines the scenario of different scales of operation.

6.2 Assessment of Bioreactor Designs

The bioreactor designs considered were:

a) microcarrier-based: Stirred Tank Reactor, Wave disposable bioreactor, and fluidised bed reactor
b) non-microcarrier-based: Roller bottles, spiral film reactor, plate heat exchanger method and multi-unit reactor (e.g. Cell factory, Cell cube)

As can be seen from this list, both stainless steel and disposable options were evaluated. The use of disposable equipment is attractive since it allows for a lower initial capital burden, and the possibility of spreading the costs over a plant's life. There is an increasing acceptance of the use of disposables in the biopharmaceutical industry sector, and this trend is set to grow, as more suppliers enter the disposables market. Thus the possibility of adopting a plant based on disposable components for the generation of tissue-engineered products is an interesting alternative for investigation.

6.2.1 Methodology

Multi-criteria decision-making (MCDM) methods provide a formal mechanism for explicitly including qualitative and non-financial aspects of performance in the evaluation. In this chapter the additive weighting sum technique was used to screen for the most preferred designs in terms of both financial and operational feasibility. A set of financial and technical criteria were compiled through discussions with industrial experts. In addition to the relative magnitude of the production cost, several operational criteria such as scalability, ease of control, and validation were considered key factors affecting

the decision. A summary of the criteria used is given in Table 6.1. Each of these criteria was assigned a weighting according to their relative importance of 1 to 3. Then each individual criterion was then given a relative score of 1-3, with 1 being the worst outcome and 3 the best outcome. The scores given by a panel of six academic and industrial experts were averaged, and the results of this are further shown in the following section in Table 6.2. The total score for each alternative was obtained as the weighted sum of all the criteria values. The financial and operational scores was then normalised and results are plotted in Fig. 6.1

Table 6.1 Criteria used in the analysis of bioreactor designs

	Criteria name	Criteria description
Financial	Projected cost per kg	Cost of biomass per kg wet weight, in the condition ready to undergo formulation into the product
Operational	Scaleability	Ability to expand the scale of the process to achieve 250 kg/year, and inclusion of flexibility into the scheduling.
	Validation burden	Combination of the perceived difficulty and duration of validation to meet FDA requirements, and the probability of success.
	Control of process	Expectation of the ability to reproduce the culture conditions and control the product composition through control of the culture environments of the cells. Ability to manipulate growth conditions.
	Versatility	Ability of the process system to accommodate changes to the cell types other than just fibroblasts and also to be able to be utilised with a range of cell support materials.
	Patent Issues	Probability of being able to acquire the rights to sell the product and potential to prevent others from replicating the product.
	R&D burden	Combination of the perceived difficulty and duration of the research and development. Consideration of the likelihood of success and the ability to demonstrate early proof of concept.
	Operability	Perceived robustness of the process

The weighting was given from an industrial perspective on the relative importance of each criterion to the company, Smith and Nephew after extensive discussion. Thus

projected costs/kg was perceived to be the most important criterion and thus given a weighting of 3, in comparison patent issues were felt to be of lesser importance and given a 1. This is because process patents are notoriously difficult to defend and Smith and Nephew had broad patents for its existing products, Dermagraft and Transcyte.

6.2.2 Results and Discussion

From Table 6.2, it can be seen that multitray units do not score favourably in terms of operability and control of process because of the perceived difficulty in retrieving the product; it would be undesirable to run an enzymatic solution to harvest since that would digest away the product, thus operability scores a low 1. It was perceived that STR with microcarrier technology would have better scalability than the Wave reactor thus this was given a score of 3, and the Wave reactor a score of 2 because the maximum working volume that a Wave reactor can have is 500L.

Table 6.2 Compiled averaged scores obtained from the panel.

Criteria	Weighting	Current existing process	Microcarrier based designs			Non-microcarrier designs		
		Roller bottle	Stirred Tank	Wave reactor	Fluidised Bed	Spiral reactor	Plate heat exchanger	Multi-Tray units
Operability [Hi =3/Med=2/Lo=1]	1	2	2	2	2	1	2	1
Scaleability [Hi =3/Med=2/Lo=1]	2	2	3	2	2	1	1	2
R&D burden [Hi =1/Med=2/Lo=3]	2	3	2	2	2	1	1	3
Validation burden [Hi =1/Med=2/Lo=3]	1	3	2	2	2	2	2	2
Projected cost/kg [Hi =1/Med=2/Lo=3]	3	1	2	2	2	2	3	1
Control of process [Hi =3/Med=2/Lo=1]	2	1	3	3	3	2	2	1
Patent Issues [Hi =3/Med=2/Lo=1]	1	2	2	2	2	3	2	2
Versatility [Hi =3/Med=2/Lo=1]	2	2	3	2	2	1	2	2
Total		26	34	30	30	22	27	25

From the aggregate weighted scores in Table 6.2, it can be seen that STR was the most favoured route with the highest total score. Additionally, the microcarrier based designs had the higher scores when compared to others.

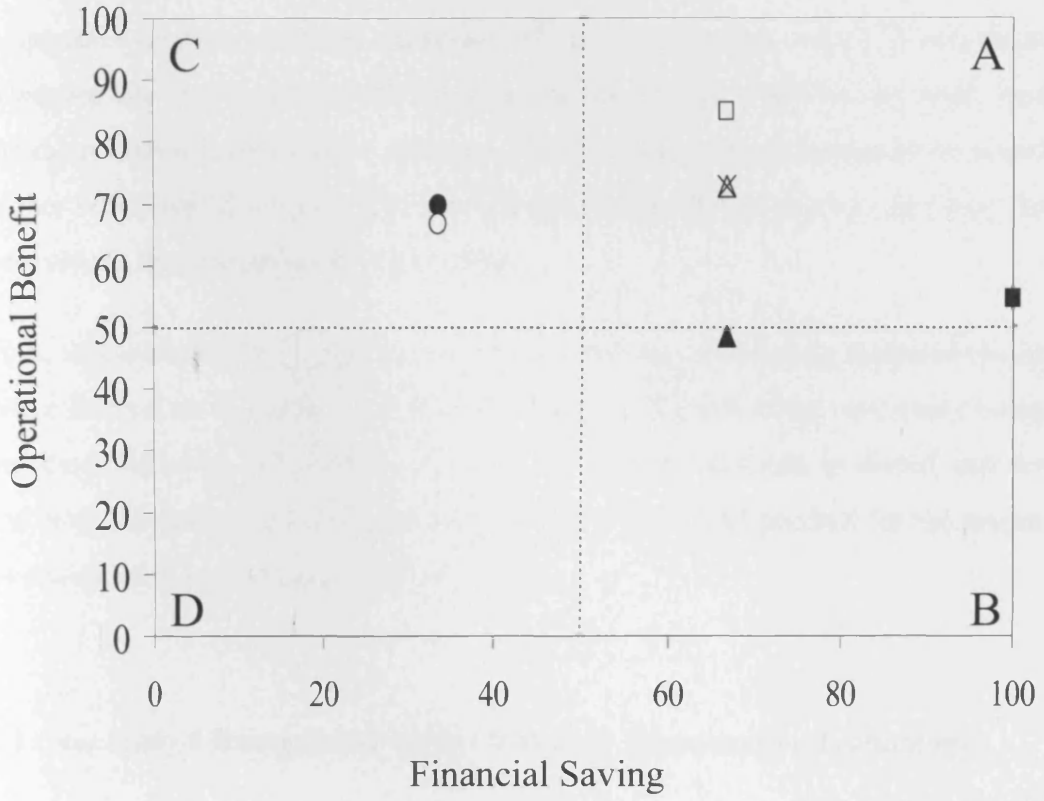

Figure 6.1. Normalised plot to show the assessment of the reactors. The horizontal axis is the financial saving and the vertical axis is the operational benefit. Reactors, which fall into quadrant A, are the most desirable as it has a high score for the financial saving and the operational benefit as well. ● denotes Roller bottles, ○ Multi-unit reactor, × Fluidised bed, ■ Plate reactor, □ STR, ▲Spiral film reactor, and Δ denotes Wave reactor.

Fig.6.1 compares the operational and financial weighted normalised scores for each alternative. It can be seen that there is a trade-off between operational benefit and

financial saving. The figure shows 4 quadrants labelled A, B, C and D; reactors which fall into the top right quadrant A are the most desirable and those in the bottom left quadrant D are the least desirable. The conventional roller bottle method for cell expansion and extracellular matrix production has a low financial saving score but a moderate operational benefit score. The reactors in quadrant A are microcarrier-based suspension reactors with the exception of the plate reactor, which is non-microcarrier. However, the plate reactor suffers from a low operational benefit score when compared to the microcarrier-based reactor options. The microcarrier-based suspension reactors has a higher score overall compared to the non-micocarrier based reactors and were deemed to best satisfy the criteria listed in the table.

From this initial analysis, the optimal reactor was the stirred tank, followed closely by the Wave Bioreactor as can be seen from the Fig 6.1. The following case study compares the processes based on roller bottles to microcarrier-based methods in stirred tank fermenters and Wave Bioreactors for the production of the bulk ECM product for the preparation of an advanced wound healing product.

6.3 Case study I Background: Roller bottle vs. Microcarrier Technology

Four flowsheets were proposed based on different bioreactor designs for the production of bulk TE-ECM product: Manual and automated roller bottle (RB) routes containing a biodegradable mesh, vs. two microcarrier-based routes, either using stirred tank fermenter (STR) or disposable wave bioreactor. These are shown in Fig 6.2.

Roller bottle (RB) technology is a simple, tried and trusted method for the cultivation of mammalian cells and can be used easily for the manufacture of biosynthetic skin substitutes. The transparency of the roller bottles allows quick visual inspection and microbial bottles that are contaminated can be quickly discarded. The losses caused by contamination can be addressed by applying corrective action, preventative action (CAPAs) before too much money has been wasted and by spreading the losses over a

campaign of production this avoids the peaks and troughs caused by the large individual batches going down as associated with STR and the Wave bioreactor route.

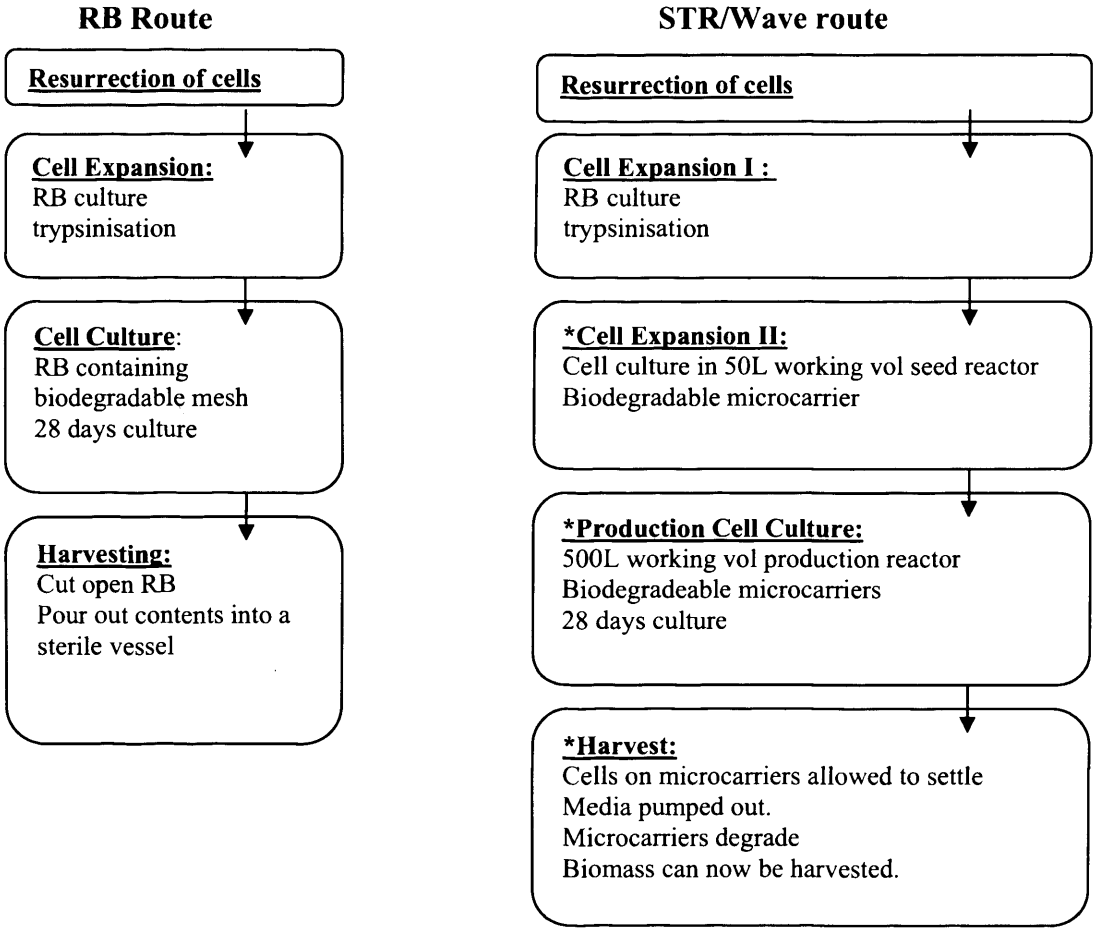

Figure 6.2 Flowsheet of the Roller Bottle (RB) Process and the microcarrier-based processed using STRs or disposable Wave Bioreactors. * indicates the choice of either the STR or the Wave bioreactor.

RBs also offer the advantage of being disposable, thus avoiding the need for ancillary cleaning and sterilising steps but incurring high consumable costs. However, the disadvantages are quickly realised for large scale manufacturing, which requires aseptic handling of numerous bottles; these are more pronounced for the manual manipulation of RBs where the risk of contamination and yield inconsistency is high and investment in

skilled labour can escalate or adoption of automation is required. The disadvantages related to skill labour are alleviated with the use of automated RB systems whereby the robotic arms are responsible for all the critical handling steps such as inoculation, media exchanges and harvesting. Such systems are currently used for the manufacture of Amgen's EPO. The operator merely removes the RB from the incubator onto the input tray of the laminar flow hood which is then rolled into the hood by a conveyor belt. The robotic arm in the hood then implement the media removal and additions and an operator is then required to move the processed roller bottle back into the incubator. This reduces the risk of repetitive strain injury on the operators, and increases the amount each operator can then process. The microcarrier-based routes in fermenters are less labour-intensive and hence the risk of contamination is lower. In addition, scaling up and automation are easier to apply and environmental conditions (e.g. temperature, pH, DO) can be finely controlled.

Conventional stainless steel STRs were compared to disposable Wave bioreactors that comprise disposable bags placed on a stainless steel rocking cradle, which tilts to generate motion of the liquid similar to waves. The trade-off between the advantages of disposables, such as a potentially lower capital investment, faster turnaround and elimination of CIP and SIP steps, and the potential disadvantages, such as increased consumable costs, and floor space for the rocking devices were analysed. This analysis compares the bulk production costs; formulation and packaging are not included since they will be the same for all options.

6.4 Deterministic analysis

6.4.1 Set up of the model

A process economic model was set up in *MS Excel XP* (Microsoft Corp, Washington) as described in previous chapter, to assess the feasibility of each manufacturing option using the following metrics: number of batches required to meet demand, cost of goods (COG),

and the profitability indicator net present value (NPV). The model comprised of spreadsheets defining the process characteristics that fed into a COG model, which in turn fed into a cashflow model to compute NPV. The flow of information through the model is illustrated in Fig. 6.3.

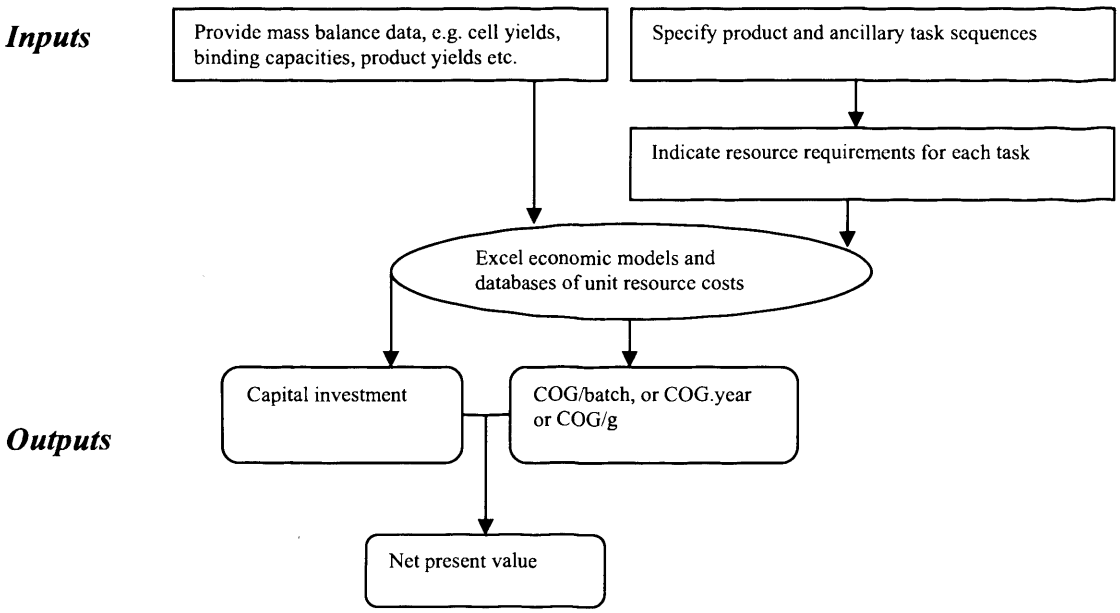

Figure 6.3 Schematic indicating the flow of information through the tool

For each option, the process characteristics were specified in terms of the product-handling activities as well as the ancillary activities required to prepare equipment (e.g. CIP, SIP, mesh prep) and intermediates (e.g. media prep) as has been suggested by other authors (Farid et al., 2000, 2005; Lim et al, 2005a and b). For each activity the resources required, such as equipment, materials, staff and utilities were estimated. Companies were consulted for verification of quantities of materials required and the activity sequences. Short-cut mass balance models were used to determine the composition of each output stream. Equipment sizes and numbers, to meet market demand, and task durations were calculated using yields derived from experimental data from Chapter 4. A

database of unit resource costs was compiled through consultation with several vendors and literature sources (as presented in Chapter 5, Table 5.1)

The COG model used was based on conventional chemical engineering facilities but with modifications to account for the additional demands placed on the manufacture such as the requirement of aseptic techniques and added cost of HVAC systems. (The breakdown of the COG/g model is presented in Chapter 5, Table 5.3). The Fixed Capital Investment (FCI) was established using the Lang factor method where the total equipment purchase cost was multiplied by the Lang factor. The Lang factor was derived based on Novais et al. 2001. See Appendix C which shows the spreadsheet for the derivation. The standard 10-year depreciation period was assumed for the COG calculation. Media was assumed purchased sterile, and the preparation consisted of adding the supplements to the basal media aseptically.

Table 6.3 lists the key assumptions and the input values for each process route, which has been validated through discussion with industrial experts. The scale for the process was decided based on analysing the market information and then process flowsheets were devised based on literature information, experimental data and discussion with the engineers from Smith and Nephew, La Jolla. Thus, inputs such as product demand, the sequence of the production and ancillary unit operations, resources required, and cost data were investigated first. By examining the sales figures for the approved skin-substitute products out on the market, a product demand based on these figures was then estimated. The input value was estimated to be 100kg of TE-product. From experimental work carried out into culturing fibroblasts, the doubling time of fibroblasts was calculated to be 55 hours. Additionally, the ECM to cells ratio was determined to be 3:5. This was used as a basis to determine what scale of operation to meet the 100kg annual demand. This allowed the estimation of how many cells were required for the 100kg scale, and thereby determined the size and number of production vessels.

Table 6.3 Key assumptions for the aRB, mRB, STR and Wave route

Key Assumptions	Input Value for mRB/aRB	Input Value for STR/Wave
Cells to ECM matrix ratio	3:5	3:5
Cell density in the mesh (cells/ cm^2)	1 x 10^5	-
Cell density in STR/Wave culture (cells/mg of microcarrier)	-	3.5 x 10^5
Area of biodegradable mesh in each RB	1500cm^2	-
Microcarrier concentration	-	10 g/L
Cost of biodegradable carrier	-	1.5* cost of commercial carrier
Serum used in the media	10% w/v	10% w/v
Time of each batch run	53 days	58 days
Labour requirement	1 skilled worker can maintain 30 RBs, automation increased this 90 RBs	
No. of production reactors	-	4 for STR, 3 for Wave
Working volume of seed reactor and production reactor	-	50L and 500L
Maximum no. of batches per year	10*	12
Lang factor	8.6, 3.1	8.1, 14.5
Annual product demand (kg)	100	100
Duration of the project (years)	10	10
Turnaround time (hours)	12	8 for STR, for Wave
Size of facility (m^2)	1500	1500
Sales Price (£/g)	200	200

*each batch consists of thousands of RBs. (All processes were designed to produce an output of 100kg TE-ECM to meet the anticipated market demand.)

For the roller bottle processing route, this meant, knowing the number of total cells required based on the cells to ECM ratio allowed working out the number of seed roller

bottles required to inoculate the production roller bottles. Additionally, from experimental work, a confluent RB generates ~50 x 10^6 cells.

Thus the total number of roller bottles used for the entire roller processing was calculated based on the equation:

Total RBs used in the expansion = $1\text{-}S^{(N/(1-S))}$ + No. of seed RBs required. (6.1)

where S = Split ratio

N = no. of whole expansions

Inputs for the target cell density were 1 x 10^5 cells/cm^2 for the RB process routes, and 3.5 x 10^5 cells/mg of microcarrier for the microcarrier routes. This in turn was also interlinked to the area that is available for the cells to grow, as human dermal fibroblasts are anchorage dependent. Thus the area of biodegradable mesh used in the rolled bottles was assumed to be 1500cm^2, and the microcarrier concentration in the STR and Wave options was assumed to be 10g/L. The facility size of 1500m^2 was assumed in all cases.

Calculations indicated that this would require a total production capacity of 83,333 RBs, in the RB route, versus 3571L in the STR and Wave routes. For the STR and Wave case, multiple bioreactors were used as they offer flexibility of operation, and a degree of robustness in the case of batch failures. This modular design minimises the production disruption (Rouf, 2000). Thus, for the base case, multiple STR bioreactors at 500L working volume were modelled rather than increasing the reactor size. Additionally, it is undesirable to have too long a reactor train, since these are primary cells, and therefore high passage numbers should be avoided. To account for the faster turnaround time with the disposable Wave bioreactor, three was thought to be required as opposed to the four stirred tank reactors. The Wave bioreactor consists of a fixed rocking cradle (investment cost) and a disposable cellbag (consumable cost), and is available in working volumes of up to 500L.

In order to model the effect of automation of roller bottle processing, certain additional assumptions were required, such as the number of RBs a robotic arm could operate within a timed duration. One of the leading companies in this field, the Automation Partnership (TAP) was consulted with regard to the cost of Cellmate, and its capabilities. Additionally, Tecan Ltd. was also consulted on the cost of the robotic arms as well, and the footprint of the equipment. Bernard et al. (2004) states that the Cellmate from the Automation Partnership (TAP) is capable of processing between 10 and 500 roller bottles or tissue culture flasks containing as many as 10 different cell lines a day and that each Cellmate can handle up to 2 to 3 times the amount of work a skilled worker can comfortably handle. Hence, the assumption that the use of the Cellmate increases the throughput of each operator by 3 times was used in the case study. The use of automation improves upon the existing manual tissue culture methods by increasing throughput, reduce the risk of contamination due to operator error, and reduce risk of repetitive strain injuries.

The key assumptions for the NPV calculations required the inclusion of the sales price for the product in order to calculate what the perceived revenue could be. Sales price was determined based on the price of the products out on the market. Thus the sales price of the TE-product per g was determined based on the information that the sales price of the formulated products on the market was estimated at £300/g; this was based on a piece of Dermgraft, which costs $475 for a patch, and $1159 for Apligraf. As the costing exercise carried out was only taking into account of the bulk product, and not the formulation or packaging, a more realistic sales price of £200/g was set for the cashflow analysis. The NPV was calculated assuming a plant operating life of 10 years, and a discount rate of 10%.

6.4.2 Results and Discussion of the deterministic analysis

The annual direct costs on a task basis for the manual RB, automated RB, STR, and Wave routes are illustrated in Fig. 6.4. The breakdown of the direct and indirect costs of the annual COG are shown in Fig 6.5.

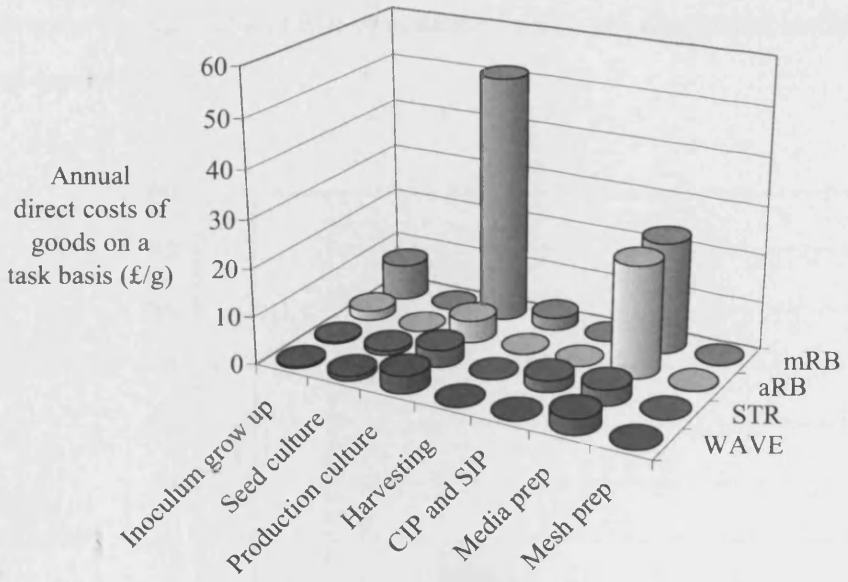

Figure 6.4 Comparison of the annual direct cost of goods per gram (COG/g) on a task basis, for the RB method (manual and automated), the Wave Bioreactor method and STR method, to produce the same product output of 100kg per year.

Most of the costs can be seen to accrue during the production reactor culture stage; the manual RB costs are significantly higher than the aRB, STR and the Wave routes. Examining Fig. 6.5 demonstrates that this can be attributed to the higher labour demands when operating such huge numbers of RBs; the impact of automation in reducing labour costs can be seen when one compares the manual RB route to the automated RB route (Fig.6.4 and 6.5). Furthermore, the RB processes use more media than the other two microcarrier processes and this is because more media exchanges are required to account for loss of moisture due to evaporation, and to reduce the build-up of lactate waste, making the culture environment undesirable as it lowers the pH considerably. This contributes to higher materials and utilities costs in Fig. 6.5.

The production reactor step has a slightly higher cost in the Wave route compared to the STR route. This is because of the higher consumable costs due to the use of disposable cellbags retailing for £312 for the small scale and £1200 for the largest size of 1000L

which has an operating volume of 500L. On the other hand, the STR route consumes extra resources for its CIP and SIP operations, which are eliminated in the disposable RB and Wave routes.

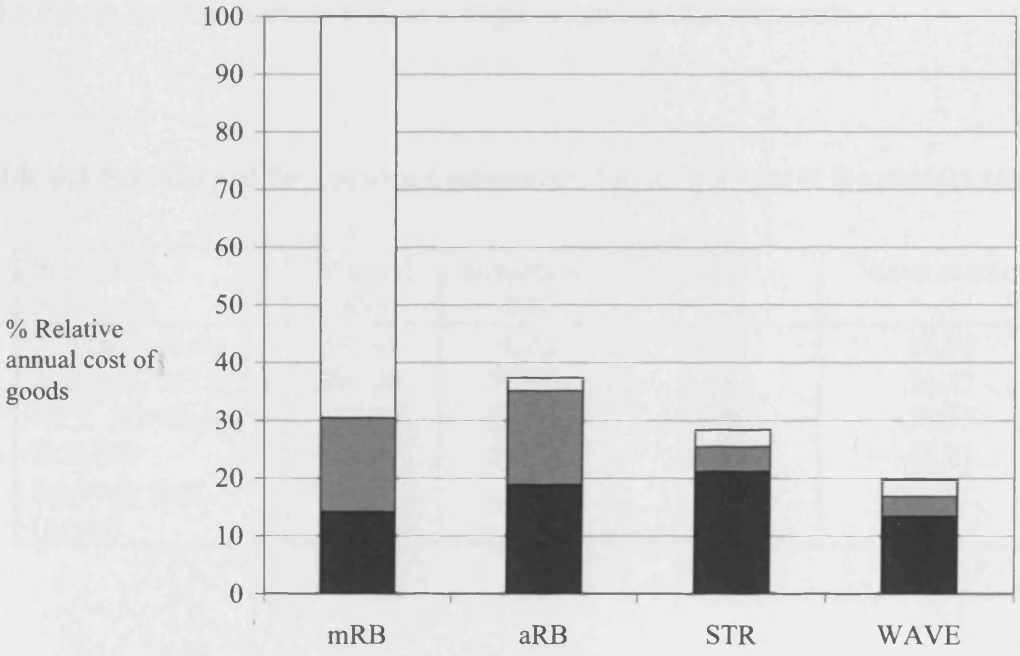

Figure 6.5 Breakdown for relative total annual cost of goods for the RB (manual and automated), STR and Wave routes. The labour component (□) comprises the costs of operating labour, supervisors, QC and QA and general management. The materials and utilities costs (▩) are displayed together. The indirect costs (■) consist of general utilities, depreciation, insurance, local taxes and general maintenance costs. The costs are displayed relative to the manual RB process.

The aRB, STR and the Wave routes can be seen to offer significantly lower costs compared to the manual RB route (37%, 28% and 20% respectively, if manual RB is 100%). The ratio of direct costs to indirect costs differs considerably and the mRB route is dominated by direct costs (materials, utilities, labour) whereas indirect costs dominate in the STR route. The indirect costs are proportional to the capital investment required which is highest in the STR case (see Table 6.4 or Fig 6.5). Interestingly, the graph

indicates that the STR and the Wave routes have similar materials and utilities costs. Although the Wave route has higher consumable costs, the utilities and chemical costs are lower given the lack of CIP and SIP operations. Therefore, when compared to the STR option the cost reduction in the Wave route can be attributed to a significant reduction in indirect costs as well as a slight reduction in labour costs.

Table 6.4 Summary of the economic parameters for comparison of the process routes.

Economic indicators	Manual RB	Automated RB	STR	Wave reactor
FCI (£) million	14.70	20.24	22.98	13.83
Annual COG (£/g)	260.70	97.49	73.97	51.47
NPV (£million)	-37.15	29.86	38.40	53.35
IRR (%)	N/A	27.68	29.66	48.83
Payback time (years)	N/A	2.7	2.5	1.4

Table 6.4 summarises the results of the economic metrics used to compare the various methods. The Fixed Capital Investment (FCI) is highest for the STR route, followed by the automated RB route, manual RB route and then the Wave route. The significantly large quantity of roller racks needed to process the roller bottles in each batch contribute to the high FCI values for the RB processes. The automated RB has a higher FCI than the manual RB route given the robotics required. The upfront cost of half a million pounds for one these units (e.g. Cellmate) does seem daunting, but there are potential savings to be gained since fewer expensive highly skilled labour are required. Dutton and Fox (2006) also showed this trend in their life cycle cost analysis. The Wave route has the lowest FCI, of which most of the cost is attributed to the rocking cradle for the reactor, and any remaining supporting equipment.

The NPV is negative for the manual RB route, and positive for the automated RB, STR Wave routes at a 10% discount rate. A positive NPV indicated a worthy investment and a

negative NPV denoted a loss, therefore, the more positive the NPV, the more profitable the process. In industry, an IRR above the 30% mark is considered a profitable project. To conclude, the deterministic analysis suggests that Wave is the most economically feasible because of its higher NPV (~£ million) and an IRR that exceeds the 30% benchmark.

By examining comparative cost ratios shown in Table 6.5 for the different process routes at the 100kg scale of operation relative to the automated RB process route, it can be seen that automation allows the RB process route to compete with the bulk reactor routes. A similar conclusion was drawn by Archer and Wood (1992), however, the difference in the labour requirement between the manual and automated operation is greater in this scenario, and a further difference lies in the STR and Wave routes having higher labour requirements than the automated RB route. Of course, the results are case study specific and highly dependent on the assumptions made and the scale of operation. This led to further analysis to examine the impact of changing the scale of operation and this is explored in the Section 6.7.

Table 6.5 Comparative cost ratios

	RB	Automated RB	STR	Wave
Annual output	1	1	1	1
FCI	0.7	1	1.1	0.7
Materials Cost	1	1	0.2	0.2
Labour Cost	31	1	1.3	1.3
COG/g	2.7	1	0.8	0.5

6.5 Sensitivity analysis

Since several variables were considered in the case study, it was important to determine which had the most impact on the NPV and hence were the key profitability drivers.

6.5.1 Setting up the sensitivity analysis

For each key variable in the model, the best case and worst case scenarios were run to monitor the impact on NPV. The variables examined along with their worst and best values are shown in Table 6.6. These results are then plotted as tornado diagrams.

Table 6.6 Scenario setups for RB, STR and the Wave

Input variable	**Worst**	**Base**	**Best**
mRB/aRB/STR/WAVE			
Cells to ECM ratio	10:1	3:5	1:10
Sales Price (£/g)	150	200	250
mRB and aRB – specific			
Cell density in mesh (cells/cm^2)	1 x 10^4	1 x 10^5	1 x 10^6
Mesh Area (cm^2)	850	1500	2150
Mesh Cost (£/m^2)	14.56	11.64	8.73
STR/Wave – specific			
Cell density in suspension (cells/mg carrier)	3.5 x 10^4	3.5 x 10^5	3.5 x 10^6
Microcarrier concentration (g/L)	5	10	15
Cost of biodegradable microcarrier (£/g)	7.20	5.40	3.60
Process route specific –Lang factor			
mRB	9.60	8.60	7.60
ARB	4.10	3.10	5.10
STR	9.13	8.13	7.13
WAVE	15.47	14.47	13.47

Additionally, the effect of the scale of operation will affect the type of process route chosen tremendously, thus, additional modelling was set up to look varying scales of annual production of 1kg, 10kg, 1000kg, and 10,000kg. By examining the NPV across the different scales of operation, the most suitable for each scale can be identified.

6.5.2 Results and discussion

Tornado diagrams are used to illustrate the sensitivity of the variables on NPV in Fig 6.6.

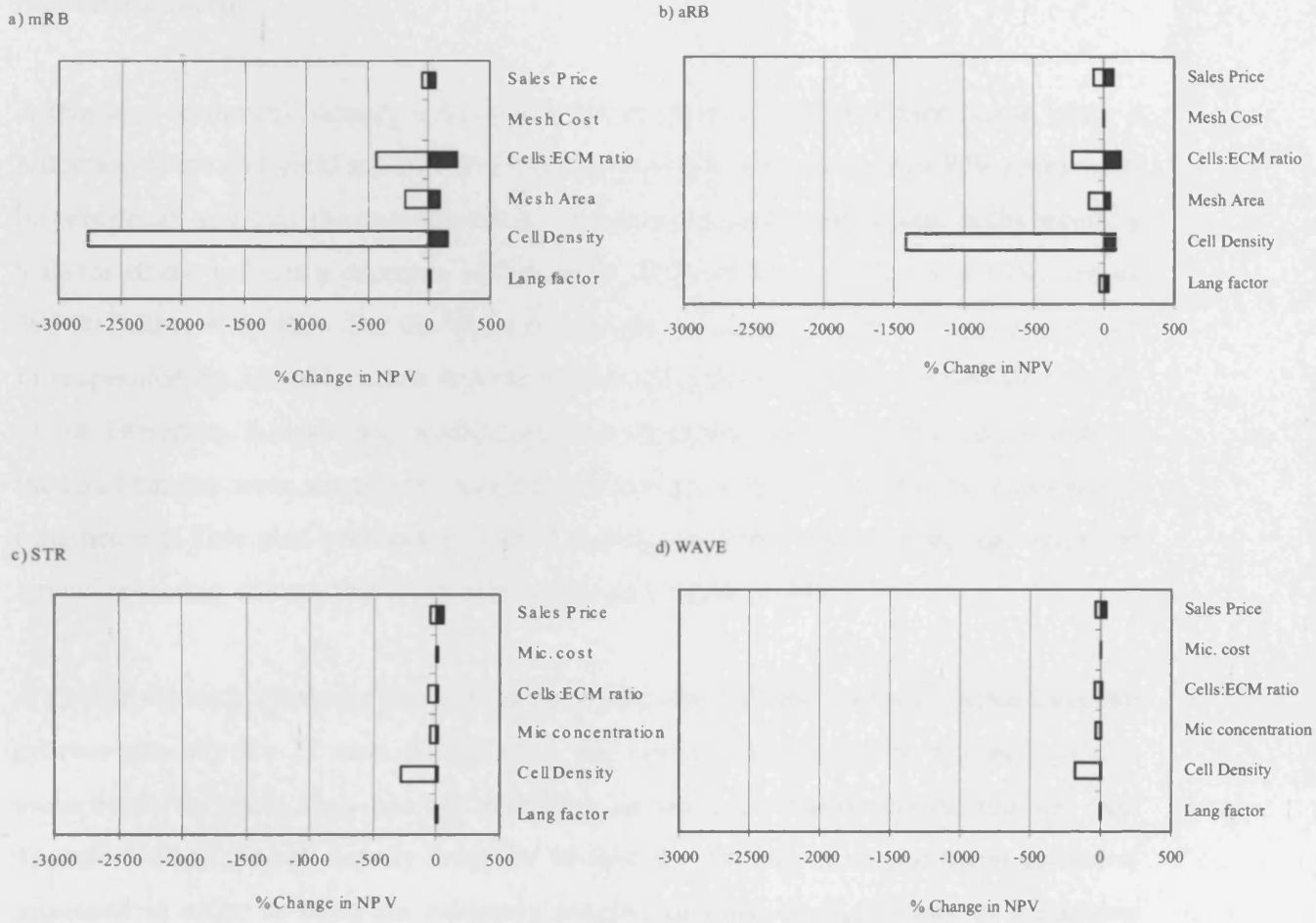

Figure 6.6 Tornado diagrams showing the %Change in NPV from the base case for the three processes. Plot a) is the manual Roller bottle option, b) is the automated Roller bottle option c) is the Stirred tank reactor and d) is the Wave reactor option. (■) denotes best case, (□) denotes worst case scenario.

This highlights that the NPV is most sensitive to the cell density in all cases, followed by the Cells:ECM ratio and then either, the mesh area (RB routes), or the microcarrier concentration (STR and Wave routes). Additionally, it can be seen from the plots, that the

worst-case scenario has more impact and cause more deviation from the base, than the best-case scenario.

Alterations to the cell density achieved in the mesh is a very important factor, since a reduction in the cell yield achievable means an increase in the number of RBs required to be processed, and thus the costs escalates. The increase in the cell density in the mesh by a factor of ten reflects a decrease of RBs by a factor of ten as well, i.e. a reduction of 80,000 RBs to 8000 RBs. For the Wave Bioreactor, a decrease in the cell density reached in suspension by 10-fold, means that the number of runs needed is increased by a factor of 10. Therefore, this not only leads to an increase in the direct costs, but an increase in the fixed capital costs, since more rocking cradles are needed to meet the sheer number of runs needed. This also becomes a case of scaling out rather than scaling up, since the largest operating volume the Wave bioreactor can provide is 500L.

A similar situation exists for the STR method since the maximum runs a reactor train can process annually are 12 runs. Additionally, the reactor train cannot be too long, as it is undesirable to reach high passage numbers, as the cells maybe considered too old. Therefore when the cell density drops by 10-fold, the number of reactor trains needed is increased in order to meet the necessary number of runs, again, leading to a massive increase in fixed capital costs.

Next, it can be seen from Fig 6.6 that the cell to ECM ratio is also very important. In the RB situation, this is because it affects the scale of the operation tremendously, and in the STR situation, it means more runs are needed when the ratio drops. A similar situation also happens in the Wave route. However, the impact is not as drastic when compared to cell density. The area of the mesh will also affect the number of roller bottles required. Likewise, a similar situation exists with the impact the microcarrier concentration has upon the process. Since a reduction in the concentration of microcarrier means less area available for the cells to proliferate and therefore a lower yield so more runs are needed. Changes in the sales prices, mesh cost, microcarrier costs and Lang factor only have a minor impact on the NPV.

To further confirm the rankings of the process route, stochastic analyses were carried out as described by the next section.

6.6 Stochastic analysis

6.6.1 Setting up the Stochastic analysis

Having identified the key uncertainties in the sensitivity analysis, triangular probability distributions were assigned to the key uncertain inputs using the worst and best case values as the minimum and maximum values of the distribution. The Monte Carlo simulation technique was then used to determine the distribution of possible outcomes for the NPV. Since the cost models were set up in Excel, VBA macros were written to allow the running of Monte Carlo simulations. 10,000 iterations were used; the running average of the results was monitored to ensure convergence was reached.

6.6.2 Results and discussion of the stochastic analysis

Fig. 6.7 illustrates the cumulative probability distribution plot for the NPV for each process route at the 100kg scale. From Fig 6.7, it can be seen that the probability of obtaining a negative NPV is greater for the manual RB route than the STR or Wave routes. This reinforces that the manual RB route is infeasible at this scale for the assumptions made. The automated RB route lies between the manual RB and the bulk reactor routes. Further examination of Fig 6.7 illustrates that the STR and Wave routes have much narrower NPV distributions implying they are more robust processes.

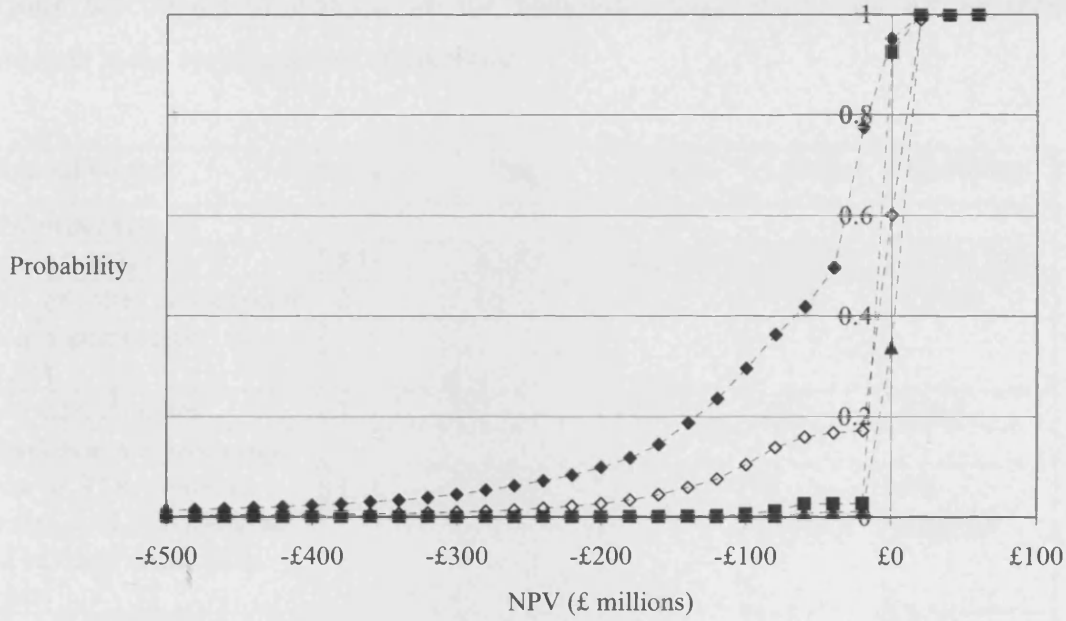

Figure 6.7 Cumulative distribution plots of the three options overlapped. (--◊--) denotes the automated RB route, (-- ♦--) denotes manual RB, (--■--) STR, and (--▲--) denotes the Wave route.

Having examined the rankings at the base case demand of 100kg, the impact of scale was explored.

6.7 Impact of Scale

6.7.1 Setting up the analysis

Spreadsheets were set up to determine the COG and NPV at demands 1kg, 10kg, 100kg, 1000kg and 10,000kg. The deterministic impact of the demand on the equipment requirements are summarised in Table 6.7. Monte Carlo simulations were then run using the triangular distributions identified with the values in Table 6.6 to compute the expected COG and NPV and their probability distributions.

Table 6.7 Impact of demand on the equipment requirements for the Deterministic analysis at the varying scales of operation

Annual Output	1kg	10kg	100kg	1,000kg	10,000kg
RB processes					
No. of RBs/year	833	8,333	83,333	833,333	8,333,333
No. of roller racks (each can accommodate 80 RBs)	2	15	151	1510	15104
No. of Cellmates	1	2	11	111	1111
Bulk reactor processes					
No. of STR process trains, and operating no. of batches required a year	1, 1	1, 1	1, 8	6, max 12	60, max 12
No. of WAVE process trains, and operating no. of batches required a year	1, 1	1, 1	1, 8	6, max 12	60, max 12
Working volume of WAVE/STR reactor	100L	500L	500L	500L	500L

6.7.2 Results of scale analysis

The impact of changing the demand and hence scale of operation on the expected NPV and COG is summarized in Table 6.8 and Fig.6.8. Table 6.8 shows that the manual roller bottle route can never reach profitability compared to the bulk reactor routes, and the disposable Wave route is always more profitable to operate in comparison to the STR route at the scales explored.

Interestingly, these results highlight that the ranking of the process alternatives is highly dependent on the scale of operation, at the smaller scale the automated RB route is more cost effective than the STR and the Wave routes. As the roller bottle systems are very easy to set up, thus the obvious advantage of the quicker to market with the RB process route makes it quite attractive at the small scale, especially the automated RB process.

However, adoption of the bulk fermenter routes is much more favourable if the demand is higher.

Table 6.8 Impact of changing the scale of operation upon the choice of process routes

		Scale				
Route	Parameter	1kg	10 kg	100kg	1,000kg	10,000kg
mRB	Expected COG (£/g)	1561	456	304	284	284
	Expected NPV (£ million)	-7.8	-15.9	-57.2	-468.1	-4689.0
aRB	Expected COG (£/g)	1545	292	114	104	101
	Expected NPV (£ million)	-6.5	-6.7	20.3	248.2	2669.0
STR	Expected COG (£/g)	3079	749	98	50	44
	Expected NPV (£ million)	-17.9	-35.9	26.6	571.5	6062.9
WAVE	Expected COG (£/g)	2165	571	74	43	40
	Expected NPV (£ million)	-12.4	-23.0	42.3	610.6	6293.8

Figure 6.8 shows that as the scale of operation increases, the bulk reactor routes are still the most favourable options. The difference at the 10kg scale and 1kg scale for the STR route is attributed to the difference in the size of the reactor required. Since for 1 kg production, the production vessel required is 100L, but for the 10kg production, the fermenter size increases to the 500L working volume. This size was set as the upper limit, since to get any bigger requires a long reactor train which was considered an undesirable for the primary cell line for making a TE product. Thus as the scale increases further, the only option to cope with production is to increase the number of reactor trains, rather than the size of the reactor. The Wave bioreactor however, merely uses differently sized bags, and the cost difference between the sizes of the rocking cradles is not as big as the differences in the cost of the stainless steel vessels for the STR routes at the smaller scale.

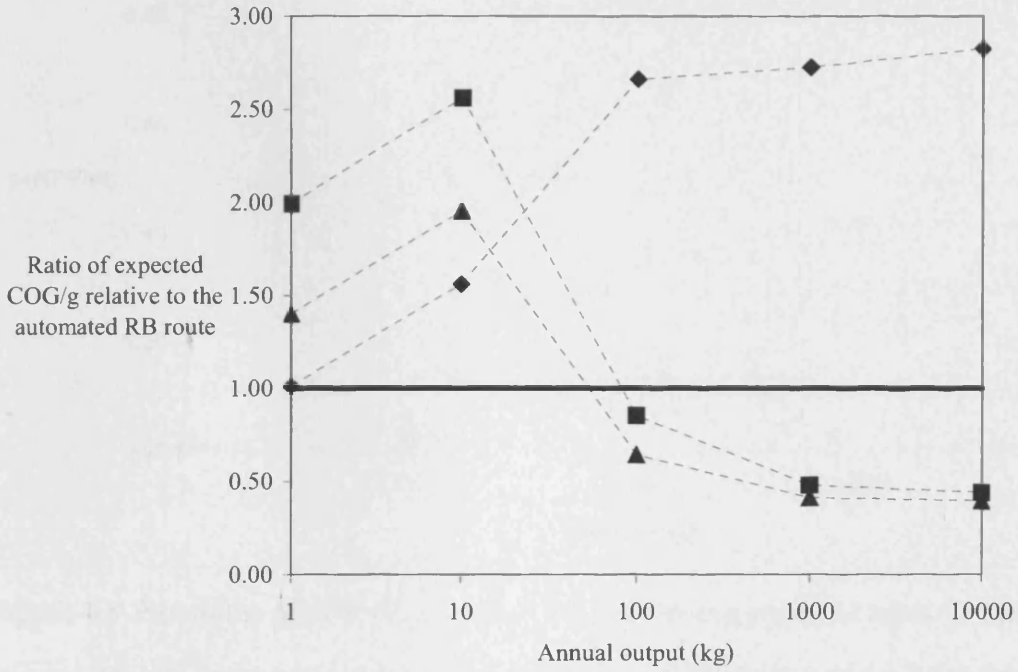

Figure 6.8 Ratio of the expected COG/g ratios across the operational scale of 1 kg to 10,000kg relative to the automated RB route. The bold black line denotes the automated RB case and the (--♦--) denotes manual RB, (--■--) for the STR, and (--▲--) for the Wave reactor route.

By examining the p(NPV>0) (Fig 6.9), as the scale of operation increases this becomes higher whereas at the lower end of the operation, the risk of failure to reach profitability is a lot higher. The best the manual roller bottle can ever achieve is ~40% success, whereas automation is able to double this and makes it more comparable to the STR and WAVE routes.

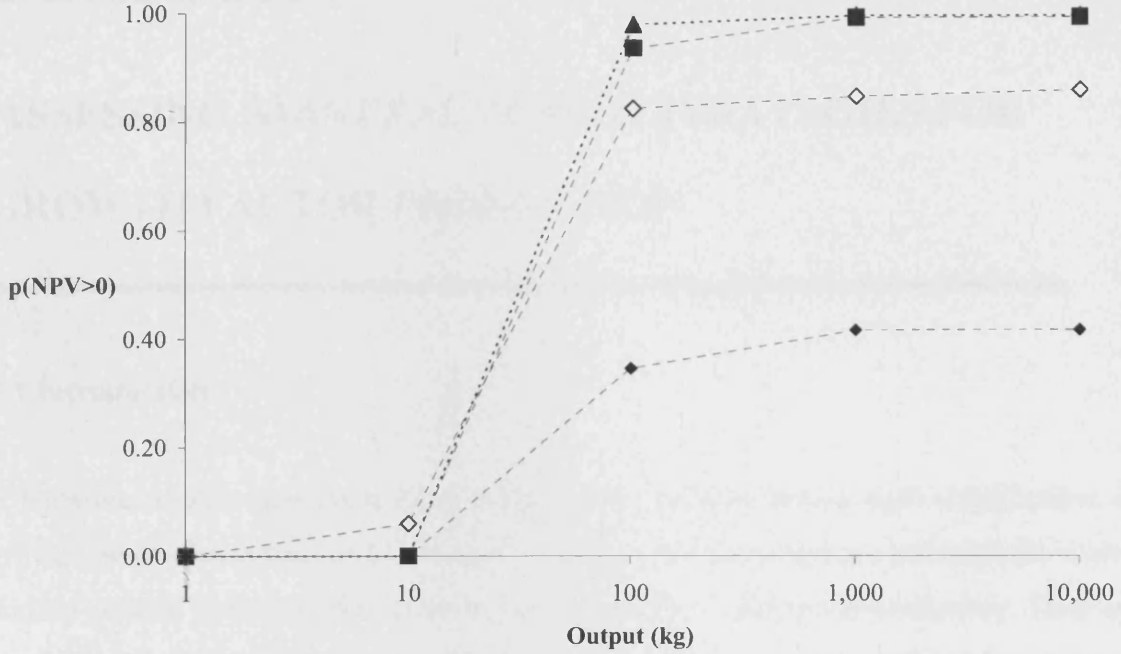

Figure 6.9 Plot of the p(NPV>0) vs. output for the various process routes. (♦) denotes manual RB, (◊) denotes automated RB, (■) denotes STR route, and (▲) denotes Wave route.

6.8 Conclusions

In conclusion, from the case study presented, the use of disposable Wave bioreactor technology could greatly benefit the process of producing bulk material for skin substitute products, and automation can lead to a massive reduction in costs if the choice of roller bottle technology is applied. However, a main limiting factor for these processes can be attributed to the general higher cost of media for mammalian cells and longer culture duration required, especially when compared to microbial cultures. Thus the next chapter examines the process economics for the production of growth factors targeting the wound market via microbial routes.

CHAPTER 7

ASSESSING MANUFACTURING STRATEGIES FOR GROWTH FACTOR PRODUCTION

7.1 Introduction

Alternatives to skin substitutes for treating chronic wounds include topical application of growth factors formulated as either a gel or spray. Growth factors are polypeptides which control cellular growth, differentiation and proliferation, and protein production. They are also referred to as cytokines and are the mediators of the multiple cellular processes of wound healing. Growth factors are required to promote tissue regeneration by inducing angiogenesis. The controlled release of growth factors for tissue regeneration will play a strong part as one of the essential technologies of the future in regenerative medicine (Tabata, 2003). This chapter evaluates the process economics behind the production of growth factors using recombinant technology.

Growth factors have been applied topically to chronic wounds giving variable results, and this is partly due to the complexity of the actions these growth factors or cytokines can instigate. Fergerson and O'Kane (2004) reported that by manipulating the various levels of the factors TGF-β1, TGF-β2, TGF-β3 and PDGF, healing can be accelerated and more impressively, scar-free healing promoted. KGF-2 (Repifermin) developed by Human Genome Sciences as a potential treatment for cancer therapy induced mucositis demonstrating that KGF-2 contributes towards healing of tissues containing keratinocytes. They are currently in Phase 2 Clinical Trials. Additionally, Amgen has also completed a Phase 3 clinical trial of KGF-1, which is similar to Repifermin showing the ability of KGF-1 to reduce the duration and incidence of oral muscositis.

Renovo (Manchester, UK) has a portfolio of therapeutic products targeted at wound healing. Among this portfolio are therapeutics based on the use of growth factors. Juvista (TGF-β3) and Prevascar (IL-10) are its lead products currently in phase II clinical trials. Tissue Repair Company (TRC), a San Diego based pharmaceutical company has focused on the development of growth factor therapeutics for the potential treatment of chronic diabetic wounds. The lead product Excellarate is currently in clinical trials.

To date, the only growth factor products to have penetrated the market and have active sales are Regranex gel (Johnson and Johnson, New Jersey) and Fiblast spray (Kaken Pharmaceuticals Co., Tokyo) (Table 7.1). Regranex (rPDGF) and Fiblast (rbFGF) are both single growth factor treatments for foot ulcers and in 2004, they reached sales of $160million and ¥3.4 billion respectively. Harding et al. (2002) commented that in future growth factors may be administered sequentially or in a combination for increased efficacy.

Table 7.1 Production methods used to produce the commercial topical growth factors

Product	Company	Product and Process Description	Cost	Year approved	Sources
Regranex gel	Johnson and Johnson	Topical application containing a secreted growth factor rPDGF Kept refrigerated . Derived from Yeast.	£275 for a 15g tube	1998	www.rxlist.com www.regranex.com
Fiblast spray	Kaken Pharmaceuticals	Topical application containing a bound growth factor rbFGF Freeze-dried powder, reconstituted upon usage. Derived from *E.coli*	£60 pounds for a 500ml spray	2001	Annual Report from Kaken Pharmaceuticals

This chapter characterises and compares the process economics of growth factor production in yeast versus *E.coli*. The critical trade-offs and success factors are identified for both single growth factor therapies and multiple growth factor therapies.

7.2 Case Study Background

The active ingredient in Regranex gel is PDGF (Platelet derived growth factor) and this is expressed using the yeast *Sacchromyces cerevisiae* in a secretory manner. Yeast cells possess secretion machinery and the ability to perform post-translational modifications; these advantages ensure bioactive product is expressed and simplifies the downstream processing. Other growth factors have been produced using *E. coli* (Meagher et al., 1994; Wu et al., 2005), however this tends to result in the formation of inclusion bodies (IBs). Advantages are the higher levels of expression that can be achieved, ease of IB isolation by host cell disruption and centrifugation, and the stability of the IBs (Graumann and Premstaller, 2006). Unfortunately, inclusion bodies can make bioprocessing difficult and increase the number of unit operations (namely solubilisation and refolding) compared to the growth factors which can be secreted instead. A process economics study was therefore set up to assess the financial impact of the relative merits and limitations of processes based on yeast and *E.coli* expression systems.

The yeast route was further extended to compare production in stainless steel fermenter versus disposable Wave bioreactors. The marketed growth factors are currently produced in stirred tank reactors. Typically, processes in industry for microbial systems have used stainless steel fermenters and not the disposable Wave bioreactor, because of oxygen transfer limitations. However, Mikola et al. (2007) reported the use of the Wave bioreactor for successful yeast cultivation, and obtained k_La values of 60 h^{-1}, thus a process route using the disposable Wave bioreactor was considered as an alternative to the stainless steel STR.

The process descriptions were derived from literature searches, and existing approved products on the market, Regranex gel and Fiblast Spray. Fig. 7.1 and 7.2 illustrate the process flowsheets derived based on the papers published by Chiron Corporation (Barr, 1998) and British Biotechology Ltd. (Cook, 1992) for the production of PDGF from yeast. Additionally, the chromatograpy steps are based on the purification process patented by Scios Nova Inc (Shadle, 1994) for bFGF.

For the *E.coli* route, the traditional route for inclusion body processing was chosen (Fig. 7.2). However, there can be other routes; Lee et al. (2006) showed that IB processing can be intensified by using chemical extraction compared to the traditional route of homogenisation, centrifugation and resuspension for the production of GM-CSF. However, it is important to remember that chemical extraction will also have to contend with proper waste stream disposal routes, for example, Triton X-100 is toxic to aquatic life and must be disposed of through specialist waste contractors.

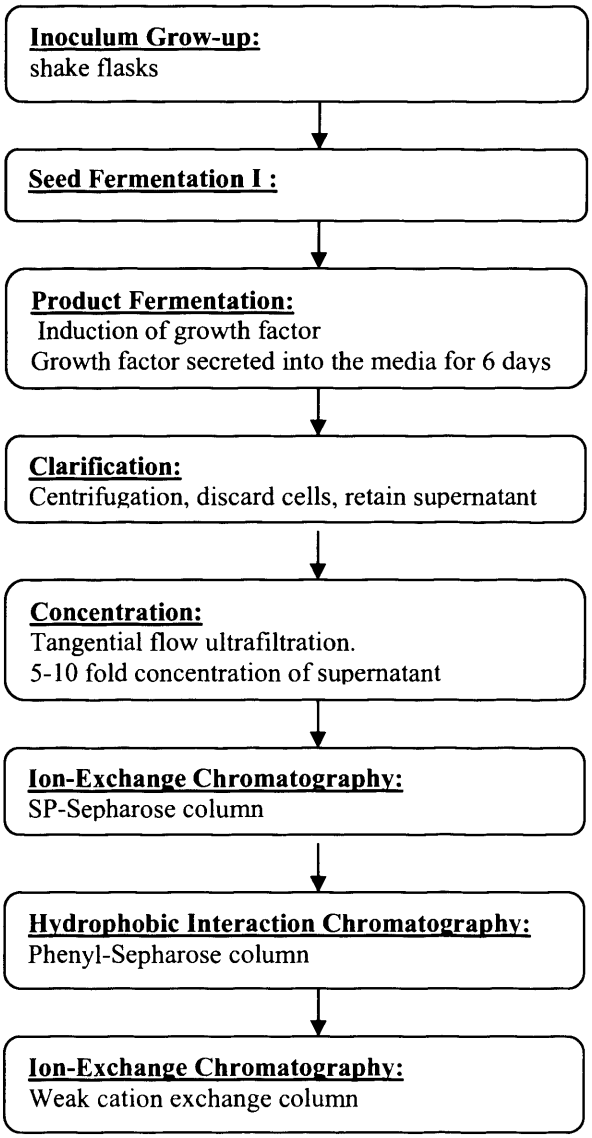

Figure 7.1 Flowsheet for the production of growth factors using the Yeast route (Secretory, STR and Wave)

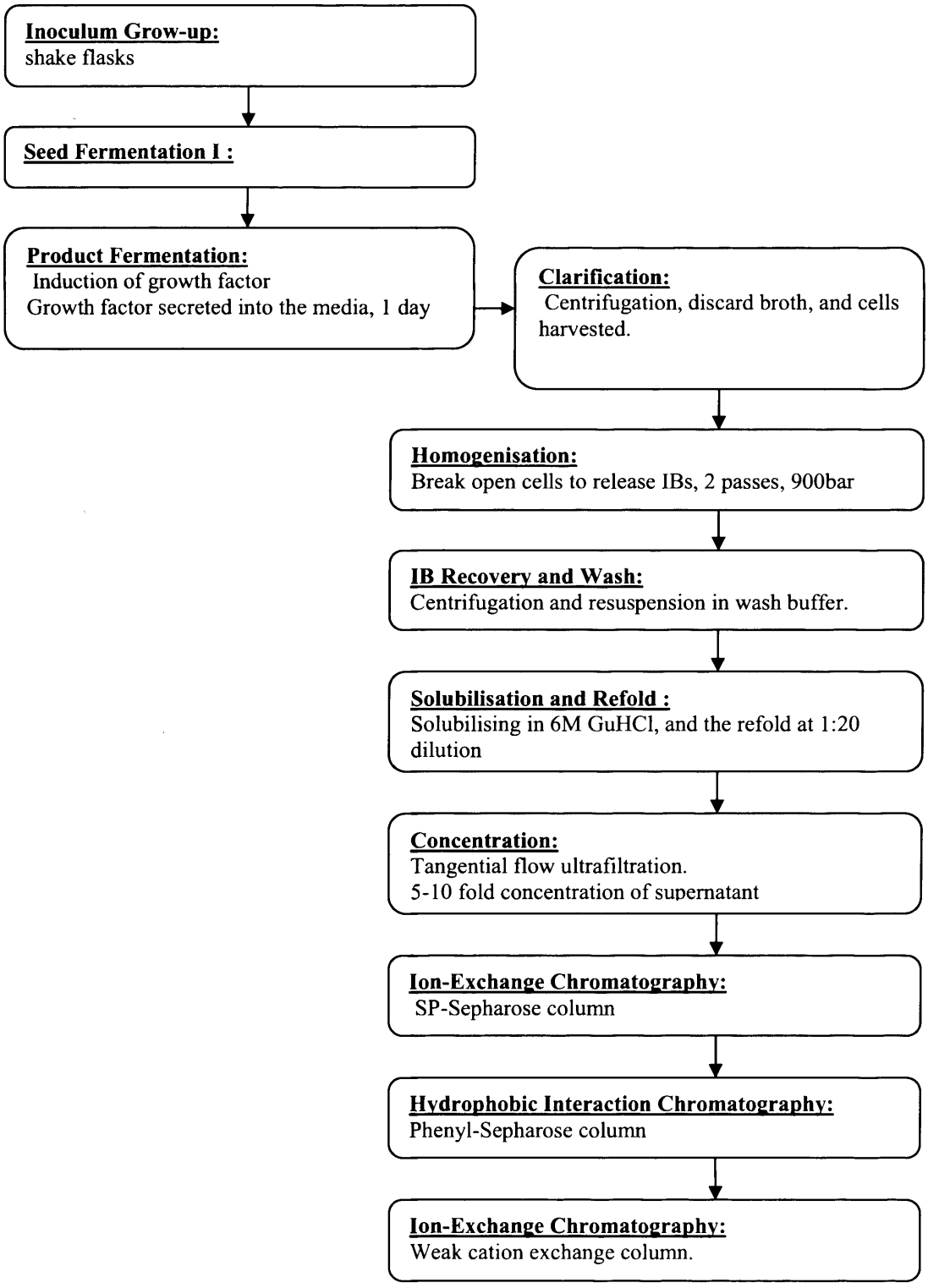

Figure 7.2 Flowsheet for the production of growth factors using the *E.coli* route (Non-secretory, STR)

7.3 Deterministic Analysis

7.3.1 Methodology

Microsoft Excel XP was set up as described by Chapter 5, and a database of required information was gathered from contacting vendors and companies. Table 7.2 lists the key assumptions made to model the scenario.

Table 7.2 Assumptions for the case base for the three process routes

	YEAST-STR	YEAST-WAVE	E.COLI-STR
Annual Production (g)	600	600	600
Production bioreactor size (L)	6000, 4500 (working volume)	1000, 500 (working volume)	1000, 750 (working volume)
Duration of Fermentration (day)	6	6	1
Sales Price per gram of API (£)	146,666	146,666	146,666
No. of Production bioreactors	1	9	1
Total number of batches	21	181	2
Titre (mg/L)	10	10	1000
Lang Factor	8.1	4.18	8.1
Overall Process Yield	0.95^5	0.95^5	0.95^8

In order to determine the scale of operation, the demand was derived based on the annual sales of Regranex gel. The number of tubes sold resulted in the predicted annual demand of API of 600g. This was based on the description that Regranex gel tube is 15 g, and the active ingredient in the gel is 0.01%.

The sizing of the production reactor was based on calculation of the annual culture broth required given the titre, overall yield and the number of batches that could be processed

in a year. The maximum annual number of batches per process train was determined as 21 batches for yeast and 24 batches for *E. coli* based on the duration of the processes and the number of working days in a year. Thus if the annual production of 600g could not be matched by 1 process train operating at the maximum, the model then increased the number of process trains to match this. However, as the Wave reactor has an upper limit of 1000L, this meant the requirement of 9 Wave reactors to feed into a DSP chain. For the *E.coli* scenario, because of the possibility of the higher titre, this meant, you could have either a bioreactor of 100L, operating 15 batches a year, or alternatively by having a 1000L reactor, 2 batches would give the required amount. Thus if this forecasted annual production of 600g increases the facility could easily accommodate or if only 2 batches are required, then consideration of choosing a contract manufacturer could be more favourable than building a facility where only 2 batches are required. For the sake of comparison for this Chapter, the scenario of operating 2 batches in a facility with 1000L reactor was chosen for the *E.coli* scenario. Fermentation for yeast culture was 6 days based on the information published by Cook et al. (1992), and 1 day for *E. coli* as is typical for *E. coli* processes (Sivakesava et al. 1999, Kim et al. 2007).

Growth factor titres of 10mg/L and 1g/L were assumed for the yeast and E.coli routes. There values were based on literature sources reporting varying titres for growth factors, some as little as 0.62mg/L to 133mg/L for yeast secreted growth factors (Siemeister, 1996; Joo-Hyung Heo, 2002; Soler, 2003; Barr, 1998; Wu, 2005). Titres reported for *E. coli* generally are in g/L as oppose to mg/L, but ranges of 10mg/L to 9.7g/L have been reported for different growth factors. (Soler et al., 2003; Seeger et al., 1995; Hu et al., 2004)

In order to generate a cashflow to calculate the economic profitability indicator, NPV, a perceived sales price was required to determine the income. The sales price per gram of growth factor was derived from the sales price of Regranex gel and Fiblast spray. As each gel tube for Regranex gel was 15g, and sold for £275, of which 0.01% was the active ingredient, this gave the estimated sales price £183,333 per gram for the API. It was

assumed that the bulk product would command 4/5 of the sales price of the final formulated product.

The Lang factor was derived as described in previous chapters, based on the method, reported by Novais et al., (2001). Calculation of overall process yield was simplified by assuming 0.95^n, where n is the number of unit operations. Thus this takes into account the extra steps that the *E.coli* process consisted of.

7.3.2 Results and Discussion

Comparison of the economic indicators across the three processing routes showed that the *E.coli* route was the most profitable route with the lowest COG/g, FCI and highest NPV and this is mainly attributed to the fact that the E.coli route can achieve the 1g/L titre mark, thereby decreasing the number of batches required and the size of reactor. This also showed the economy of scale. The Yeast-WAVE route was the most unfavourable because of the size limitation of the reactor, which meant the increasing the number of rocking cradles and the number of batches required. The Yeast-STR had the higher FCI due to the higher Lang factor but when compared to the WAVE there is the reduction in COG/g and higher NPV which showed the benefit of the economies of scale, whereby less batches are required.

Table 7.3 Summary of COG/g, FCI and NPV across the three routes

	COG/g (£)	FCI (£ millions)	NPV (£ millions)
Yeast-STR	17,202	35.3	302.5
Yeast-WAVE	45,363	25.5	235.4
E.coli-STR	5,656	11.7	345.8

7.3.2.1 Total Equipment Purchase Costs (TEPC)

Examining the breakdown of the equipment costs in terms of ratios as shown by Fig 7.3 indicated that DSP formed the majority of the cost for the STR options when compared to the Wave option. The difference between the Yeast-STR and E.coli-STR was due to higher titre of the *E.coli* and this was examined further in the sensitivity analysis. Yeast WAVE had the higher USP when compared to the Yeast STR was due to the requirement of 9 production bioreactors versus one production reactor.

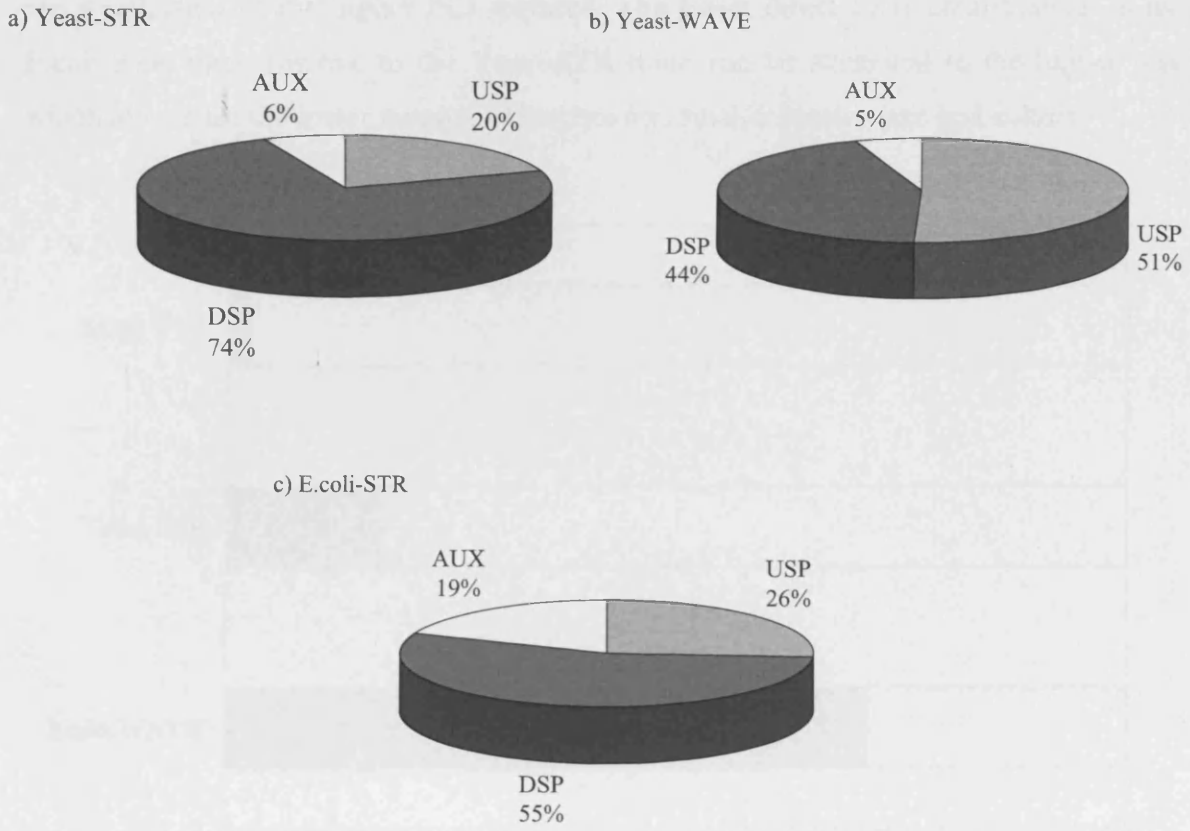

Figure 7.3 Breakdown of the equipment costs for the three processing routes. a) Yeast-STR, b) Yeast-WAVE, and c) *E.coli*-STR. USP = Upstream processing equipment, DSP = Downstream processing equipment, and AUX = Auxillary equipment.

7.3.2.2 Annual COG/g

The breakdown of the annual COG/g in terms of direct and indirect costs for the three process routes is shown by Fig. 7.4. The ratio of direct to indirect costs is dominated by the indirect costs for the Yeast-STR (17:83), and *E.coli*-STR (3:97) routes whereas direct costs dominate in the Yeast-WAVE route (71:29). This is due to the disposable nature of the Yeast-WAVE route which lowers the FCI and hence the indirect costs whilst also increasing the materials costs due the increased use of Cell bags, and other miscellaneous costs such as general tubing usage. The higher indirect costs in the stainless steel routes are a reflection of the higher FCI required. The lower direct costs contributions in the E.coli STR route relative to the Yeast-STR route can be attributed to the higher titre which allows for the lower number of batches and smaller reactor size and culture.

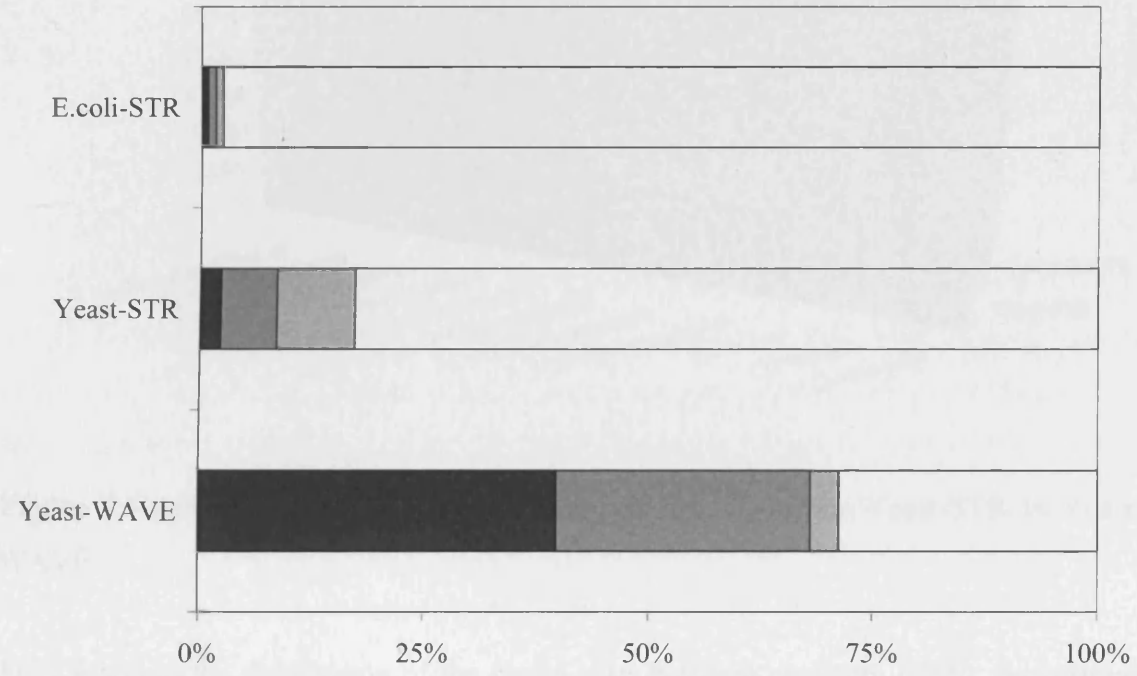

Figure 7.4 Comparison of the direct to indirect costs across the three routes with (■) Materials, (■) Labour, (■) Utilities and (□) Indirect costs.

7.3.2.3 Direct COG/g

Breakdown of the direct costs onto a task basis (as shown by Fig 7.5) revealed that CIP and SIP were dominant costs. Although there is a reduction in the costs of the Yeast-WAVE route but the inflated costs of the upstream and higher media prep costs can be observed due to the need for 9 WAVE bioreactors working at full capacity. Thus this showed the economy of scale for the stainless steel route.

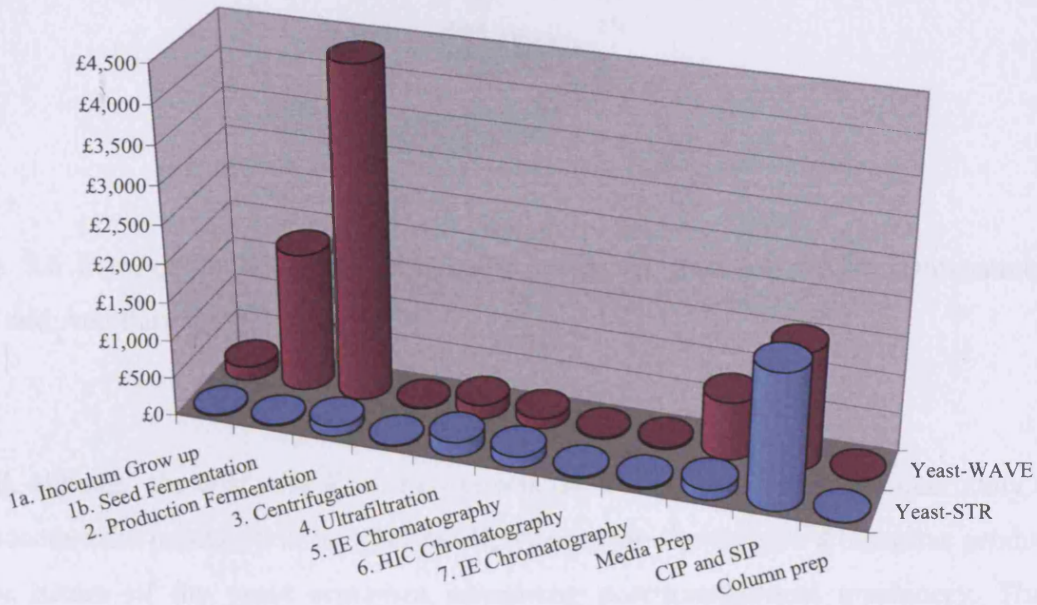

Figure 7.5 Annual direct cost of goods/g on a task basis for the Yeast-STR vs Yeast - WAVE.

Fig 7.6 shows the distribution of the direct costs between upstream (USP), downstream (DSP) and ancillary (ANC) activities. The breakdown ratio of the costs was very similar for both *E.coli*-STR and Yeast-STR. For the Yeast-WAVE there was the reduction in the ancillary unit operations cost which was balanced by the increase in the costs for USP.

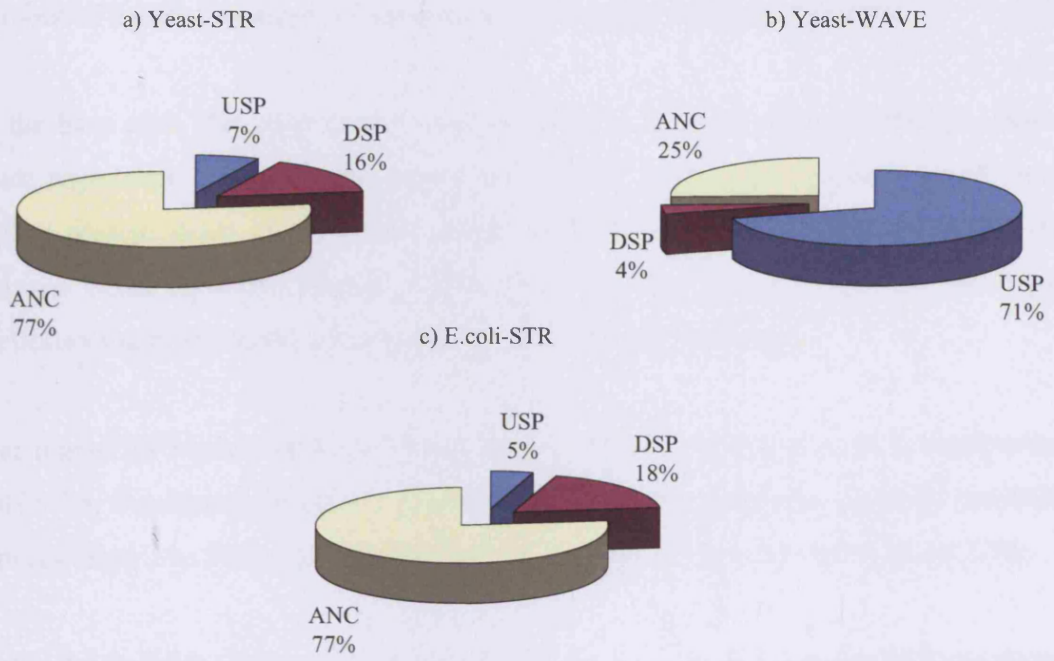

Figure 7.6 Breakdown of the direct costs in terms of Upstream (USP), Downstream (DSP) and Ancillary (ANC) activities.

Overall, although the cost with *E. coli* route was the lowest, there was the uncertainty of how bioactive the product will be whereas the yeast route should give a bioactive product due the nature of the yeast organism possessing post-translational machinery. Thus sensitivity analysis on the effect of titre was carried out on the process routes that used yeast. Additionally, the effect of changing the scale of operation was examined, such as what happened when the scale doubled or halved.

7.3.3 Sensitivity Analysis

Sensitivity analysis was undertaken to examine the impact of titre upon the process routes as titre was a critical process economic driver. Additionally, the annual demand affects the scale of operation, and the number of batches required per year. Therefore the process models were used to examine what happened if the demand was halved, or doubled.

Again, for the process models, the variables: fermenter size, and no. of reactors and the number of batches changed in response to the changes in demand or titre.

In the base case, the yeast routes were assumed to achieve a titre of 10mg/L, however, yeast expression systems have improved over the years, and typically result in much higher protein titres, with typical values of 4g/L for *S. cerevisiae* and 15g/L for *P. pastoris* being reported (Werner, 2005). The sensitivity analysis explored the impact of the following titires in the yeast routes: 1, 10, 100, and 1000mg/L.

The impact of increasing titres in the facility size and running costs is summarised in Table 7.4. Increasing titre has a dramatic impact on the fermenter capacity required and moving from 1 to 1000mg/L decreases the annual capacity from 775,413L to 775L.

Table 7.4 Impact of Titre on the USP:DSP (COG/g) ratio, and direct to indirect costs (COG/g)

Titre (mg/L)	1	10	100	1000
Annual capacity required for the yeast routes (L)	775,413	77,541	7,754	775
Yeast-STR				
Reactor size (L)	6000	6000	1000	1000
No. of batches	173	18	11	2
No. of reactor trains	9	1	1	1
Direct:Indirect ratio	25 : 75	17 : 83	14 : 86	3 : 97
USP:DSP ratio	16: 84	19 : 81	48 : 52	46 : 54
Yeast-WAVE				
Reactor size	1000	1000	1000	1000
No. of batches	1551	156	16	2
No. of reactor trains	74	8	1	1
Direct:Indirect ratio	87 : 13	71 : 29	21 : 78	4 : 96
USP:DSP ratio	98 : 2	87 : 13	39 : 61	36 : 64
E.coli-STR				
Reactor size	N/A			1000
No. of batches				2
No. of reactor trains				1
Direct:Indirect ratio				2 : 98
USP:DSP ratio				28 : 72

For the Yeast-WAVE route, as the titre increased, the focus of the cost shifted from USP to DSP. This trend has been observed for monoclonal antibody production; Sommerfeld and Strube (2005) showed that increasing the fermentation titre 10 fold from 0.1 g to 1g/L caused the ratio of USP:DSP to change from 55:45 to 30:70. The Yeast-STR does show this increase in DSP when comparing the 0.1g to 1g/L, but not for the 1mg/L and 10mg/L and this was due to the changes in the number of batches, and size of fermentation. However, DSP is more of a dominant factor the Yeast-STR routes, as the ability to operate large tank sizes for the USP meant economy of scale. Overall, DSP cost more for the *E. coli* than the yeast routes because there are more DSP unit operations when compared at the same titre.

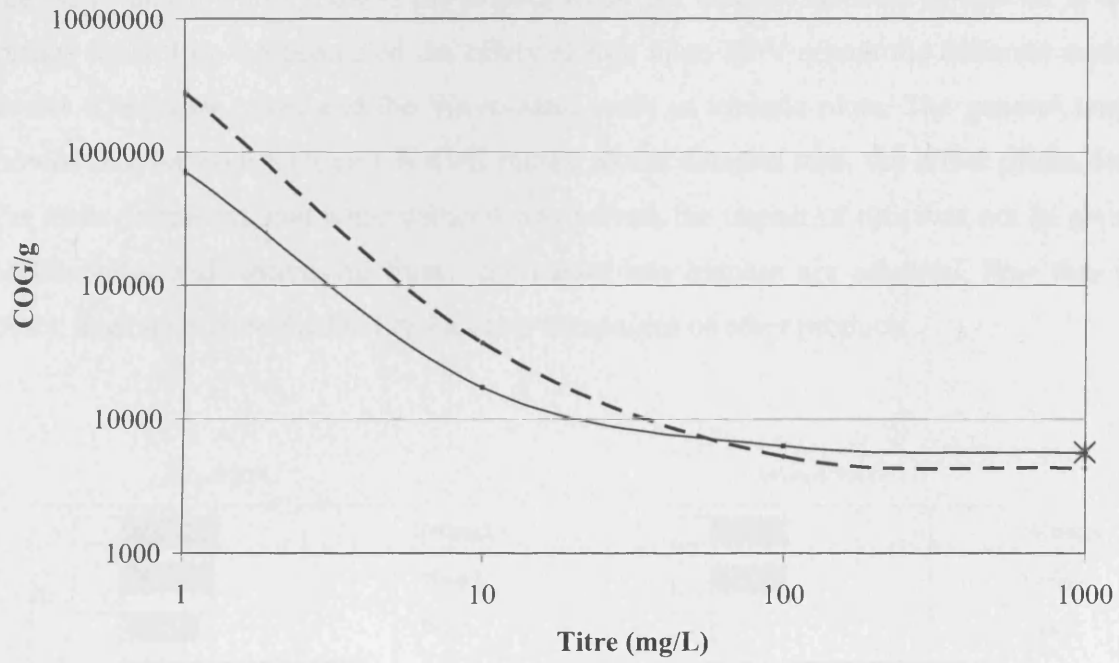

Figure 7.7 COG/g for the three process options across titres. The solid line represents the STR-yeast and the dotted line is the WAVE-yeast. The symbol × marks the STR-E.coli option.

Additionally, the ratio of direct to indirect costs shifted towards indirect costs as the titre increased, simply because, as the number of batches decreased, process trains are

decreased, and therefore the ratio of amount of direct costs decreased more dramatically, as opposed to the indirect costs.

Fig.7.7 shows the impact of changing the titre on the cost of goods. As the titre increased, the COG/g is reduced and there is a rapid change initially, and then a plateau is reached. Indeed, when the titre goes beyond 100mg/L, the yeast processing routes are equally favourable as the E.coli route. Interestingly, above the 100mg/L, the Yeast-WAVE route is more favourable than STR-routes, as the FCI is lower for the Yeast-WAVE route due to the ease of installation of the flexible disposable fermentation system in comparison to the amount of stainless piping that is required for the STR routes.

The NPV analysis also showed the impact when the demand doubled or halved at the various titres. Fig. 7.8 presented the effect of titre upon NPV across the different scales for the STR-yeast route, and the Wave-yeast route as tornado plots. The general trend showed that for both STR and WAVE routes, as the demand rose, the effect of the titre was more prominent, and when demand was halved, the impact of titre was not as great. Additionally, with increasing titres, this meant less batches are required, thus this in effect, frees up time in the facility for other campaigns of other products.

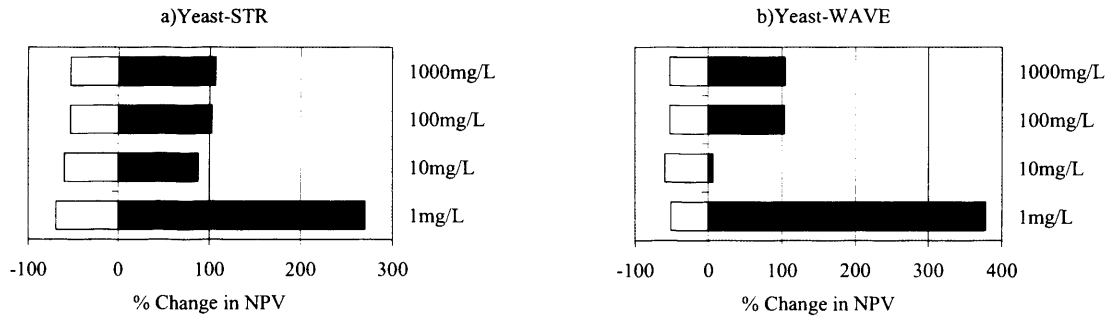

Figure 7.8 NPV for the a) STR-Yeast and b) WAVE-yeast across titres and demonstrating the effect of demand upon the NPV. ■ denote doubling of the demand and □ denote halving the demand.

An additional consideration would be the scenario of multiple growth factor applications, since culture supernatant from human dermal fibroblasts has been used as a potential treatment in wound healing or as anti-ageing products. The culture supernatant contains a cocktail of growth factors, examples of such products being commercialised are Epigrow (Clinical Cell Culture C3, Australia), Retivitx (Organogenesis US), Bio-restorative skin cream with PSP (Neocutis, Inc, US). Thus the next section examined the process economics of multiple growth factor application and compared this to the TE approach using dermal fibroblasts.

7.3.4 Multiple growth factor production

It was estimated that Dermagraft possessed 15 different growth factors thus this was compared to the microbial approach of producing 15 different growth factors in a multi-product facility. As the levels of growth factors in the skin-substitute product were not fully identified or known, to rationalise the comparison, it was assumed that 8 patches for treating a chronic ulcer were equivalent to 56g of growth factor gel. (See Appendix C for full details on assumption). Thus by comparing to the 100kg of ECM matrix production, this meant that the annual amount of growth factor to be produced would be 15 lots of 95g each growth factor. From this, it was calculated that a 200L reactor was required for fermentation, to process ~120L to 150L for each batch of growth factors. For the calculation of the NPV, the sales prices was assumed at the worst case scenario where the tube would still be sold for the same price, but containing 15 growth factors instead of one. This was calculated to be £9777 per gram of growth factors. [£275 for 15g tube, of which 0.15% contains the growth factors rather than 0.01%]

Table 7.5 presents a summary of the results of the multi-growth factor analysis. It displays the economic parameters, and shows that a multi-growth factor facility is very economically feasible and the most profitable route would be to go down the disposable route.

Table 7.5 Multi-growth factor production via the 3 production routes

	E.coli-STR	Yeast-STR	Yeast-WAVE
Inputs			
Titre (g/L)	1	1	1
Number of GFs	15	15	15
Lang Factor	8.13	8.13	5.44
Reactor size (L)	200	200	200
Sales Price (£)	9,777	9,777	9,777
Economic parameters			
Number of reactor	1	1	1
Total number of batches	15	15	15
COG/g (£)	2,473	2,523	2,049
FCI (£ millions)	10.6	10.3	7.3
NPV (£ millions)	36.9	36.8	41.5

From the results presented by Table 7.5, the most favourable route for multi-growth factor production would be the Yeast-WAVE route, followed by the Yeast-STR and finally, *E.coli*-STR. Thus the results show that if the titre was the same, yeast was preferable to the *E.coli* route. Furthermore, utilising the disposable WAVE route would need the reduction of CIP and SIP for the upstream processing, which is very attractive especially when producing 15 lots of different growth factors. The FCI is the highest for the *E.coli*-STR route because of the extra unit operations when compared to the yeast route.

NPV across the three routes are very similar, and the COG/g values are the same order of magnitude. As the Yeast-WAVE has the most positive NPV, and the lowest COG, this would indicate the Yeast-WAVE would be the most ideal route to choose. However, this would be dependent on achieving the necessary titre in the fermentation culture, and concerns with oxygen transfer limitations and being dependent on a sole supplier for the cellbags would mean choosing the Yeast-STR route.

Comparison of the NPV for the microbial growth factor approach to the TE-ECM approach from the previous chapter showed that making several growth factors from the microbial approach and recombining to form a growth factor gel was not as favourable.

Table 7.6 summarises this and shows that they are in the similar region with a positive NPV.

To a certain extent, the NPV values are dictated by the sales price, thus instead of taking the worst case scenario for the price of the growth factor, this would then make the growth factor production using the microbial approach more favourable than the TE approach. However, the NPV values indicated that production of growth factors was commercially possible.

Table 7.6 Summary of the COG and NPV values for the different approaches

	Annual COG (£millions)	NPV (£millions)
Automated RB-TE	9.7	29.9
STR-TE	7.4	38.4
WAVE -TE	5.1	53.4
E.coli –STR	3.5	37.0
Yeast –STR	3.6	36.8
Yeast –WAVE	2.9	42.5

7.4 Conclusions

From the process simulation models, this shows that if the titre of growth factor for the yeast processing route was above the 100mg/L, then the process economics are more favourable than the IB processing route using *E.coli*, even when demand doubled. Indeed, assessing which processing route to take would probably depend on whether the growth factor produced via the *E.coli* IB route have the necessary bioactivity, otherwise, the default choice would be the yeast processing route.

If the plant was to be making multiple growth factors then the disposable yeast processing route would be more favourable, however, the risk of only having a sole supplier for the cell bag would mean that the traditional STR route was chosen. For production of growth factors aimed at treating wound-healing, the multifactorial complexity that exists means that combinations of growth factors would be the more desirable option. However, the analysis showed that to make the same number of different growth factors via the microbial approach was not as economically favourable as using the dermal fibroblasts to produce to the range of growth factors, but the difference was not as dramatic as imagined.

CHAPTER 8

REGULATORY ISSUES

8.1 Introduction

This chapter examines the regulatory issues that are faced by the TE-products. The pioneering skin-substitute products first brought to market cited that regulatory barriers were one the main reasons for high cash-burn rate and by falling into the gap between the definitions of a medical device/drug meant significant delays in obtaining approval (Naughton, 2001, Bouchie, 2002). There is a comprehensive need to prove the safety and efficacy of these cell-based therapy products and this presented a major challenge to the companies as well as the regulating bodies, but clearly, the 'one size fits all' solution does not apply and the clear guidelines needs to be established.

8.2 Autologous vs Allogenic

The first critical component to be decided in these TE-products will be the identification of cell source: autologous vs allogenic. This will affect the manufacturing route, and the commercial strategy taken by the company, and additionally what regulatory path to take. Material from other mammalian sources has also been used in humans (xenogenic) but this has its potential risks (e.g. transmission of viruses crossing the species barrier). Autologous means using the cells obtained from the patient whereas allogenic focuses on the use of one or few donors to generate a supply for others. The autologous route is considered the more straight forward route because it is easier to comply with the regulatory and safety requirements in comparison to the allogenic route. By following the autologous route, this becomes more like a service based industry, and the patient actively seek out the treatment and relocate to the treatment centre, whereas the allogenic route will mean the product is transported to the patient, probably in the cryopreserved format. Autologous products are unlikely to require any long term tissue storage and thus

cold preservation is likely to suffice. The allogeneic route offers the relative compatibility to large-scale manufacturing at single sites and part of the regulatory costs will be to prove the safety of cell banking and expansion.

8.3 Regulatory frameworks

There is no specific regulatory framework for TE-products in the UK currently but reference should be made to the guidance document, *A Code of practice for the production of Human-derived therapeutic products, 2002.* It seems the situation in the UK is reviewed on case by case. Additionally, the Department of Health have produced certain reference documents, which advises on the various actions required. The *Guidance on the Microbiological Safety of Human organs, tissue and cell used in Transplantation, 2000*, and *A Code of practice for tissue banks – providing tissues of human origin for therapeutic purposes, 2001* should be consulted.

The announcement of the *Regulation of Advanced Therapies: Tissue Engineering, Cell therapy, and Gene therapy* on 16th November 2005 by the EC means a clearer way forward for the companies to take. The provisions in the proposal were that TE-products falling within the definition of medicinal product are to be regarded as advanced medicinal therapy product and grouped with gene therapy, and somatic cell therapy. The TE-product is defined as containing engineered cells or tissues and is presented to have properties of treating or preventing disease in humans. It is proposed that a centralised Community marketing authorisation would apply, and a Committee for Advanced Therapies (CAT) should be established to give scientific advice on advanced therapy medicinal products.

In the US, the FDA has grasped the implications of creating and implanting a product that contains cells as well as biomaterials and regulates on a case-by-case basis. In 1998, Genzyme's Carticel was launched where chrondral cells removed from the patient are cultured and then reintroduced to repair the cartilage defect, marketed as a surgical device. The FDA had it withdrawn until a biologic license application had been made. Fig. 8.1 shows the blueprint for the FDA's approach to regulating human cell and tissues

in its *Proposed Approach to Regulation of Cellular and Tissue-Based Products* released in 1997. This document also outlines the determination of donor suitability. Additionally, proposed rules for good tissue practice and final rules on establishment registration and listing were issues in 2001.

Figure 8.1 Flow-chart to determine the regulatory pathway (361 HCT/P or 351 HCT/P). A 361HCT/P must comply with the tissue rules. A 351 HCT/P must comply with the tissue rules and premarket approval authorities (BLA/PMA). (Darin Weber, 2004)

In 2002, the FDA established a specific Office of Combination Products. The FDA's Tissue Reference Task Group will assess the product's primary mode of action and thus decide which agency (CBER, CDER, or CDRH) will take the lead in the regulation of the product. Additionally, the FDA also decided that should the TE-product contain biopharmaceuticals such as growth factors, cytokines, enzymes or immunomodulators, as well as cells and biomaterials it will be assessed by all three centers.

Implications of the regulatory frameworks will ultimately dictate the level of revenue the company can make. In the States, if classed as a biologic rather than a device, then reimbursement is available at the Average Selling Price plus 6%, allowing the customers to make some money upon acquisition of the product. This enhances product penetration into the market, plus additionally, under Medicare, procedures codes are billed in the region of $400-700 for the level of debridement or surgical prep needed. This makes the use of the products more profitable for the centres, and ultimately leads to product uptake.

8.4 Conclusions

Although the microcarrier cultures could generate the biomass which could be formulated into gel, the problems with aggregation in culture makes the monitoring of cell numbers very difficult and therefore compromising the ease of culture. From a regulatory point of view, this could cause problems, as the need to demonstrate control of process is required. Thus ability to link the amount of nutrients are utilised by the cells and more understanding of this could help then form a correlation between nutrient usage to cell numbers over the progress of the culture to demonstrate the necessary control of process. However, because of the varying regulatory burden from country to country, this makes the marketing of tissue-engineered products hard, and as such, until more rules become defined, charting uncertain territory will be one of the key risks to be faced.

CHAPTER 9

FUTURE WORK

9.1 Introduction

As Archer and Williams (2005) wrote, it is time to study tissue production from an engineering point of view. There is the need to consider what type of automation could be applied to each case. The application of economic modelling to enhance the decision making has been demonstrated here and could be applied to other tissue-engineered products. Depending on which organ is to be produced, the need to develop scalable automated systems for manufacturing will always exist. This chapter summarises the conclusions drawn from the previous chapters and points out the future developments that could further enhance the quality of decision making, and the path for companies to take.

9.2 Summary of the technical and future work

The work in this thesis demonstrated that microcarrier culture is a viable and efficient way of culturing human dermal fibroblasts to generate extracellular matrix on a large scale. The use of microcarriers opens up the variety of reactor configurations to give space savings and more efficient media utilisation, and ultimately a route for automated manufacture.

Future work is recommended to evaluate the potential of microcarrier culture for the cell expansion for other cell types. Critically, overcoming or controlling the aggregation that occurs would be required for this approach to ensure reliable measurements and thus, to have greater control. Ways to reduce the aggregation may be to alter the media utilised, impeller design and speeds. This could be coupled to shear studies to fully understand the

flow profiles and avoid applying lethal stresses. The shear studies could also help explore aggregation studies. By controlling the level of shear applied, it may be possible to reduce the aggregation and also to stimulate growth and extracellular matrix production of the cells. Furthermore investigation into possible methods for improving the monitoring capabilities would be useful with the aim of more automated online monitoring.

Further investigation into the optimal culture duration is required. This would require clinical data on the required levels of collagen and growth factors for wound-healing. If collagen is not the most critical component, then it may be possible to shorten culture time. This would result in a more cost-effective option, a reduction in the risk of batch failures due to contamination, and allow more repeatable robust batches.

Different microcarriers were explored in this thesis: commercial smooth discs and microporous spheres, and biodegradeable discs made in-house. It would be ideal to work with a commercial biodegradable microcarrier that is designed to similar density to that of cells, or different degradation profiles to fit the culture time required. At present, no commercial biodegradeable microcarriers exist and so further studies on creating ones with robust characteristics would be useful. Indeed, having the microcarriers as biocompatible constructs would further reinforce the principle of the 'the process is the product'.

The need for serum-free culture is required, and a process that avoids the use of raw materials of animal origin would be favoured by the regulatory authorities. Future work could investigate the nutrient needs of the cell line, and apply metabolic pathway analysis to determine the correct medium formulation at the right time. Application of factorial design to find the optimal conditions for growth and production of growth factors by the cells would be desirable. This would help define an operating space. Due to the high expense of these materials, scaling down to using microwells would be beneficial, especially when discovering the best media formulation. Therefore incorporating the

concept of quality by design to the design of these processes would also help to cope with the regulatory burden and risk.

9.3 Economic analysis summary and modelling improvements

The analyses presented in Chapters 6 and 7 highlighted the importance and benefits of linking technical data with process economic modelling to allow more rigorous evaluation of various production methods that could be adopted. Chapter 6 presented an economic analysis of different bioreactor designs for generation of skin substitute in the form of bioactive extracellular matrix (RBs, STR, and the disposable Wave bioreactor). This highlighted the advantages of using disposables such as the Wave bioreactor, to lower the initial upfront cost and thus allow the spread of the risk over the lifetime of the process as running costs. This is particularly attractive for an industry which many consider to have the risks of biopharmaceuticals and the profit margins of devices. If the regenerative medicine market were to adopt a service-based business model then the scale of operation would indicate the use of automated RB type reactor processing route as this would be operating at the smaller scale of the spectrum, where speeding up production and trying to apply the 'just-in-time' manufacturing philosophy would be more appropriate. However, solving the transportation and storage issues would indicate the bulk scale up method where there would be a centralised manufacturing site and a distribution network of smaller warehouses/medical centres/hospitals.

Chapter 7 examined the process economics for the production of growth factors using recombinant technology (yeast vs *E. coli*) as alternatives to skin substitutes. Critical titre levels that needed to be reached in each expression system were identified. For treatments requiring multiple growth factors the recombinant production route was compared to using dermal fibroblasts to generate the growth factors. The latter route appeared more favourable though the difference was not as dramatic as imagined.

Final formulation costs were not included in the modelling, and this could be expanded upon. Additionally, sales and distribution costs were assumed to be 30% of the sales

revenue based on the rule of thumb from chemical engineering cost appraisals. However, from discussion with experts in the industry this figure could be as high as 70% due to the need to ship at constant temperature and within a certain timeframe. Discussion with courier companies, and examining the technical processing required would allow sufficient modelling of this step. There is the need to consider the logistics for a distribution network required and the costs involved. Additionally, rules and regulations for shipping, certain security measures could impact upon the product in transit, all this will incur costs which should be modelled. Discussion with industry on pricing models would allow more precise prediction of NPV, once additional costs for formulation are included.

Simplification of implementation of the studies meant omission of certain factors. Namely, process validation and quality control activities were not modelled to the same extent as, say, direct materials cost. The need to have realistic estimates from industry as input in to validation is required.

Development of more sophisticated modelling software will allow more rigorous modelling of the manufacturing activities such as tracing the exact fermentation profile based on experimental data to calculate the media utilisation with more precision and future work could incorporate more risk analysis to assess uncertainties such as contamination rates, batch failures, and delays in a unit operation extending processing times. It is envisioned that such modelling efforts will become a critical component of process design when considering the needs of manufacture.

REFERENCES

Anthony E.T., Syed M., Myers S, Moir G., Navsaria H. The development of novel dermal matrices for cutaneous wound repair. Drug Discovery Today:Therapeutic Strategies **3**(1):81-86 (2006)

Archer R., Wood L. Production tissue culture by Roberts. In: Animal Cell Technology: Developments, Processes and Products (11th ESACT annual meeting). Spier RE et al. (Eds.) Butterworth Heninemann 402-408 (1992)

Archer R., Williams D. Why tissue engineering needs process engineering. Nature Biotechnology **23**(11):1353-1355 (2005)

Aunins J.G., Bibila T.A., Gatchalian S., Hunt G.R., Junker B.H., Lewis J.A., Licari P., Ramasubramanyan K., Ranucci C.S., Seamans T.C., Seifert D.B. Zhou W., Waterbury J., Buckland B.C. Reactor Development for the Hepatitis A Vaccine VAQTA. In: Animal Cell Technology. M.J.T. Carrono et al. (Eds.) 175-183 (1997)

Aunins J., Glazomitsky K., Buckland B., Cell culture reactor design: known and unknown. In: Nienow AW. Ed. Third International conference on Bioreactor and Bioprocess Fluid dynamics, BHR Group Conference Series, Publication No.5 MEP, London 175-190. (1993)

Baker J., Barsh G., Darrell C., Cunningham D. Dexamethasone modulates binding and action of epidermal growth factor in serum-free cell culture. Proceedings of the National Academy of Sciences of the Unite States of America **75**(4):1882-1886 (1978)

Balasubramani M., Ravi Kumar T., Babu M. Skin substitutes: a review. Burns **21**: 534-544 (2001)

Balin A.K., Pratt L., and Allen R.G. Effects of ambient oxygen concentration on the growth and antitoxidant defenses of human cell cultures established from fetal and postnatal skin. Free Radical Biology and Medicine **32**(3): 257-267 (2002)

Barnabe N., Butler M. The effect of glucose and glutamine on the intracellular nucleotide pool and oxygen uptake rate of a murine hybridoma. Cytotechnology **34**:47-57 (2000)

Barr P.J., Cousens L.S., Lee-Ng C.T., Medina-Selby A., Masiarz F.R., Hallewell R.A., Chamberlain S.H., Bradley J.D., Lee D., Steimer K.S. Expression and processing of biologically active fibroblast growth factors in the yeast *Sacchromyces cerevisiae.* Journal of Biological Chemistry **263**(31):16471-16478 (1988)

Barteling S. J., Vreeswijk J. Developments in foot-and-mouth disease vaccines. Vaccine **9**(2):75-88 (1991)

Bell E., Ehrlich H.P., Buttle DJ., Nakatsuji T.A. A living tissue formed in vitro and accepted as a living skin equivalent. Science **211**:1042-54 (1981).

Bell E., Ehrlich H.P., Sher S., Merrill C., Sarber R., Hull B., Nakatsuji T.A., Church D., Buttle DJ. Development and use of a living skin equivalent. Plastic Reconstructive Surgery **67**(3):386-92 (1981)

Benazzoug Y., Borchiellini C., Labat-Robert J. Robert L. Kern P. Effect of high glucose concentrations on the expression of collagens and fibronectin by fibroblasts in culture. Experimental Gerontology **33** (5): 445-455 (1998)

Bennet S.P., Griffiths G.D., Schor A.M., Leese G.P., Schor S.L. Growth factors in the treatment of diabetic foot ulcers. British Journal of Surgery **90**:133 (2003)

Bernard C.J., Connors D., Barber L., Jayachandra S., Bullen A., Cacace A. Adjunct automation to the Cellmate cell culture robot. Journal of the Association for Laboratory Automation (JALA) **9**:209-17 (2004)

Bettger W., Boyce S., Walthall B., Ham R. Rapid clonal growth and serial passage of human diploid fibroblasts in a lipid-enriched synthetic medium supplemented with epidermal growth factor, insulin, and dexamethasone. Proceedings of the National Academy of Sciences of the Unite States of America **78**(9):5588-5592 (1981)

Boedecker B., Newcomb R., Yuan P., Braufman A., Kelsey W. Production of recombinant factor VIII from perfusion cultures. I. Large-scale fermentation. In Spier R.E. Griffiths J., Berthold W. (eds) Animal cell technology: products of today, prospects for tomorrow. Butterworth Heinemann, Oxford pp580-583 (1994)

Booth A.B, Polak K.L. and Uitto J. Collagen biosynthesis by human skin fibroblasts I. Optimization of the culture conditions for synthesis of type I and type III procollagens. Biochimica et Biophysica Acta (BBA) – Nucleic Acids and Protein synthesis **607** (1):145-160. (1980)

Bouchie A. Tissue Engineering firms go under. Nature Biotechnology **20**:1178-1179 (2004).

Boyce S.T. Design principles for composition and performance of cultured skin substitutes. Burns **27**:523-533 (2001)

Briggs M., Nelson E.A. Topical agents or dressings for pain in venous leg ulcers (Cochrane Review). The Cochrane Library. Issue 1. Chichester, UK: John Wiley & Sons. Ltd. (2003)

Butler M. Growth limitations in microcarrier cultures. Advances in Biochemical Engineering **34**:57-841987

Butler M., Nuzel N., Barnabe T., Gray T., Bajno L. Linoleic acid improves the robustness of cells in agitated cultures. Cytotechnology **30**:27-36 (1999)

Buckland B. Seminar given at UCL. Development of a vaccine to prevent cervical cancer. (2006)

Cherry R., Papoutsakis E. Hydrodynamic effects on cells in agitated tissue culture reactors. Bioprocess Engineering **1**:29-41 (1986)

Cherry R., Papoutsakis E. Physical mechanisms of cell damage in microcarrier cell culture bioreactors. Biotechnology and Bioengineering **32**:1001-1014 (1988)

Christi Y. Animal-cell damage in sparged reactors. Trends in Biotechnology **18**:420-432 2000

Cook A.L., Kirwin P.M., Craig S., Bawden L.J. Green D.R., Price M.J.., Richardson S.J., Fallon A., Drummond A.H., Edwards R.M. Purification and anlaysis of proteinase-resistant mutants of recombinant platelet-derived growth factor-BB exhibiting improved biological activity. Biochemical Journal **281**:57-65 (1992)

Cox S., Cole M., Tawil B. Behaviour of human dermal fibroblasts in three-dimensional fibrin clots: Dependence on fibrinogen and thrombin concentration. Tissue Engineering **10** (5/6):942-954 (2004).

Croughan M., Hamel J.,Wang D. Effects of microcarrier concentration in animal cell culture. Biotechnology and Bioengineering **32**:975-982 (1988)

Croughan M., Hamel J.,Wang D. Hydrodynamic effects on animal cells grown in microcarrier cultures. Biotechnology and Bioengineering **29**:130-141 (1987)

Croughan M., Wang D. Growth and death in overagitated microcarrier cell cultures. Biotechnology and Bioengineering **33**:731-744 (1989)

Currie L., Martin R., Sharpe J., James S. A comparison of keratinocyte cell sprays with and without fibrin glue. Burns **29**(7):677-85 2003

Curran S.J, Chen R., Curran J.M, Hunt J.A. Expansion of human chondrocytes in an intermittent stirred flow bioreactor, using modified biodegradable microspheres. Tissue Engineering **11** No.9/11 (2005)

Davidson J.M., LuValle P.A., Zoia O., Quaglino D. Jr, Giro M. Ascorbate differentially regulates elastin and collagen biosynthesis in vascular smooth muscle cells and skin fibroblasts by pretranslational mechanisms. The Journal of Biological Chemistry **272** (1): 345-352 (1997)

Del Guerra S., Bracci C., Nilsson K., Belcourt L., Kessler R., Lupi L., Marselli P., De Vos P., Marchetti P. Entrapment of dispersed pancreatic islet cells in cultisphere –S macroporous gelatin microcarriers: Preparation, in vitro characterization, and microencapsulation. Biotechnology and Bioengineering **75**(6):741-744 (2001)

DePalma A. Bioprocessing: Options for anchorage-dependent cell culture. Genetic Engineering News **22**(11):58-62 (2002)

Doctor J., Petraglia C., Loveland A., Dietz M., Munich E., Leung J., Hollinger J. and Campbell P. Evaluating microcarriers for delivering human adult mesenchymal stem cells in bone tissue engineering. Developmental Biology **247**(2):505(2002)

Dutton R.L., Fox J.S. Robotic processing in Barrier-Isolator environments: A life cycle cost approach. Pharmaceutical Engineering **September/October 2006**:36-48. (2006)

Eagle H., Barban S., Levy M., Schulze H. The utilization of carbohydrates by human cell cultures. Journal of Biological Chemistry **235**:551-557 (1958)

Eaglstein W.H., Falanga V. Tissue engineering and the development of Apligraf, a human skin equivalent. Clinical Therapeutics **19**(5):894-905 (1997)

Eaglestein W/H., Falanga V. Tissue engineering for skin: An update. Journal of American Academy of Dermatology **39**:1007-10 (1998)

Ehrenreich M., Ruszczak Z. Update on Tissue-engineered biological dressings. Tissue Engineering **12**(9):1-18 (2006)

Eridani S. Animal cell technology. **4**: 469-488. (1990)

Farid S.S, Novais J.L, Karri S, Washbrook J., & Tichener-Hooker N.J. A tool for modeling strategic decisions in cell culture manufacturing. Biotechnology Progress **16**: 829-836 (2000).

Farid S. A decision-support tool for simulating the process and business perspectives of biopharmaceutical manufacture. University College London. PhD thesis (2001).

Farid S.S., Washbrook J., Titchener-Hooker N. J. Decision support tool for assessing bio-manufacturing strategies under uncertainty: stainless steel versus disposable equipment for clinical trial material preparation. Biotechnology Progress **21**:486-497 (2005)

Farid S.S., Washbrook J., Titchener-Hooker N. J. Modelling biopharmaceutical manufacture: design and implementation of SIMBIOPHARMA. Computers and Chemical Engineering **31**:1141-58. (2007)

Farndale R.W., Buttle D. J., Barrett A.J. Improved quantitation and discrimination of sulphated glycosaminoglycans by use of dimethylmethylene blue. Biochimica et Biophysica Acta **883**:173-177 (1986)

Fergerson M., O'Kane S. Scar free healing:from embryonic menchanisms to adult therapeutic intervention. Philosophical Transactions of the Royal Society of London B: Biological Sciences **359**: 839-850 (2004)

Fisher E., McLennan S.V., Tada H., Hefferman S., Yue D.K., Turtle JR. Interaction of ascorbic acid and glucose on production of collagen and proteoglycan by fibroblasts. Diabetes **40:** 371-375 (1991)

Forestell S., Kalogerakis N., Behie L.A. The extended serial subculture of human diploid fibroblasts on microcarriers using a new medium supplement formulation. Biotechnology and Bioengineering **40**:1039-1044 (1992)

Frame K.K., Hu. W-S. Oxygen uptake of mammalian cells in microcarrier culture – responses to changes in glucose concentration. Biotechnology Letters **7**(3):147-152 (1985)

Freed LE., Vunjal-Novakovic G., Langer R. Cultivation of cell-polymer cartilage implants in bioreactors. Journal of Cell Biochemistry **51**:257-64 (1993)

Frost and Sullivan. Global Advanced Wound Management Markets. [Market research report published by agency Frost and Sullivan]. (2004)

Garke G., Deckwer W-D., Anspach F.B. Preparative two-step purification of recombinant human basic fibroblast growth factor from high cell-density cultivation of *Escherichia coli*. Journal of Chromatography B **737**:25-38 (2002)

Gentzkow G. Iwasaki S., Hershon K., Mengel M., Prendergast J., Ricotta J., Steed D., Lipkin S. Use of Dermagraft, a cultured human dermis, to treat diabetic foot ulcers. Diabetes Care **19**:350-354 (1996)

Genzel Y., Olmer R.M. Schafer B., Reichl U. Wave microcarrier cultivation of MDCK cells for influenza virus production in serum containing and serum-free media. Vaccine **24**:6074-6087. (2006)

Gold M.H., Goldman M., Biron J. Efficacy of novel skin cream containing mixture of human growth factors and cytokines for skin rejuvenation. Journal of Drugs in Dermatology **6**:197-201. (2007)

Goldberg B., Green H. An analysis of collagen secretion by established mouse fibroblast lines. The Journal of Cell Biology **22**: 227-258(1964)

Gorodetsky R., Clark R., An J., Gailit J., Levdansky L., Vexler A., Berman E., Marx G. Fibrin microbeads (FMB) as biodegradable carriers for culturing cells and for accelerating wound healing. Journal of Investigative Dermatology **112**:866-872 (1999)

Graumann K., Premstaller A. Manufacturing of recombinant therapeutic proteins in microbial systems. Biotechnology Journal **1**:164-186 (2006)

Griffith L.G., Naughton G. Tissue engineering - current challenges and expanding opportunities. SCIENCE. **295**:1009-1016 (2002)

Griffiths B. Scale up of suspension and anchorage-dependent animal cells. Molecular Biotechnology **17** (3):225-238 (2001)

Griffiths M., Ojeh N., Livingstone R., Price R. Navsaria H. Survival of Apligraf in acute human wounds. Tissue Engineering **10**(7-8):1180-1195 (2004)

Green H., Goldberg B. Collagen and cell protein synthesis by established mammalian fibroblast line. Nature **204**:347-9 (1964)

Gustafson C-J., Birgisson A., Junker J., Huss F., Salemark L., Johnson H., Kratz G. Employing human keratinocytes cultured on macroporous gelatin spheres to treat full thickness-wounds: an in vivo on athymic rats. BURNS **33**:726-735 (2007)

Harding K.G, Jones V., Price P. Topical treatment: which dressing to choose. Diabetes Metabolism Research and Reviews **16**(1):S47-50 (2000)

Harding K.G., Morris H.L., & Patel G.K. Clinical review: healing chronic wounds. British Journal of Medicine **324**:160-163 (2002).

Heng BC, Liu H., Cao T. Transplanted human embryonic stem cells as biological 'catalysts' for tissue repair and regeneration. Medical Hypotheses. **64**(6):1085-1088 (2005)

Hildebrand A., Romaris M., Rasmussen L. Heinegard D., Twardzik D., Border W., Ruoslahti E. Interaction of the small interstitial proteoglycans biglycan, decorin and fibromodulin with transforming growth factor beta. Biochemical Journal **302**(2):527-34 (1994)

Horino Y., Takahashi S., Miura T., Takahashi Y. Prolonged hypoxia accelerates the posttranslational process of collagen synthesis in cultured fibroblasts. Life Sciences **71** 3031-3045 (2002)

IPTS report. Human tissue-engineered products – today's markets and future prospects. (2003) http://www.jrc.es

Ito A., Mase A, Takisawa Y., Shinkai M., Honda H., Hata K., Ueda M., Kobayashi T. Transglutaminase-mediated gelatin matrices incorporating cell adhesion factors as a

biomaterial for tissue engineering. Journal of Bioscience and Bioengineering **95**(2):196-199 (2003)

Joo-Hyung Heo, Hye Soon won, Hyun Ah Kang, Sang-Ki Rhee, Bong Hyun Chung Purification of recombinant human epidermal growth factor secreted from the methylotrophic yeast *Hansenula polymorpha*. Protein Expression and Purification **24**:117-122 (2002)

Jones I., Currie L., Martin R. A guide to biological skin substitutes. British Journal of Plastic Surgery **55**(3):185-193 (2002)

Karna E., Miltyk W., Wolczynski, Palka J.A. The potential mechanism for glutamine-induced collagen biosynthesis in cultured human skin fibroblasts. Comparative Biochemistry and Physiology Part B **130**(1):23-32 (2001)

Kidchob T., Kimura S., Imanishi Y. Thermoresponsive release from poly (Glu(OMe))-block-poly(Sar) microcapsules with surface-grafting of poly(N-isopropylacrylamide). Journal of Controlled Release **50**:205-214 (1998)

Kim N.H., Jung H.H., Cha D. R. and Choi D.S. Expression of vascular endothelial growth factor in response to high glucose in rat mesangial cells. Journal of Endocrinology **165**:617-624 (2000)

Kim S., Mohamedali K. Cheung L., Rosenblum M. Overexpression of biologically active $VEGF_{121}$ fusion proteins in *Escherichia coli*. Journal of Biotechnology **128**:638-647 (2007)

Kong D., Chen M, Gentz R. and Zhang J. Cell growth and protein formation on various microcarriers. Cytotechnology **29**:149-156 (1999)

Kretzmer G. Industrial processes with animal cells. Applied Microbiology and Biotechnology **59**:135-142 (2002)

Kuroyangi Y. Yamada N., Yamashita R., Uchinuma E. Tissue-engineered product: allogeneic cultured dermal substitute composed of spongy collagen with fibroblasts. Artificial Organs **25**:180 (2001)

LaFrance M. L. and Armstrong D.W. Novel living skin replacement biotherapy approach for wounded skin tissue. Tissue Engineering **5**:153 (1999)

Lakhotia S., Papoutsakis E. Agitation induced cell injury in microcarrier cultures. Protective effect of viscosity is agitation intensity dependent: Experiments and modeling. Biotechnology and Bioengineering **39**:95-107 (1992)

Lauer G. Solberg S., Cole M., Flamme I., Sturzebecher J., Mann K., Krieg F., Eming S. A. Expression and proteolysis of vascular endothelial growth factor is increased in chronic wounds. Journal of Investigative Dermatology **115**:12-18 (2000)

Lee G.H., Cooney D., Middelberg A.P.J., Choe W.S. The economics of inclusion body processing. Bioprocess and Biosystems Engineering **29**:73-90 (2006)

Leventon W. Synthetic skin. IEEE Spectrum
(2002) http://www.spectrum.ieee.org/WEBONLY/publicfeature/dec02/skin.html

Lim AC., Zhou Y. Washbrook J., Sinclair A., Fish B., Francis R., Titchener-Hooker N., Farid S. S. Application of decision-support tool to access pooling strategies in perfusion culture processes under uncertainty. Biotechnology Progress **21**(4):1231-1242 (2005)

Lim A.C., Washbrook J., Tictchener-Hooker N., Farid S. S. A computer-aided approach to compare the production economics of fed-batch and perfusion culture under uncertainty. Biotechnology and Bioengineering **93**(4):687-697 (2006)

Lindskog U., Lundgren B., Billig D., Linder E. Alternatives for harvesting cells grown on microcarriers: effects on subsequent attachment and growth. Developments in Biological Standardization **66**:307-13 (1987)

Leveque N. Robin S., Makki S., Rougier A., Humbert P. Iron and ascorbic acid concentrations in human dermis with regard to age and body sites. Gerontology **49**(2):117-122. (2003)

Lundgren B., Blüml G. Microcarriers in cell culture production. In: Bioseparations and Bioprocessing Volume II: Processing, Quality and Characterization, Economics, Safety and Hygiene. Eds G. Subramanian. Wiley-VCH. (1998)

Lysaught M. J., Hazlehurst A.L. Tissue engineering: the end of the beginning. Tissue Engineering **10**(1/2):309-320 (2004)

Ma J., Wang H., He B., Chen J. A preliminary in vitro study on the fabrication and tissue engineering applications of anovel chitosan bilayer material as a scaffold of human neofetal dermal fibroblasts. Biomaterials **22**(4):331-336 (2001)

Ma L., Gao C., Mao Z., Zhou J., Shen J., Hu X., Han C. Collagen/chitosan porous scaffolds with improved biostability for skin tissue engineering. Biomaterials **24** (26): 4833-4841 (2003)

Malda J., Frondonza C. Microcarriers in the engineering of cartilage and bone. Trends in Biotechnology **24**(7): 299-304 (2006)

Mason C., Hoare M. Regenerative medicine bioprocessing: building a conceptual framework based on early studies. Tissue Engineering **13**(2): 301-311 (2007)

McKenna N. Broad applications of biocompatible materials. Genetic Engineering News **22**(8):8-9 (2002)

Meagher M.M., Barlett R.T., Rai V.R. Khan F.R. Extraction of rIL-2 inclusion bodies from *Escherichia coli* using cross-flow filtration. Biotechnology and Bioengineering. **43**: 969-977 (1994)

Medcalf N. Body works. The Chemical Engineer 22 JULY (1999)

Meisenholder G. Postmodern culture: maximizing cell culture output at every level. The Scientist **13**(14):21 (1999)

Mercille S., Massie B. Induction of apoptosis in nutrient-deprived cultures of hybridoma and myeloma cells. Biotechnology and Bioengineering **44**(9):1140-1154 (1994)

Mikola M., Seto J. Amanullah A. Evaluation of novel Wave bioreactor cellbag for aerobic yeast cultivation. Bioprocess Biosystems Engineering **30**:231-241 (2007)

Montagnon B. Vincent-Falquet J., Fanget B. Thousand liter scale microcarrier culture of Vero cells for killed polio virus vaccine. Developments in Biological Standandardization **55**:37-42 (1984)

Moran E. A microcarrier-based cell culture process for the production of a bovine respiratory syncytial virus vaccine. Cytotechnology **29**:135-148 (1999)

Moore S.K. Tissue Engineering Pioneers Fall to Financial Troubles. IEEE Spectrum (2002) [http://www.spectrum.ieee.org/WEBONLY/wonews/dec02/tissue.html]

Murhammer D.W., Goochee C. F. Sparged animal cell bioreactors: mechanism of cell damage and pluronic F-68 protection. Biotechnology Progress **6**:391-397 (1990)

Nakao N., Pi-Chao W., Kaoru S., Tadao O., Masatoshi M. Production of human growth hormone by protein-free cultivation of anchorage-dependent cells with porous cellulose carrier. Journal of Fermentation and Bioengineering **82**(5):469-474 (1996)

Naughton G.K. From lab bench to market: critical issues in tissue engineering. Annals of New York Academy of Sciences **961**: 372-385 (2002)

Neves A., Medcalf N., Brindle K. Influence of stirring-induced mixing on cell proliferation and extracellular matrix deposition in meniscal cartilage constructs based on polyethylene terephthalate scaffolds. Biomaterials **26**:4828-4836 (2005)

Ng Y-C., Berry J.M., Butler M. Optimization of physical parameters for cell attachment and growth on macroporous microcarriers. Biotechnology and Bioengineering **50**:627-635 (1996)

NHS CRD. University of York. Compression therapy for venous leg ulcers. Effective Health Care **3**(4) (1997)

NHS CRD. University of York. Getting evidence into practice. Effective Health Care **5**(1) (1999)

Nilsson K., Buzsaky F., Mosbach K. Growth of anchorage-dependent cells on macroporous microcarriers. Bio/Technology **4**:989-990 (1986)

Nikolai T. J., Hu W.S. Cultivation of mammalian cells on macroporous microcarriers. Enzyme Microbial Technology **14**:203-208 (1992)

Noriko K. Kyoichi M., Norio K. Effects of hyperglycemic conditions on growth of fibroblasts and secretion of growth factors. St. Marianna Medical Journal **30**(4):447-453 (2002)

Novais J. L., Titchener-Hooker, Hoare M. Economic comparison between conventional and disposables-based technology for the production of biopharmaceuticals. Biotechnology and Bioengineering **75**(2):143-153. (2001)

Omori K., Naruishi K., Nishimura F., Yamada-Naruishi H., Takashiba S. High glucose enhances interleukin-6-induced vascular endothelial growth factor 165 expression via activation of Gp130-mediated p44/42 MAPK-CCAAT/Enhancer binding protein signaling in gingival fibroblasts. Journal of Biology Chemistry **279**(8):6643-6649 (2004)

Parenteau N., Bilbo P., Nolte C., Mason V., Rosenberg M. The organotypic culture of human skin keratinocytes and fibroblasts to achieve form and function. Cytotechnology **9**(1-3):163-171 (1992)

Parenteau N., Sabolinski M., Prosky S., Nolte C., Oleson M., Kriwet K., Bilbo P. Biological and physical factors influencing the successful engraftment of a cultured human skin substitutes. Biotechnology and Bioengineering **52**(1):3-14 (1996)

Parenteau NL, Hardin Young J and Ross RN. "Skin." In: Lanza, R., Langer, R. and Vacanti, J., Editors. Principles of Tissue Engineering, 2nd Edition, Academic Press, pp. 879-890. (2000)

Peterkofsky B. The effect of ascorbic acid on collagen polypeptide synthesis and proline hydroxylation during the growth of cultured fibroblasts. Archives of Biochemistry and Biophysics **152**:318-328 (1972)

Petrides DP., Calandranis J., Cooney C. Computer-Aided design techniques for integrated biochemical processes. Genetic Engineering News Sept pp10 35:28-29 (1995)

Phillips C.L., Combs S.B. Pinnell S.R. Effects of ascorbic acid on proliferation and collagen synthesis in relation to the donor age of human dermal fibroblasts. Journal of Investigative Dermatology **103**(2): 228-32 (1994)

Pinney E., Liu K., Sheeman B., Mansbridge J. Human three-dimensional fibroblast cultures express angiogenic activity. Journal of Cellular Physiology **183**:74-82 (2000)

Pruitt BA. Jr., Levine N. Characteristics and uses of biologic dressings and skin substitutes. Archives of Surgery **119**(3):312-322 (1984)

Qiu Q-Q., Ducheyne P., Ayyaswamy P.S., New bioactive, biodegradable composite microspheres as tissue engineering substrates. Journal of Biomedical Materials Research **52**(1):66-76 (2000)

Recum H., Okano T., Kim S. Growth factor release from thermally reversible tissue culture substrates. Journal of Controlled Release **55**:121-130 (1998)

Remer D.S., Mattos F.B. Cost and scale up factors, international inflation indexes and location factors. International Journal of Production Economics **84**:1-16 (2003)

Remer D.S, Idrovo J.I. Cost-estimating factors for biopharmaceutical process equipment. Pharmaceutical Technology International. March (1991)

Rheinwald J G., Green H. Serial cultivation of strains of human epidermal keratinocytes: the formation of keratinizing colonies from single cells. Cell **6**(3):331-343 (1975)

Robson M.C., Phillips L. G., Lawrence W. T., Bishop J.B., Youngerman J.S., Hayward P.G., Broemeling L.D., Heggers J. P. The safety and effect of topically applied recombinant basic fibroblast growth factor on the healing of chronic pressure sores. Annals of Surgery **216**(4):401-406 (1992)

Robson MC, Phillips LG, Thomason A, Robson LE, Pierce GF. Platelet-derived growth factor BB for the treatment of chronic pressure ulcers. Lancet **339**:23 (1992)

Rouf S.A., Moo-Young M., Scharer J.M, Douglas P.L. Single versus multiple bioreactor scale-up: economy for high-value products. Biochemical Engineering Journal **6**:25-31 (2000)

Royal College of Nursing. The management of patients with venous leg ulcers. Audit protocol. (2000a) www.rcn.org.uk

Saed G.M., Diamond M. Effect of glucose on the expression of type I collagen and transforming growth factor-β1 in cultured human peritoneal fibroblasts. Fertility and Sterility **79**(1):158-163 (2003)

Shadle P. J., Silverness K.B., King R.S. Process for purification of basic fibroblast growth factor. Patent US 5331095 (1994)

Siemeister G., Schnurr B., Mohrs K., Schachtele C. Marme D., and Martiny-Baron G. Expression of biologically active isoforms of the tumor angiogensis factor VEGF in *Escherichia coli.* Biochemical and Biophysical research communications **222**:249-255 (1996)

SIGN. Scottish Intercollegiate Guidelines Network. Management of Diabetes. (2001)

Simon D. A., Fix F.P., and McCollum C.N. Management of venous leg ulcers. British Medical Journal **328**(7452):1358-1362 (2004)

Singh V. Disposable bioreactor for cell culture using wave-induced agitation. Cytotechnology **30**:149-158 (1999)

Sivakesava S., Xu Z., Chen Y., Hackett J., Huang R., Lam E., Lam T., Siu K., Wong R., Wong W. Production of excreted human epidermal growth factor (hEGF) by en efficient recombinant *Esherichia coli* system. Process Biochemistry **34**:893-900 (1999)

Smith D. J. Jr. Use of Biobrane in wound management. Journal of Burn Care and Rehabilitation **16**:317 (1995)

Soler L.F., Cedano J., Querol E., Llorens R. Cloning, expression and purification of human epidermal growth factor using different expression systems. Journal of Chromatography B **788**:113-123 (2003)

Sommerfeld S., Strube J. Challenges in biotechnology production – generic process and process optimization for monoclonal antibodies. Chemical Engineering and Processing **44**:1123-1137 (2005)

Sone H., Kawakami Y, Okuda Y., Kondo S., Hanatani M., Suzuki H., and Yamashita K. Vascular endothelial growth factor is induced by long-term high glucose concentration and up-regulated by acute glucose deprivation in cultured bovine retinal pigmented epithelial cells. Biochemical and Biophysical Research Communications **221**(1)193-198. (1996)

Steed DL. Modifying the wound healing response with exogenous growth factors. Clinical Plastic Surgery **25**:397 (1998)

Tabata Y. Tissue regeneration based on growth factor release. Tissue Engineering **9**:5-15 (2003)

Tajima S., Pinnell S.R. Ascorbic acid preferentially enhances type I and III collagen gene transcription in human skin fibroblasts. Journal of Dermatological Science **11**:250-253 (1996)

Takahashi Y., Takahashi S., Shiga Y., Yoshimi T., Miura T. Hypoxic induction of prolyl 4-hydroxylase α(I) in cultured cells. The Journal of Biological Chemistry **275**(19):14139-14146 (2000)

Tatard V.M., Venier-Julienne M.C.,Saulnier P.,Prechter E., Benoit J.P., Menei P., Montero-Menei C.N. Pharmacologically active microcarriers: a tool for cell therapy. Biomaterials **26**:3727-3737 (2005)

Trabold O., Wagner S., Wicke C., Scheuentuhl H., Hussain M.Z., Rosen N., Seremetiev A., Becker H.D., Hunt T.K. Lactate and oxygen constitute a fundamental regulatory mechanism in wound healing. Wound Repair and Regeneration **11**(6):504-509 (2003)

Tsao E. Bohn M., Numsuwan, Omstead D.R., Munster M. Effects of heat shock on the production of human erythropoietin from recombinant CHO cells. Biotechnology and Bioengineering **40**(10):1190-1196 (1992)

Tsao E. Bohn M., Numsuwan, Omstead D.R., Munster M. Optimization of a roller bottle process for the production of recombinant erythropoietin. Annals of New York Academy of Sciences **665**:127-136 (1992)

Valanga V. Wound healing and its impairment in the diabetic foot. Lancet **366**:1736-43 (2005)

Vallejo L.F., Rinas U. Strategies for the recovery of active proteins through refolding of bacterial inclusion body proteins. Microbial Cell Factories **3**:11 (2004)

Van der Pol L., Tramper J. Shear sensitivity of animal cells from a culture-medium perspective. Trends in Biotechnology **16**:323-328 (1998)

Van Wezel A. Growth of cell strains and primary cells on microcarriers in homogeneous cultures. Nature **216**:64 (1967)

Varani J., Bendelow M., Chun J., Hillegas W. Cell growth on microcarriers: comparison of proliferation on and recovery from various substrates. Journal of Biological Standardization **14**(4):331-336 (1986)

Varani J., Dame M., Rediske J., Beals T.F., Hillegas W. Substrate-dependent differences in growth and biological properties of fibroblasts and epithelial cells grown in microcarrier culture. Journal of Biological Standardization **13**(1):67-76 (1985)

Varani J., Josephs S., Hillegas W.J. Human diploid fibroblast growth on polystyrene microcarriers in aggregates. Cytotechnology **22**(1-3):111-117 (1996)

Veazey W.S., Anusavice K.J., Moore K. Mammalian cell delivery via aerosol deposition. Journal of Biomedical Materials Research Part B: Applied Biomaterials **72B**(2):334-338 (2004)

Vogt. G. Multi-axis robots bring automation to life sciences. Industrial Robot: An International Journal **29**(1)49-52 (2002)

Wagner S., Hussain M.Z., Hunt T.K. Bacic B., Becker H.D. Stimulation of fibroblast proliferation by lactate-mediated oxidants. Wound Repair and Regeneration **12**:368-373 (2004)

Waymouth C., Ham R. Chapple P.C. In Book: The growth requirements of vertebrate cells invitro. pg105-117. Cambridge University Press, NY (1981)

Weber D. Navigating FDA regulations for human cells and tissues. Bioprocess International **2**(8):22-27 (2004)

Werner R.G. Economic aspects of commercial manufacture of biopharmaceuticals. Journal of Biotechnology 113(1-3):171-82 (2004)

Wilkins L.M., Watson S.R., Prosky S.J. Development of a bilayered living skin construct for clinical applications. Biotechnology and Bioengineering **43**:747-56 (1994)

Williams B. Factors regulating the expression of vascular permeability/vascular endothelial growth factor by human vascular tissues. Diabetologia **40**:S118-S120 (1997)

Williamson D., Harding K. Wound healing. Medicine **32**(12):4-7 (2004)

Woessner J.F. The determination of hydroxyproline in tissue and protein samples containing small proportions of this imino acid. Archives of Biochemica et Biophysica **93:** 440-7 (1961)

Wu X., Su Z., Li X., Zheng Q., Huang Y., Yuan H. High level expression and purification of a nonmitogenic form of human acidic fibroblast growth factor in *Escherichia coli.* Protein Expression and Purification **42**:7-11 (2005)

Wurm F. Production of recombinant protein therapeutics in cultivated mammalian cells. Nature Biotechnology **22**:1393-1398 (2004)

Yamato M., Utsumi M., Kushida A., Konno C., Kikuchi A., Okano T. Thermo-responsive culture dishes allow the intact harvest of multilayered keratinocyte sheets without dispase by reducing temperature. Tissue Engineering **7**(4) 473-480 (2001)

Zabriskie D.W. Bioreactor Design, Operation and Control. In: Comprehensive Biotechnology II (Moo-Young M ed.) 175-189, Pergamon Press, New York (1985)

Zielke H.R., Ozand P.T., Tildon J.T., Sevdalian D.A., Cornblath M. Growth of human diploid fibroblasts in the absence of glucose utilization. Proceedings of the National Academy of Sciences of the United States of America **73** (11): 4110-4114 (1976)

Zielke H.R., Ozand P.T., Tildon J.T., Sevdalian D.A., Cornblath M. Reciprocal regulation of glucose and glutamine utilization by cultured diploid fibroblasts. Journal of Cell Physiology **95**:41-48 (1978)

Zielke R., Zielke C., Ozand P. Glutamine: a major energy source for cultured mammalian cells. Federation Proceedings **43**:121-125 (1984)

Zielke H.R., Submilla C., Ozand P.T. Effect of glucose on aspartate and glutamate synthesis by human diploid fibroblasts. Journal of Cell Physiology **107**:251-254 (1981)

Zwietering T. N. Suspension of solid particles in liquids by agitators. Chemical Engineering Science **8:**244 (1958)

APPENDIX A

Betty Lin, Mary-Ann Dowling, Mark Smith, Nick Medcalf, Susana Levy, Suzanne Farid. *Process economic evaluation of 2nd generation tissue-engineered skin substitutes*

Betty Lin, Mary-Ann Dowling, Mark Smith, Nick Medcalf, Susana Levy, Suzanne Farid. *Process economics for the manufacture of growth factor based products for wound-healing*

To be submitted to Tissue Engineering.

APPENDIX B

This section provides a full description of the various protocols and assays mentioned in Chapter 3.

.

B1: Protocol for resurrection of frozen cells:

This protocol thaws one vial of (HuFFs) human dermal foreskin fibroblasts and seeds the cells into 1xT75 flask.

Record date thawed:
Passage 5, Date_____ (Vials frozen at P5, so the first passage will be P6.)

Pull the following media for passaging of the cells from the fridge prior to obtaining the vial:-

Complete DMEM medium, stored at 4°C , subsequently warmed to room temperature.

Procedure:

1. Using a 25ml pipette, add 15 ml of complete medium to the new 1 x T75 flask [Corning, Cat#430825, vented cap]
2. Label flask with HuFFs, passage number, initials, and date.
3. Place the flask into the CO_2 incubator to equilibrate.
4. Turn the water bath on and set to 37°C.
5. Remove one vial from frozen, liquid nitrogen storage and place the vial into the styrofoam container of dry ice/normal ice. Transfer to the lab as soon as possible.
6. Rapidly thaw the vial in a 37°C in the water bath by a swirling motion for about 2-3minutes. Avoid submerging the vial cap to avoid contamination from the water, which can travel up the wick threads. Wear a face shield during thawing.
   Time started thawing: _____ am/pm
   Time completed thawing: _____am/pm
7. Wipe the vial with a tissue soaked in 70%(v/v) prior to opening.
8. Quickly transfer the cells to a 10ml centrifuge tube and add cold (4°C) complete medium slowly up to a total volume of 10ml.
9. Spin the cells in the Megfuge 1.0R (Heraeus) at 1000rpm (300g) for 5 minutes at 4°C.
10. Remove the supernatant.
11. Gently resuspend the cells in 1ml pre-warmed complete medium by aspirating through a plugged sterile Pasteur pipette. Then further dilute the cell suspension to 5ml.
12. Now take a sample to assess the cell number and viability. (0.5 to 1ml sample)

13. Now bring the 1 x T-75 flask from the incubator and add the cell suspension, thus the total volume in the flask is ~ 20ml.
14. Incubate at 37°C.

B2: Protocol for passaging and maintenance of cells:

This protocol passages 1xT-75 flasks to 4 x T-75 flasks using a 1:4 split ratio. Any combination can be substituted and at 1:3 or 1:4 split ratio, confluent cultures are achieved after 2-3 days. A 1:6 split ratio will generate confluent cultures after 4-5 days.

Record the passage number and date. Passage____, Date_____

Reagents:

Complete DMEM medium
Trypsin/EDTA
DPBS without Ca^{2+} and Mg^{2+}, [Sigma Cat #D8537]

Procedure:

1. Add 17.5ml of complete medium to the new 4 x T-75 flasks
2. Label the flasks with HuFFs, passage number and date
3. Place the new flasks into the 37°C, 10%CO_2 incubator.
4. Remove the 1xT-75 flask from the incubator. Time removed from incubator:_____am/pm
5. Observe the cells under the microscope and check for confluency, absence of microbial contamination, abnormal pH, excessive detached cells, or degeneracy of the cell monoloayer.

   _____

   _____

6. Remove the spent tissue culture medium from the tissue culture flask. Take a sample of this.
7. Add 10ml of DPBS to the flask to rinse the sheet.
8. Remove the DPBS and discard.
9. Add 3ml of trypsin/EDTA. Rinse trypsin/EDTA over the cell growth surface and allow the flask to sit for about 5minutes. Occasionally rock the flask to ensure the even coating of trypsin. Inspect the cells frequently to observe the rounding up of the cells and lifting from the plastic.
   Start time of trypsinization:_____am/pm
10. Gently tap the flask to dislodge the cells
11. Add 10ml of complete medium to the flask to quench the trypsin activity.
    Time quenched:_____am/pm
12. Transfer the contents of the flask to a 10ml centrifuge tube and spin at 1000rpm (300g) for 5 minutes in the Megafuge 1.0R (Heraeus) at 4°C.
13. Remove the supernatant above the cell pellet

14. Add 1 ml of the complete medium to gently re-suspend the pellet
15. Add 10ml of complete medium to the cell suspension to make up the required volume.
16. Take 2.5ml of cell suspension and inoculate the 4 x T-75 flasks.
17. Using the remaining 1ml for cell counting.

B3: Protocol to determine the level of ammonia present in the media samples:

Reagents:

Sodium phenate solution – 2.5g sodium phenate, 80mls of UHQ water, 7.5ml of 4M NaOH. Make up to a final volume of 100mls using UHQ water.

Sodium nitroprusside stock solution – 1% w/v sodium nitroprusside in UHQ water. Dilute to 1/100 (v/v) to use in assay.

Sodium hyperchlorite solution – 1.25ml of sodium hypochlorite solution (10-14% w/v). Make up to 100mls in UHQ water, ~0.02M in water.

Ammonium chloride standards – Make up 10mM NH_4Cl as stock solution. Then in 1.5ml eppendorfs, make a range of standards from 0 to 3.5mM concentrations, as shown in the table below.

Standards (concentrations mM)	Microlitres of 10mM NH_4Cl	Microlitres of water
0	0	1000
0.5	50	950
1	100	900
1.5	150	850
2	200	800
2.5	250	750
3	300	700
3.5	350	650

All reagents were obtained from Sigma, UK.

Procedure:
Add the reagents in the following order and quantity into the wells of a microplate:

1. Sample/standard 8µl
2. Sodium phenate solution 80µl
3. Sodium nitrusside working solution 120 µl
4. Sodium hypochlorite solution 120µl

Wrap the plate with foil immediately after the addition of the sodium hypochlorite solution and incubate for 30mins at room temperature. Read the plate at 640nm.

B4: **Protocol to determine the level of VEGF present in the media samples:**

Reagents:

The Capture antibody is goat anti-human VEGF and is diluted with PBS.

The Detection antibody is biotinylated goat anti-human VEGF and diluted with 1% BSA in PBS, pH7.2-7.4 and 0.2μm filtered.

Streptavidin-HRP is diluted with 1% BSA in PBS, pH7.2-7.4 and 0.2μm filtered.

Standards are recombinant human VEGF and reconstituted and diluted with 1% BSA in PBS, pH7.2-7.4, 0.2μm filtered.

(The above 4 reagents are obtained from R&D Systems Cat. DY293, and prepare to the working concentrations as according to the instructions leaflet that comes with it.)

Substrate solution = 1:1 mixture of Colour reagent A (H_2O_2) and colour reagent B (Tetramethylbenzidine) (R&D Systems, cat. DY999)

Stop Solution = 2N H_2SO_4 (Sigma, UK)

Block Buffer = 1% BSA, 5% Sucrose in PBS with 0.05% NaN_3.

Wash Buffer = 0.05% Tween 20 in PBS (pH7.2-7.4).

Procedure:

1. Coat 96-well plate (e.g. COSTAR EIA plate Cat. No. 2592, or Nunc immunoplate) with 100μl per well with the diluted capture antibody. Seal the plate with cling film and incubate overnight at room temperature in a humidified chamber.
2. Remove the capture antibody by washing the plate with Wash buffer. Wash three times to ensure the removal of the capture antibody. Invert the plate and blot against clean paper towels.
3. Cover the plates with 300ml per well of blocking buffer and seal with cling film and place in the humidified chamber overnight in the cold room or in the refrigerator.
4. Remove the block buffer by washing the plates with the wash buffer. Wash three times. Invert the plates and blot against paper towels as before.
5. Add 100μl of the sample/standards into the designated wells in the plate. Cover with adhesive strip and incubate for 2 hours at room temperature.

6. Remove the sample/standards by washing the plates with the wash buffer. Wash three times. Invert the plates and blot against paper towels as before.
7. Add 100µl of the Detection antibody to all wells in the plate. Cover with new adhesive strip and incubate for 2 hours at room temperature.
8. Remove the detection antibody by washing the plates with the wash buffer. Wash three times. Invert the plates and blot against paper towels as before.
9. Add 100µl of the diluted Streptavidin-HRP to all wells in the plate. Cover and incubate for 2 hours at room temperature away from direct light. (Advisable to cover with foil, and try to avoid light as much as possible).
10. Remove the Streptavidin-HRP by washing the plates with the wash buffer. Wash three times. Invert the plates and blot against paper towels as before.
11. Add 100µl of the Substrate solution to each well, and incubate for 20min at room temperature in the dark.
12. Add 50µl of Stop solution to each well. Gently tap the plate to ensure the
13. colour formation on the plate is homogeneous and the read the plate immediately at 450nm and either 540nm or 570nm. Then subtract the reading at 540nm/570nm from the 450nm, to take into account of optical imperfections on the plate.

NB. The washing steps must be observed to ensure good results.

B5: Protocol for LIVE/DEAD staining:

Reagents:

LIVE/DEAD stain - Add 20µl of the ethidium dibromer and 5µl of calcein AM to 10mls of PBS. (Molecular Probes, Cat. No. L3224, Lot No. 02E2-1).

Procedure:

1. If the sample is from the bioreactor, gently pipette it into a six-well plate.
2. Remove the spent media from the sample, and rinsed with PBS.
3. Then add the LIVE/DEAD stain incubated in the dark in the incubator at 37°C for 30minutes.
4. Remove the stain by aspirating it off and gently cover the sample with PBS.
5. View under the confocal microscope using fluorescence.

B6: Protocol for the preparation of the SEM samples

Reagents:

PBS
Formalin
100% ethanol, make a series of alcohol solutions, of 10%, 20%, 30%, 40%, 50%, 60%, 70%, 80% and 90%.

Procedure:

1. Remove the media using a pipette and rinse with PBS to ensure removal of media.
2. Fix the sample by addition of formalin, (diluted at 10 parts PBS and 1 part formalin), and leave to fix for 2 hours.
3. Rinse 3 times with PBS, and then proceed with the alcohol rinses. (Taking it through an alchol dehydration series)
4. Rinse with 10%, 20%,30%,40%, 50%, 60%, 70%, 80%, 90%, and finally 100%. Leave it to soak for 20minutes between rinses.
5. Then final three rinses in 100% ethanol ans leave for overnight in 100% ethanol.
6. When ready to use, remove most of the alchol with pipette. Air dry and ready for SEM.

B7: Protocol for the preparation of the histology samples

1. Dehydrate the sample through an alcohol series, by rinses from 10% through to 100% ethanol.
2. Processed in wax and embedded by placing the sample in chloroform first, leave for an hour and carry out three chloroform changes. This is to remove any traces of moisture.
3. The using wax at 60°C, place sample into the wax for an hour, and carry out two wax changes. Use the R.A. Lamb embedding centre.
4. Allow the wax to solify, and samples can be processed when desired.
5. Using the Leica RM2165 rotary microtome, slice sections at 5micon thick. Float these out onto the waterbath at 45°C.
6. Each slides can put up to two sections.
7. Then load the slides once it is dry. Load the stains desired into the Autostainer.
8. Hit start button and collect the slides later for microscopy.

B8: Protocol for the MTT Assay:

Reagents and prior preparation:

Establish the test cultures in 96-well microtiter plates using 0.2ml of growth medium and up to 10^4cells/well. (This depends on proliferation of cell type)

Place in incubator for a period of time (1-3 days) so the cells reach exponential phase.

Prepare the dilutions in growth medium of the factors/drugs for testing, covering a range of concentrations.

Prepare a solution of MTT by dissolving 50mg/ml in 0.1 glycine buffer at pH10.5. Remove any particulates and sterilize through membrane filtration.

Procedure:

1. Remove the medium from the each of the wells and add the 0.2ml of the factors/drugs dilutions to the wells. Add medium to control wells.
2. Place the plates in the incubator for a period of timed exposure.
3. Remove all medium from wells and replace with fresh medium with no drugs/factors. Repeat daily to have about 2-3 cell divisions
4. After the final feeding, add the MTT solution of 50µl and wrap the plate in foil and place into the incubator for 3-8 hours.
5. Remove medium from wells and dissolved the retained formazan by addition of 0.2ml of DMSO, and then add 25µl of glycine buffer and read absorbance immediately in ELISA plate reader at 570nm.

B9: Protocol for the immunostaining of the tissue mass for collagen:

Reagents:

Wash Buffer – PBS-Tween 20 (0.1%)

Blocking Buffer – 10% swine serum in PBS-Tween 20 or 5% BSA in PBS-Tween 20

Primary Antibody – Rabbit polyclonal to human collagen type I (Biogenesis)

Secondary Antibody – Swine anti-rabbit IgG conjugated with FITC (DAKO) diluted in 20% swine serum or 0.5% BSA in PBS-Tween 20

Mounting Media – Vectorshield Mounting Agent with Propidium Iodide

Procedure:

1. Wash the slides with PBS-Tween20 (0.1%)
2. Block the slides with 10% swine serum in PBS-Tween20 for 30 minutes at room temp.
3. Add the primary antibody diluted to 1:10 and incubate at room temperature for 2 hours.
4. Wash three times use PBS-Tween20, and from this moment on, avoid direct light by keeping the slides covered in foil.
5. Add the secondary conjugate antibody and incubate for 30 minutes at room temp.
6. Wash the slides three times with PBS-Tween 20 and add a drop of Mounting Media and look under the microscope using fluorescence.

B10: Protocol for the hydroxyproline assay:

Reagents:

Papain Buffer (Store at 4°C, shelf-life of 3months)
1.42 g Sodium Phosphate, dibasic, and monobasic
0.0788g Cysteine Hydrochloride
0.1861g Ethylenediaminetetraacetic acid (EDTA)
Add 90 ml of UHQ Water and stir until dissolved. Adjust pH to 6.5 using 1M HCL, and make up to a volume of 100ml with UHQ water.

Papain solution (Made fresh on the day, and use on the day of preparation)
0.0264g Papain (P4762 100mg, Sigma)
Add 25ml of papain buffer and stir until dissolved.

0.25M Sodium Phosphate pH6.5 (Store at 4°C, shelf life is 3months)
7.5g of sodium phosphate, monobasic, anhydrous. Dissolve in UHQ water and make up to a final volume of 250ml, making a solution of pH5.
8.875g of sodium phosphate, dibasic, anhydrous. Dissolve in UHQ water and make up to a final volume of 250ml, making a solution of pH9.
Add 125ml of the monobasic solution to the 80ml of dibasic solution. Check the pH is pH6.5, adjust the pH accordingly, by adding either the monobasic or dibasic solution.

Hydroxyproline assay Stock solution (Store at 4°C, shelf life is 3 months)
5g citric acid and 12g sodium acetate and dissolve in 65ml of UHQ water
3.4g of sodium hydroxide in 25ml of UHQ water.
Mix two solutions together and add 1.2ml glacial acetic acid. Make up to 100ml of UHQ water. Add 5 drops of toluene.

Hydroxyproline assay Working solution (Store at 4°C, shelf life is 3 months)
15ml of isopropanol to 50ml of hyroxyproline stock solution.
Mix well and adjust to pH6, using conc. HCl. Make up to a final volume 75ml with UHQ water.

Chloramine T solution (Store in glass container at room temp, shelf life 2 days)
Take 20ml of the hydroproline working solution and add 2.5ml of isopropanol.
Weigh out 0.3525g of chloramines T and add to the solution, and stir

p-Dimethylaminobenzaldehyde (p-DAB) solution (Store in a glass container at room temperature, shelf life is 2 days)
3.75g of pDab
15ml of isopropanol
6.5ml of perchloric acid

Procedure:

Preparation of the samples

1. Rinse the sample in PBS
2. Place the sample in the preweighed glass tube_____ g_ and freeze at -70°, or use liquid nitrogen
3. Dry the samples in the freeze drier, for about 2 days
4. Record the weight of the tube and sample, _____and calculate the dry-weight of the sample in grams._____ g
5. Add the 0.5ml to 1ml of papain solution and record volume used._____ ml
6. Incubate the samples in a 60°C oven overnight
7. Allow the samples to come to room temperature
8. Do not disturb the settled pellet, to dry and weigh for microcarrier weight
9. Retain supernatant for analysis.
10. Now take 250µl of the supernatant, and add 250µl of concentrated HCl in Pyrex screw cap glass tube. Cap the vial tightly with a black phenolic PTFE lined screw caps and incubate overnight at 120°C.
11. Next day transfer the contents to small glass vials and incubate them uncapped at 90°C until dry. Cool the sample to room temperature and dissolve the residue in 1ml of 0.25M sodium phosphate buffer.

Preparation of blanks and sample diluent

1. Heat the papain solution in the oven at 60°C.
2. Hydrolyse this blank solution with equal volume of conc. HCl.
3. Incubate at 90°C until dry and then redissolve with 0.25M sodium phosphate.

This hydrolysed papain solution (HPS) will act as the blank and as the diluent for samples and standards.

Preparation of Standards

Make up a stock of 1mg/ml of hydroxyproline in UHQ water. Dilute down to 100µg/ml with the hydrolysed papain solution. Prepare the standards in 1.5ml eppendorfs

Standard value(µg/ml)	µl of 100µg/ml	µl blank HPS
30	60	140
20	40	160
15	30	170
10	20	180
8	16	184
6	12	188
5	10	190
4	8	192
2	4	196
1	2	198
0	0	200

Now load the standards and samples into the 96 well plate.

Load 50 µl of HPS as the blank
Load 50 µl of the standards
Load 50 µl of the sample, and do a range of dilutions from neat to a 1 in 10.
Add 50 µl of Chloramine T solution to each well and incubate for 20 min.
Add 50 µl of p-DAB solution to each well and incubate at 60°C for 30 min.

Ensure self-adhesive film and lids are placed over the wells to prevent evaporation.
Allow the plate to come to room temperature for 10 min and the read on the plate at 540nm.

% collagen in sample = (Conc. in ug/ml x Dil. factor x proportion of digest hydrolysed)/(Dry weight of the sample (g) x 0.143 x 1000,000) x 100%

B11: Protocol for the DMB assay for the GAG quantification:

This assay is applied after the papain digestion step used for B10.

Reagents:

1,9 Dimethylene blue (DMB) solution – Dissolve 16mg 1,9-dimethylene blue, and 2g sodium formate, in 100ml of UHQ water. Then add 5ml of 100% ethanol, and 2ml formic acid. Make up this solution to 1000ml using UHQ water and store the solution in foil wrapped brown bottle at room temperature. (Shelf life of 3months)

Standards – make a 1mg/ml stock solution of chrondroitin-4-sulphate (Chrondroitin sulphate A, bovine trachea) in UHQ water. Dilute this to 100µg/ml using the blank papain solution (i.e. 50µl of stock solution and 450 µl of blank papain solution). Prepare the standards in 1.5 ml eppendorf tubes from the diluted standard.

Standards (concentrations µg/ml)	µl of 100µg/ml of stock solution	µl of blank Papain Solution
0	0	100
5	5	95
10	10	90
15	15	85
20	20	80
25	25	75
30	30	70
40	40	60
50	50	50
75	75	25

Procedure:

1. Load the following reagents in the following order into a 96 well plate:
   20µl blank papain solution or the papain digested sample or the standards
   200 µl of 1,9-dimethylene blue (DMB) solution

2. Read the plate immediately using dual wavelength of 540nm (measurement) and 595 nm (reference). NB. The GAG/dye complexes may start to precipitate with time and plates should be read within 10 minutes of addition of the DMB solution.

B12: Range of suspension speeds used for the microcarriers:

1. Nunc 2D Microhex, minimum: 45rpm, maximum: 60rpm
2. Cytodex 2 microcarriers, minimum:60rpm, maximum:85rpm
3. Vicryl biodegradable discs, minimum:60rpm, maximum:85rpm (this was chosen empirically, i.e. to keep suspending the discs as much as possible, and the maximum was chosen to be the same as the Cytodex 2 microcarriers)

APPENDIX C

This section details on the cost and mass balance data used in Chapters 6 and 7.

C1 Cost data gathered for Chapters 6 and 7

Table C1: Resource cost information gathered for Chap 6.

Resource	Cost
Equipment	
70L fermenter, working volume 50L	£56,366
700L fermenter, working volume 500L	£559,606
CIP skid	£73,200
Roller bottle apparatus	£3,782
Cryogenic freezers – 150°C	£18,849
Freezer -80°C	£2,562
Wave reactor system 500 +KIT1000	$350,000 +$30,000
Wave reactor system 200	$105,000
Laminar flow hoods	$2,800
CELLMATE	£475000
Materials	
Consumables	
RB	£3.78 /RB
Disposable CellBags – 200L	£312 /unit
Disposable CellBags – 1000L	£1200 /unit
Chemicals	
DMEM	£4/L
Glutamine	£22/L
Serum	£32.97/L
MEM (Non-Essential amino acids)	£29/L
DPBS (buffer)	£4.20 /L
Ascorbic acid	£0.12 /g
Trypsin	£1.10/L
Commercial microcarrier	£3.60 /g
Biodegradable microcarrier	£5.40 /g (see assumptions table)
Biodegradable mesh	£11.64 / m^2
Staff	
Operator	£30k/annum
Utilities	
WFI	£5.30/L
Steam	£0.03/kg
Cooling water	$0.001/L

Table C2: Resource cost data gathered for Chapter 7.

Resource	Unit	Cost
Equipment		
Shake flask incubator		£7,000
Wave reactor system 500+KIT1000		£240,000
Wave reactor system 200EH		£70,000
Centrifuge	1000L	£100,000
Ultrafiltration Rig		£37,500
Chromatography Rig.	Diameter 11dm	£140,000
Chromatography columns (height 1100mm)	Diameter 0.7	£4,947
	Diameter 1.0	£5,686
	Diameter 1.4	£7,740
	Diameter 2.0	£8,529
	Diameter 2.5	£14,065
	Diameter 3.0	£18,591
	Diameter 3.5	£25,372
	Diameter 4.5	£46,332
Vessel/Holding Tank	50L	£2,600
	1500L	£20,000
CIP vessel		£60,000
Materials		
Consumables		
Cell Bag	1000L	
Cell Bag		
Shake flasks	0.5L	£30
Prostak UF Modules	0.93m^2	£883
	1.9 m^2	£1763
Spiral Wound Ultrafiltration Module	3.7 m^2	£3228
Ion Exchange Chrom. Matrix – CM Sepharose		£470/L
Gel Filtration Chrom. Matrix – G25M		£200/L
Affinity Chrom. Matrix – Heparin Sepharose		£4720/L
Chemicals		
Media		£5/L
PBS buffer		£0.66/L
1.0M NaOH		£1.80/L
1.0M NaCl		£0.78/L
0.01MTris/HCl		£0.55/L
H_3PO_4 pH 1.5		£0.63/L
CIP Buffer		£1.5/L

FCI is derived by multiplying the equipment purchase costs by a Lang factor, and this factor constitutes the sum of the individual factors f_1 to f_{10}. Thus deriving Lang factor for a disposable situation would be the same but the factors can be calculated based on the disposable costs rather than conventional costs. See inserted spread sheet as example.

Table C3: Derivation of Lang Factors

This method is based on Novais et al. (2001) where the Lang factor is the sum of the factors F1 to F10, multiplied by a contingency factor. Below is the example of the how the Lang factor (4.18) of the disposable plant using the Wave reactor is derived:

Process route	**Equipment Cost of each process route**	Ratio A (STR/WAVE)	Ratio B (WAVE/STR)
STR	£4,336,883	0.67	1
WAVE	£6,443,853	1	1.49

WAVE	**A**	**B**	**C**	**D**
	Conventional	Disposable on conventional	Disposable on conventional	Disposable on disposable
F1 Equipment	1.00	1.49	1.49	1.00
F2 Pipework	0.90	0.33	0.30	0.20
F3 Process control	0.37	1.00	0.37	0.25
F4 Instrumentation	0.60	0.66	0.40	0.27
F5 Electrical power	0.24	1.00	0.24	0.16
F6 Building works	1.66	0.80	1.32	0.89
F7 Detail Engineering	0.77	0.50	0.39	0.30
F8 Construction	0.40	0.75	0.30	0.20
F9 Commissioning	0.07	1.00	0.07	0.05
F10 Validation	1.06	0.50	0.53	0.36
Contingency factor	1.15	1.15	1.15	1.15
Lang Factor	**8.13**		**6.21**	**4.18**

Column A = individual (F1 to F10) factors for a conventional stainless steel biotech plant (Source: Novais et al. 2001)

Column B = Relative change in factors F1 to F10 for a disposable plant relative to a conventional plant.

Column C = Factors (F1 to F10) would be based on a conventional case i.e. Column A x Column B

Column D = Factors (F1 to F10) normalized to relative equipment costs for a disposable plant. (i.e. Column C divided by Ratio B)

Therefore the sum of Column D (F1 to F10) multiplied by the contingency factor gives 4.18 as the Lang factor to use.

C2 Mass balance and demand data

C2.1 Mass balance calculations

This following table shows the various mass balances implemented into spreadsheets for various unit operations for the processing calculations in Chapter 7

Table C4 :Process models adopted for the various unit operations used in Chapter 7

Unit Operations	*Process Models*
Fermentation	Stoichiometry, extent of reaction, e.g. $m_{out} = m_{in} - m_{inlimiting} \times x \times \frac{a_i}{a_{\lim}}$
Centrifugation	Solids carry-over, Solids volume fraction in sediment e.g. $m_{ssed} = (1-S) \times m_{s\,inlet}$ $m_{s\,\sup} = m_{\sin} \times m_{s\,sed}$
UFDF	Flux, Rejection coefficients, Number of Diavolumes e.g. $J = \frac{V_0(1-CF^{-1})}{A_T \times n \times t}$ e.g. $J = \frac{D \times V_0}{A_T \times n \times t}$
Chromatography	Flowrates, Column volumes, yields, binding capacities e.g $t = \frac{H \times CV}{u}$

C2.2: Derivation of the amount of steam used for vessels

An example calculation for the deriving how much steam that might be used for SIP

Amount of steam required for a 400L vessel:

At sterilization temperature of 121°C, the pressure is 2.4 bar (look in steam tables)
V= 400L i.e. 0.4 m^3
R = 8.314 (Gas constant)
T = 121°C

PV = nRT So n = PV/RT = 2.4 x 10^5 x 0.4 / (8.314 x (121+273)) = 29.3 moles

Moles = mass/mr therefore Mass of steam needed = 29.3 x 18 = 527.4 kg of steam
Thus expect to use about 528kg of steam and each need to use it before and after each batch run, therefore at 8 batches a year that is **8448**kg per year

C2.3: Demand data

A rationale was prepared based on market information and then the estimated demand was then calculated for the comparison of the growth factor with the TE-approach in Chapter 7. This is shown below:

Manufacture of GF (Growth Factors) individually as a treatment to chronic wounds:

Background information for what's on the market:

Regranex gel (US): main active ingredient is rPDGF (recombinant Platelet-derived growth factor), secreted by yeast of the strain Sacchromyces cerevisiae. This is a non-sterile, low bioburden gel. Price is £275 for a 15g tube, of which 0.01% is the active ingredient, i.e. 1.5mg.
This product is sold by Johnson & Johnson, sales in 2004 was $160 million (£100 million).

Fiblast spray (Japan): main active ingredient is rbFGF (recombinant basic fibroblast growth factor), loosely bound to the periplasm of the yeast strain Sacchromyces cerevisiae. This is sold in two vials – one of solution and one freeze-dried active ingredient to be reconstituted with the solution vial. Thus 500ml spray with 500μg of rbFGF is ¥12,339.70 (£60.70).
This product is sold by Kaken Pharmaceutical, sales in 2004 was ¥3.4 billion. (£16.7 million)

For a ulcer size of 4cm x 4cm, and treatment of 8 weeks:
DG (Dermagraft), 1 piece per week, thus total of 8 pieces of DG.
Regranex gel, 1 gram of gel used per day, thus total of 56g of gel i.e. 4 tubes.

[length of gel applied daily = 4cm x 4cm /4 = 1 g , 15 g per tube, 56/15 = 3.7 tubes, i.e. 4 tubes.]

so 8 units of DG is about 4 tubes, i.e. each piece of DG is 2 tubes.

So if comparison to previous ECM project of making 100kg production,

100kg is about 126,904 units of DG [= 100*1000/0.788] , each piece of DG weighs 0.788 g
so 126904 units of DG is about 63,452 tubes of GF gel.

therefore if each tube has 15 g of gel and at 0.01%w/w active of each single GF

Then 63,452*15*0.01% = 95.178 g
So, demand of growth factor is **95200mg** of growth factor.

C3 Calculating Cashflow and the NPV

Spreadsheet was set up as shown below and the net cashflow was utilized to then feed into the NPV calculation and the cumulative cashflow to calculate payback time.

Table C5: Example of spreadsheet set up to calculate cashflow

Year	-1	0	1 to 9	10
Production (kg)				
Sales price per kg				
Sales revenue				
Sales and Distribution Cost				
FCI		N/A	N/A	N/A
Working capital		N/A	N/A	N/A
Total indirect costs				
Total direct costs				
Total running costs				
Gross Profit				
Interest				
Profit before Tax				
Corporate Tax @ 30%				
Profit After Tax				
Depreciation Recouped				
Working Capital Recouped	N/A	N/A	N/A	
Net Cashflow				
Cumulative Cashflow				

	Base Case	Discount Factor			
	0%	10%	20%	30%	40%
Year -1	Net cashflow				
Year 0	Net cashflow				
Total 1	Year-1+year0	Year-1+year0	Year-1+year0	Year-1+year0	Year-1+year0
Year 1	Net cashflow				
Year 2	Net cashflow				
Year 3	Net cashflow				
Year 4	Net cashflow				
Year 5	Net cashflow				
Year 6	Net cashflow				
Year 7	Net cashflow				
Year 8	Net cashflow				
Year 9	Net cashflow				
Year 10	Net cashflow				
Total 2	Sum(Year 1:year 10)	Sum(Year 1:year 10)	Sum(Year 1:year 10)	Sum(Year 1:year 10	Sum(Year 1:year 10)
NPV	total1+total2	total1+total2	total1+total2	total1+total2	total1+total2

NPV : to calculate the values in the blank spaces in the table shown above :

= Base case x $(1+(\text{discount factor})^{\text{year}}$.